澳門大學
UNIVERSIDADE DE MACAU
UNIVERSITY OF MACAU

# Outstanding Academic Papers by Students
# 學生優秀作品

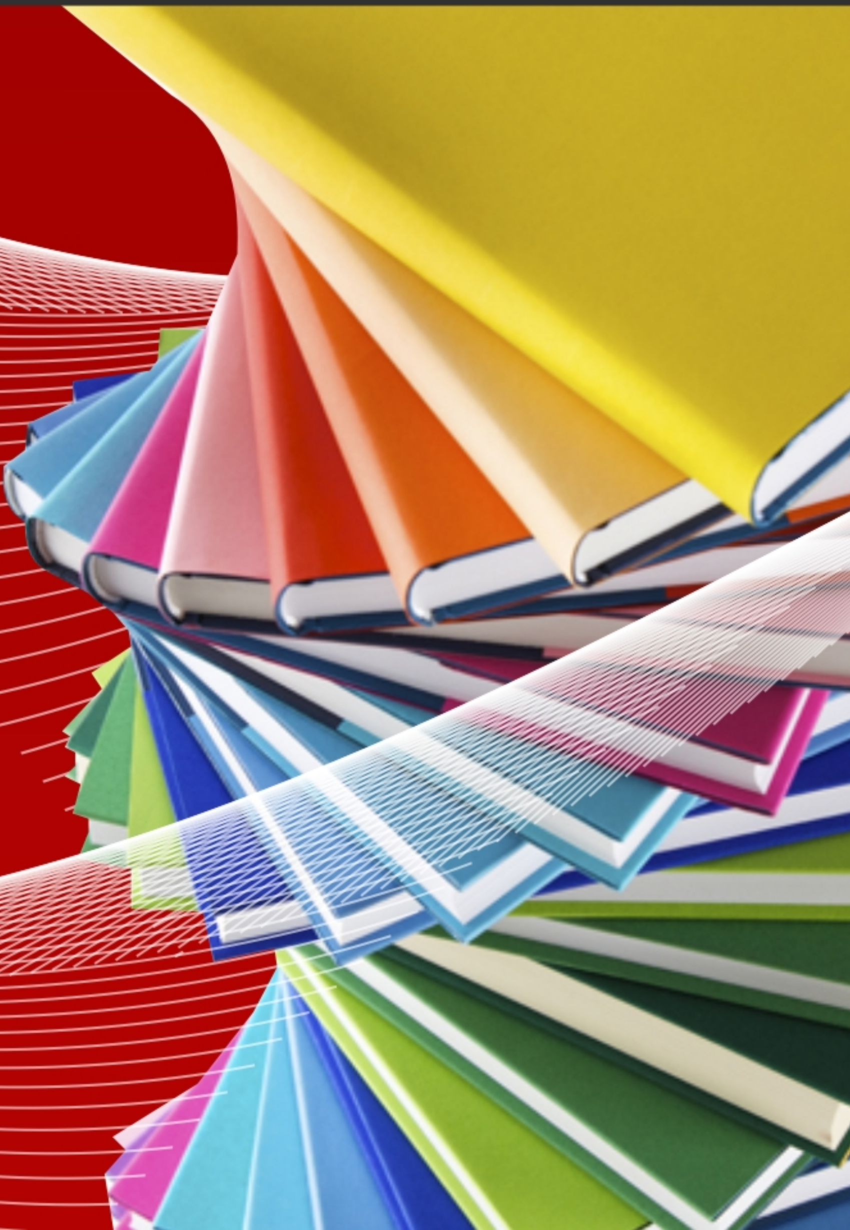

# Analysis of Air-Supported Structures Subjected to Vertical and Horizontal Loads

by

**Lao Hong Wan**

Final Year Project Report submitted in partial fulfillment of the requirement of the Degree of

**Bachelor of Science in Civil Engineering**

**2014-2015**

**Faculty of Science and Technology**
**University of Macau**

# DECLARATION

I declare that the project report here submitted is original except for the source materials explicitly acknowledged and that this report as a whole or any part of this report has not been previously and concurrently submitted for any other degree or award at the University of Macau or other institutions.

I also acknowledge that I am aware of the Rules on Handling Student Academic Dishonesty and the Regulations of the Student Discipline of the University of Macau.

Signature : 留鴻運

Name : LAO Hong Wan

Student ID : DB127628

Date : 2015/05/18

# APPROVAL FOR SUBMISSION

This project report entitled "**Analysis of Air-Supported Structures Subjected to Vertical and Horizontal Loads**" was prepared by Lao Hong Wan in partial fulfillment of the requirements for the degree of Bachelor of Science in Civil Engineering at the University of Macau.

Endorsed by,

Signature: ____________________

Supervisor: Dr. IU Vai Pan

~~Signature:~~ ____________________

~~Examiner: Dr. ER Guo Kang~~

# ACKNOWLEDGEMENTS

In such a long time fighting, I was really learning how to torment myself. But I know that the pleasure and success come after the pain. I am very lucky to have these experiences to grow me up.

Firstly, Professor Iu is really a kind person who did not give me negative emotion even though my progress is behind the schedule. Every time I was learned much more than the FYP should be after the regular meeting. In here, I am grateful to the Professor Iu's support and I will keep learning as what you teach me.

Secondly, I am thankful to myself. Most of the time is alone and doing the FYP. I have to be stronger to deal with the problems from the FYP and the depression from myself. I hope I can keep going until I have a desired job.

Thirdly, I deeply appreciate to my dear families, relatives and friends. Your concern, care and encouragement are being a part of my work.

Finally, the FYP is just a part of study; everything will go forward tirelessly.

# ABSTRACT

An air-supported structure is usually an inflated membrane which derives its stiffness from tension caused by pressurized air. The structure is commonly made of fabric material. Because of its lightweight, thinness and extensible geometry, the feasibility in terms of the cost, material and aesthetic aspect makes it became more significant in the structure engineering. It has been extensively applied to different types of structural design, for instance, sports facilities, car park, airport, and among other applications. In fact, the application of a membrane structure has the difficulties which need to be considered. At first, the membrane structure is weak in taking compression and hence is a tension structure. The utilization would be based on the theory of membrane material and that is the fundamental principle of the membrane structure modeling. Besides, the property of membrane material is assumed to be inextensible in the practical concern so as to perform a proper model. In the study, a typical shape of long cylindrical membrane is the modeling object. Its nonlinear behaviour is what the study is concerning and looking for a deep discussion in analysis. The long cylindrical membrane would be modeled as infinite in longitudinal direction by one-dimensional bar elements in the computer program. For the analysis, the different geometry ratio and load patterns such as wind loads, snow loads and concentrated load which defined as lateral or vertical load are the main concern in this paper.

# TABLE OF CONTENTS

**CHAPTER 7 CONCLUSION**

# LIST OF TABLES

# LIST OF FIGURES

# LIST OF SYMBOLS

| *Symbol* | Unit | Property |
|---|---|---|
| $AncF$ | kN | Anchor force at the supports of membrane |
| $\Delta AncF$ | kN | Difference of anchor force |
| $Anc\theta$ | degree | Anchor angle at the supports of membrane |
| $\Delta Anc\theta$ | degree | Difference of anchor angle |
| $a_{o}, a_{1}, a_{2}$ | m | Radius of curvature |
| $B$ | m | Base width |
| $Co, C_{1}$ | - | Location point in membrane |
| $C_{p}$ | - | Wind load coefficient |
| $\mathrm{d}_{\mathrm{max}}$ | m | Maximum displacement |
| $\Delta \mathrm{d}_{\mathrm{max}}$ | m | Difference of maximum displacement |
| $F_{i}$ | kN | Point load component |
| $H$ | m | Height |
| $\Delta_{H}$ | m | Horizontal displacement |
| $\bar{k}$ | - | Dimensionless loading parameter |
| $\ell,\ \ell_{1},\ \ell_{2}$ | m | Arc length |
| $L$ | m | Equal length in membrane model |

| | | |
|---|---|---|
| $N_z$ | kN/m | Longitudinal membrane stress resultants |
| $N_\varphi$ | kN/m | Circumferential membrane stress resultants |
| $P$ | kN | Point load |
| $P_i$ | kN | Equivalent nodal load |
| $P_{xi}$ | kN | Equivalent nodal load in horizontal component |
| $P_{yi}$ | kN | Equivalent nodal load in vertical component |
| $p_0$ | kPa | Internal pressure |
| $\rho$ | $kg/m^3$ | Air density |
| $q_r$ | kPa | Internal pressure only used in Eq.2.3 |
| $q'$ | kPa | Dynamic wind pressure |
| $R$ | kPa | Snow load |
| $Sw$ | m | Radius of curvature used in Eq.2.3 |
| $T, T_1, T_2$ | kN | Tension |
| $T_o$ | kN | Initial tension |
| $T_i$ | kN | Tension at node number = i |
| $T_{xi}$ | kN | Tension in horizontal component |
| $T_{yi}$ | kN | Tension in vertical component |
| $v$ | m/s | Wind speed |

| | | |
|---|---|---|
| $\Delta_v$ | m | Vertical displacement |
| $\bar{\Delta}_v$ | - | Vertical displacement factor |
| $W_g$ | kN | Weight of membrane |
| $X_i$ | m | X coordinate at node number = i |
| $\Delta X_n$ | m | Misclosure of final X coordinate |
| $W_d$ | kPa | Wind pressure |
| $Y_i$ | m | Y coordinate at node number = i |
| $\Delta Y_n$ | m | Misclosure of final Y coordinate |
| $z$ | m | Z coordinate |
| $\alpha$ | degree | Angle for the calculation of *Cp* |
| $\varphi, \varphi_C, \varphi_A$ | degree | Opening angle in Eq2.2 |
| $\theta_o$ | degree | Initial angle |
| $\theta_i$ | degree | Internal angle at node number = i, used in formulation |

# CHAPTER 1 INTRODUCTION

## *1.1 Cylindrical Membrane*

An air-supported structure is any building that derives its structural integrity from the use of pressurized air to maintain the stability of structural fabric material such as cylindrical membrane. The cylindrical membrane structure mainly resists tensile stresses but the utilization also should be applied if it is subjected to compression. Referring to Merritt and Ricketts (1958), there are two methods of utilization. One of the methods is to utilize the membrane by hanging it with initial tension of the two supports on the ground. Besides of it, pretensioning a membrane, which is to pressurize the interior with air, is another way to utilize the membrane. Actually, the tension has an equation related to the internal pressure that they are adjusting mutually in order to provide the structural equilibrium. That is by assigning a value to the internal pressure (usually this number is controllable in reality), then the tension could be predicted from the equilibrium in the numerical computation. Moreover, in the research of air-supported cylindrical membranes written by Robert Maaskant and John Roorda (1985), they had used a linear equation to explain the relation of the tension and internal pressure under the assumption of inextensible membrane. By integrating these equations and the loading patterns, the equilibrium could be formed. The equilibrium system explains why both method of utilization is a stable membrane structure should be considered. In general, the principle of membrane is based on the equilibrium system.

### *1.2 Membrane Material*

The membrane material has two kinds of extremes, one is extensible and another is inextensible which would have detail discussion in Chapter 3. In order to perform a realistic model, first assumption of membrane material is inextensible. On the other hand, the study is not supported to the cylindrical membrane that is extensible.

According to the previous paragraphs, the computer program would follow the theory of equilibrium system and inextensible assumption to create a proper model for the analysis of nonlinear behaviour in both vertical and horizontal loadings.

# CHAPTER 2 LITERATURE REVIEW

## *2.1 Theoretical Behaviour of Cylindrical Membranes*

The following discussion is based on the research that written by Robert Maaskant and John Roorda (1985) for a long cylindrical membrane. The first assumption is infinite in the longitudinal direction, such that end effect could be ignored. Thus, the result is only suitable to the application of air-supported membrane structure whose longitudinal dimension is considerable long respect to the sectional dimension. Furthermore, an idealized model of using one-dimensional bar could be applied as the principal structure in sectional membrane under the assumptions above. The internal pressure that exists in circumferential direction only, is acting on the sectional membrane. Hence, for a weightless material, the simplified equation of membrane is,

$$\frac{\partial N_z}{\partial z} = 0 \qquad \text{Eq2.1}$$

$$\frac{\partial N_\varphi}{\partial \varphi} = 0 \qquad \text{Eq2.2}$$

$$N_\varphi - q_r R = 0 \qquad \text{Eq2.3}$$

where $N_z$ and $N_\varphi$ are the membrane stress resultants in the longitudinal and circumferential directions; $q_r$ is the internal pressure and $R$ is radius of curvature. From the equation Eq2.1 to Eq2.3, the variations respected to $\varphi$, and radius of curvature $R$ is inversely proportional to the internal pressure $q_r$. The membrane will be a circle shape if the internal pressure is a constant value.

The undeformed cross section of membrane is assumed as circular shape in Figure 2.1.1 (a). The sectional dimensions are correspondingly to the Figure 2.1.1 which *2B* is the width, *H* is the height, $\psi$o is the opening angle, $a_o$ is radius of curvature, $p_o$ is internal pressure and *P* which acting on the location *C* is the concentrated line load along the longitudinal direction. The location of *Co* is ideally in the central of undeformed section and the horizontal and vertical displacement $\Delta_H, \Delta_V$ could be derived from the location *Co* and *C* after the loading is fully developed, which shows on the Figure 2.1.1 (b).

The deformed shape in Figure 2.1.1(b) is separated into another two circular form which $\ell_1$ and $\ell_2$ is the arc length, $a_1$ and $a_2$ is the radius of curvature, $\psi_A$ and $\psi_C$ is the internal angle between the vertical axis and the line of radius of curvature respected to the end of arc and the subscribe is corresponding to the circular form 1 and 2.

The equilibrium of membranes AC and BC derive from the Eqs 2.1-2 is given by

$$T_1 = p_0 a_1 \qquad \text{Eq2.4}$$

$$T_2 = p_0 a_2 \qquad \text{Eq2.5}$$

where *T* is the circumferential tension of path AC and BC Then, the equilibrium at the loading location is

$$T_1 sin\varphi_{C1} + T_2 sin\varphi_{C2} = P \qquad \text{Eq2.6}$$

$$T_1 cos\varphi_{C1} - T_2 cos\varphi_{C2} = 0 \qquad \text{Eq2.7}$$

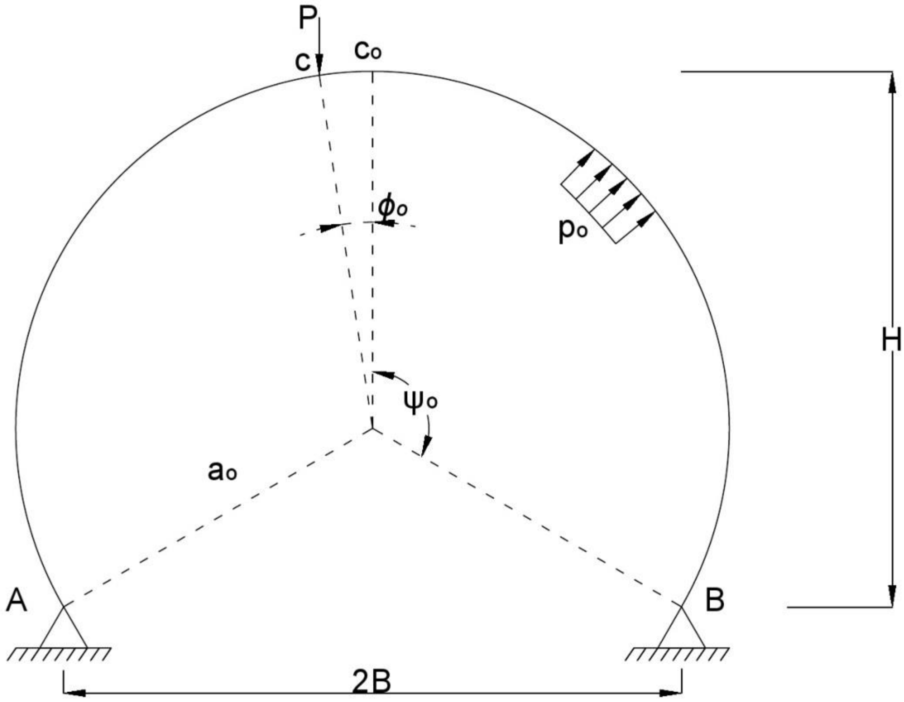


**( a )**

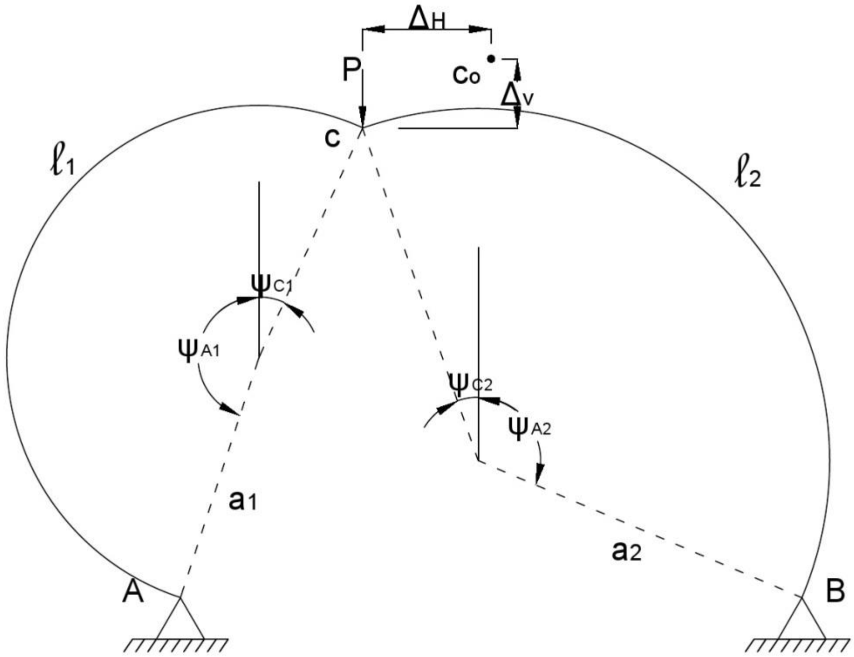


**( b )**

Figure 2.1.1 Sectional dimensions of cylindrical air-supported membrane of undeformed shape (a) and deformed shape (b)

$$a_1(sin\varphi_{C1} + sin\varphi_{A1}) + a_2(sin\varphi_{C2} + sin\varphi_{A2}) = 2B \qquad \text{Eq2.8}$$

$$a_1\left(cos\varphi_{C1} - cos\varphi_{A1}\right) - a_2(cos\varphi_{C2} - cos\varphi_{A2}) = 0 \qquad \text{Eq2.9}$$

The inextensible assumption of membrane material is represented by

$$a_1(\varphi_{C1} + \varphi_{A1}) = \ell_1 \qquad \text{Eq2.10}$$

$$a_2(\varphi_{C2} + \varphi_{A2}) = \ell_2 \qquad \text{Eq2.11}$$

where $\ell_1 + \ell_2 = \ell$

Eqs 2.4-2.11 is the behaviour of cylindrical membrane under the concentrated line load with full development. The vertical and horizontal displacements could be determined from the change in geometry

$$\Delta_V = H - a_1(cos\varphi_{C1} - cos\varphi_{A1}) \qquad \text{Eq2.12}$$

$$\Delta_H = B - a_1(sin\varphi_{C1} + sin\varphi_{A1}) \qquad \text{Eq2.13}$$

The idea of displacement shown in the Eqs 2.12 and 2.13 is also appropriate to other displacements that caused by different loading cases, which using a coordinate system to explain the movement at a particular location.

### *2.2 Symmetric Membrane Displacements*

For long cylindrical membrane subjected to central vertical point load, the membrane is deformed as path AC and BC in the same arc length and results in a symmetric displacement. Thus, the horizontal displacement does not exist (Figure 2.2.1).

The following equations describe the equilibrium under a centric line load with the sectional dimensions are simplified into single properties because of the inextensible property, where $\varphi_{C1} = \varphi_{C2} = \varphi_C$, $\varphi_{A1} = \varphi_{A2} = \varphi_A$, $a_1 = a_2 = a$, $\ell_1 = \ell_2 = \ell$;

$$\frac{P}{p_0} = 2asin\varphi_C \qquad \text{Eq2.14}$$

$$a(sin\varphi_A + sin\varphi_C) = B \qquad \text{Eq2.15}$$

$$a(\varphi_A + \varphi_C) = \ell \qquad \text{Eq2.16}$$

$$\Delta_V = H - a(cos\varphi_C - cos\varphi_A) \qquad \text{Eq2.17}$$

Eqs.2.14-2.17 contains a large amount of nonlinear relations that is applicable to a numerical analysis.

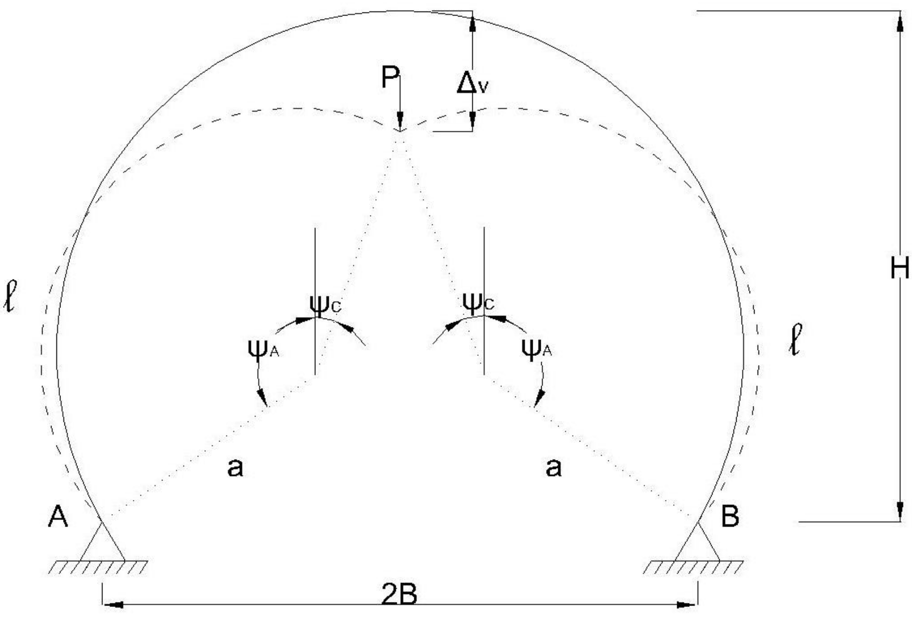


Figure 2.2.1 sectional properties of membrane in symmetrical displacement

The behaviour of symmetric membrane could be deduced by the numerical computation of the relation between the dimensionless loading parameter $\bar{k}$ and the vertical displacement factor $\bar{\Delta}_v$ Eqs. 2.18-2.19

$$\bar{k} = \frac{P}{Hp_o} \qquad \text{Eq2.18}$$

$$\bar{\Delta}_v = \frac{\Delta_V}{H} \qquad \text{Eq2.19}$$

Where *P* is point load, *H* is height of membrane, *po* is internal pressure of unit length, $\Delta_V$ is vertical displacement.

From the dimensionless numerical solution of $\bar{k}$ and $\bar{\Delta}_v$, the nonlinear behaviour (Figure 2.2.2) is similar to the strain-stress curve since the loading and displacement are involved in two equations, respectively.

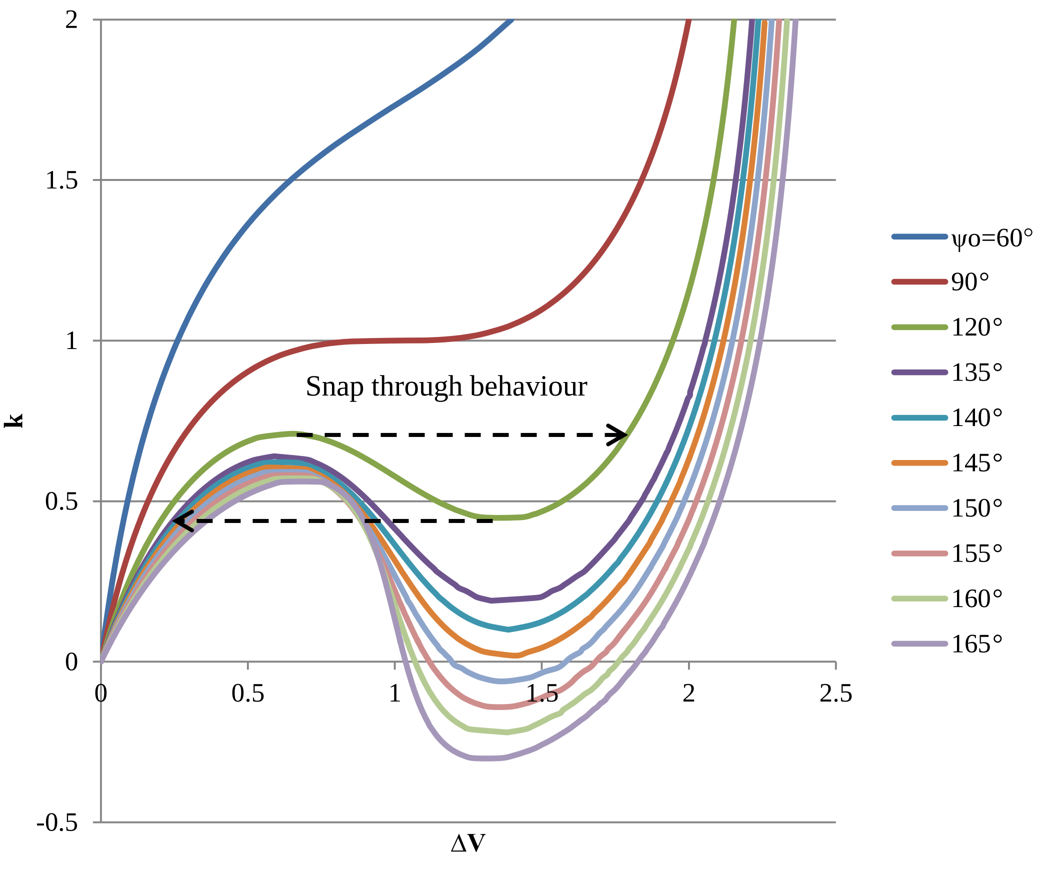


Figure 2.2.2 Equilibrium solution: Symmetrical displacements

In the Figure 2.2.2, the main factor which causing the change in behaviour is the initial opening angle $\psi$o. When the angle is equal or less than 90 degrees, the membrane is able to resist an amount of loading without many displacements. It is apparently to see that the positive slopes mean the stable equilibrium. In the opening angles equal or greater than 90 degrees, while little change in the loading would affect a considerable displacement, at this stage, the peak point is the limit of practicability which the membrane is in a statically unstable situation, correspondingly, this action could be seen graphically in the portions of the slope comes to zero at the first time. Another series of behaviour occurs in the opening angle large than 90 degrees, which is snap-through behaviour. After the limit of practicability, the membrane structure is suddenly shifted to unstable shape with large displacement that even may be twice of its original height. Obviously, the negative slopes mean the unstable configuration. Although the behaviour in portion of negative slopes do not happen in real structure, the hidden relation still could be found theoretically since the mathematical model allowed the two portion of membrane to overlap to each other.

Although this case only introduces a situation of symmetrical membrane displacement, the principle of force equilibrium and coordinate system could be also available for other geometry ratio of cylindrical membrane structure with different loading combinations, which will study in the chapter 3. In addition, the theory of membrane modeling process is required a practical data (Figure 2.2.2) as the evidence to prove the credibility of computer program that will discuss in the chapter 4.

# CHAPTER 3 METHODOLOGY

### *3.1 Membrane Modeling in Inextensible One-Dimensional Bar Elements*

In the conceptual material of membrane, it could be derived into two extremes (Turkkan and Srivastava, 1992). One extreme is like a high elastic inflatable balloon, the shape of membrane could be stretched when internal pressure or external force is applied. Another extreme is a blown-up paper dome, which the membrane material is inextensible and the pretensioning of membrane is necessary to keep a desired shape under the inflation pressure. In the reality, the membrane is most likely to be inextensible instead of extensible due to the material properties that used presently in civil or architectural structures. Moreover, large deflection will result unstably in the extensible shape and occupy available space when an extensible membrane is subjected to large loading. Hence, the following presentation assumes that membrane material is inextensible, consistently with the previous chapters.

There are four basic analytical and design aspects of such a flexible membrane structure:

(a) form finding,

(b) determination of sectional properties,

(c) determination of loads typical to these kinds of structure,

(d) static and dynamic analysis and design under the loading equilibrium

The design process involves some simplified methods of analysis and design which could be readily applied to all kind of design loads and computed by the computer program as accurate as possible to the reality.

### *3.2 Formulation of Cylindrical Membrane Structure Subjected to Vertical and Horizontal Loads*

The formulation is based on a network approach modified by the paper (Turkkan and Srivastava, 1992) which is a continuous flexible membrane with finite displacement that is idealized as a space net connected by tension one-dimensional bar element (Figure 3.2.1).

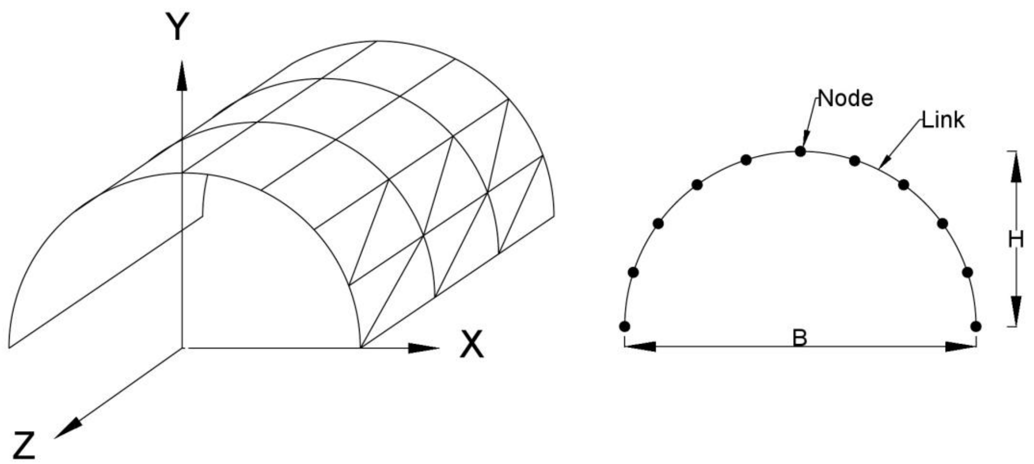


Figure 3.2.1 Description of simplified model and correspond axis

The end effect could be ignored since the long cylindrical membrane has assumed to be infinite in the longitudinal direction that has been mentioned in the beginning of chapter 2. Moreover, the non-transverse strips are set to prevent the longitudinal displacements. Thus, the design and analysis process is under the consideration of a sectional membrane, the formulation is deduced as follows.

A one-dimensional bar element is divided into *n* finite tension element of equal length *L* connected by *n-1* number of nodes (Figure 3.2.2). The equivalent load includes the distributed load, internal pressure and the weight of membrane. The load equilibrium formula from node *i = 0 to n*, are given by

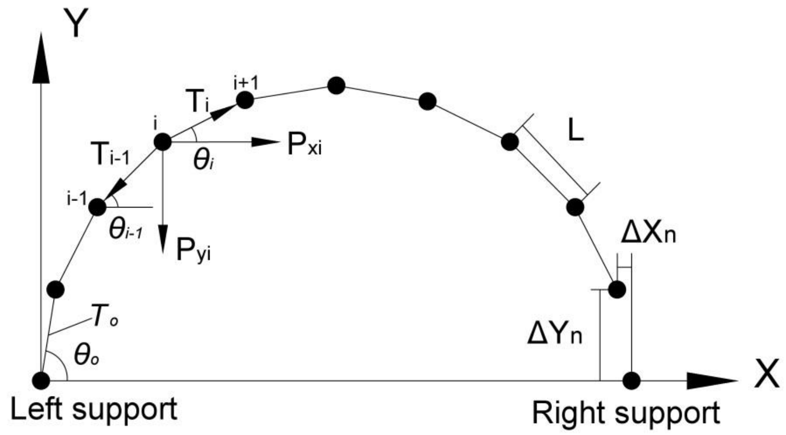


Figure 3.2.2 Node equilibrium, initial dimension and misclosure

$$P_{xi} - T_{i-1}cos\theta_{i-1} + T_i cos\theta_i = 0 \qquad \text{Eq3.1}$$

$$P_{yi} - T_{i-1}sin\theta_{i-1} + T_i sin\theta_i = 0 \qquad \text{Eq3.2}$$

where $P_i$ is the equivalent nodal load, $T_i$ and $\theta_i$ is the tension and angle at each node respectively (Figure 3.2.2). Since the initial tension $T_o$ could be estimated by the Eq 2.4 and the angle $\theta_o$ is predictable from the initial geometry, in this condition, by the known value of previous tension $T_{i-1}$, the angle $\theta_{i-1}$ and the loads, the next tension $T_i$ and the angle $\theta_i$ could be determined by the substitution of tension components

$$T_{xi} = T_i cos\theta_i = T_{i-1}cos\theta_{i-1} - P_{xi} \qquad \text{Eq3.3}$$

$$T_{yi} = T_i sin\theta_i = T_{i-1} sin\theta_{i-1} - P_{yi} \qquad \text{Eq3.4}$$

The equivalent nodal load is the combination of the weight of membrane $W_g$, the internal pressure $p_o$ and the specific loading pattern of the analytical cases which could be assumed to be point load $F_i$ in the node equilibrium system, the formulas as describe in follows

$$P_{xi} = F_{xi} - p_o sin\theta_{i-1} \qquad \text{Eq3.5}$$

$$P_{yi} = -F_{yi} + p_o cos\theta_{i-1} - W_g \qquad \text{Eq3.6}$$

All loads are transferred into vertical and horizontal components. The load components remain the same direction in the equilibrium of each node. The internal pressure acts on the circumferential direction with an approximate angle to the vertical direction. In the Eq3.5 and Eq3.6, the angle is predicted from the geometry which is similar to the angle defined in Figure 3.2.2 if a certain number of nodes are applied in the system. Moreover, in order to avoid the effect of distributed load which should be continuous along the membrane, the number of finite element is necessarily developing to a reasonable value. Therefore, the number of node would be determined once the results are approaching to the theoretical data that obtained from the Figure 2.2.2.

Then, the new coordinates are simply expressed as

$$X_{i+1} = X_i + L\frac{T_{xi}}{T_i} \qquad \text{Eq3.7}$$

$$Y_{i+1} = Y_i + L\frac{T_{yi}}{T_i} \qquad \text{Eq3.8}$$

where $T_i = \sqrt{T_{xi} + T_{yi}}$

At the ends of membrane, the boundary conditions should be remained

$$X_1, Y_1, X_n, Y_n = constant \qquad \text{Eq3.9}$$

The entire process is repeating until the final node coordinates $X_n$ and $Y_n$ are known. The misclosure $\Delta X_n$ and $\Delta Y_n$ (Figure 3.2.2) usually exist and correlate to the accumulation of error in numerical finite elements. If the misclosure is not acceptable, the Newton-Raphson iterative method would be applied for the correction:

$$\begin{bmatrix} T_o{}' \\ \theta_o{}' \end{bmatrix} = \begin{bmatrix} T_o \\ \theta_o \end{bmatrix} - \begin{bmatrix} \frac{\delta \Delta X_n}{\delta T_o} & \frac{\delta \Delta X_n}{\delta \theta_o} \\ \frac{\delta \Delta Y_n}{\delta T_o} & \frac{\delta \Delta Y_n}{\delta \theta_o} \end{bmatrix}^{-1} \begin{bmatrix} \Delta X_n \\ \Delta Y_n \end{bmatrix} \qquad \text{Eq3.10}$$

where $\Delta X_n = B - X_n = B - (X_{n-1} + L\frac{T_{x(n-1)}}{T_{n-1}})$,

$\Delta Y_n = Y_n = Y_{n-1} + L\frac{T_{y(n-1)}}{n-1}$

$B$ is the base width; $X_n$ and $Y_n$ are the final coordinate that could express in Eq3.7 and 3.8. A better value of initial tension $T_o{}'$ and opening angle $\theta_o{}'$ are calculated by the Eq3.10.

The Newton-Raphson method is available to the equation of $T_o{}'$ and $\theta_o{}'$ which involve an amount of nonlinear computation.

For the calculation of the derivations $\Delta X_n$ and $\Delta Y_n$ by $T_o$ and $\theta_o$, four series of calculations are necessary.

1) The derivation $\Delta X_n$ by $T_o$, which shows in follows:

From i(=1, 2, …, n) node, the derivation of $\Delta X_n$ by $T_o$ is

i=1 $$\frac{\delta \Delta X_1}{\delta T_o} = \frac{\delta B}{\delta T_o} - \left[\frac{\delta X_o}{\delta T_o} + L\frac{\delta}{\delta T_o}\left(\frac{T_{xo}}{T_o}\right)\right] \quad \text{Eq3.11a}$$

i=2 $$\frac{\delta \Delta X_2}{\delta T_o} = \frac{\delta B}{\delta T_o} - \left[\frac{\delta X_1}{\delta T_o} + L\frac{\delta}{\delta T_o}\left(\frac{T_{x1}}{T_1}\right)\right] \quad \text{Eq3.11b}$$

$$\vdots$$

i=n-1 $$\frac{\delta \Delta X_{n-1}}{\delta T_o} = \frac{\delta B}{\delta T_o} - \left[\frac{\delta X_{n-2}}{\delta T_o} + L\frac{\delta}{\delta T_o}\left(\frac{T_{x(n-2)}}{T_{n-2}}\right)\right] \quad \text{Eq3.11c}$$

i=n $$\frac{\delta \Delta X_n}{\delta T_o} = \frac{\delta B}{\delta T_o} - \left[\frac{\delta X_{n-1}}{\delta T_o} + L\frac{\delta}{\delta T_o}\left(\frac{T_{x(n-1)}}{T_{n-1}}\right)\right] \quad \text{Eq3.11}$$

where the sub-derivation $\frac{\delta}{\delta T_o}\left(\frac{T_{x(n-1)}}{T_{n-1}}\right)$ is also a series of calculations:

i=1 $$\frac{\delta}{\delta T_o}\left(\frac{T_{xo}}{T_o}\right) = \left(\frac{\frac{\delta T_{xo}}{\delta T_o} T_o - T_{xo}\frac{\delta T_o}{\delta T_o}}{{T_o}^2}\right) \quad \text{Eq3.12a}$$

i=2 $$\frac{\delta}{\delta T_o}\left(\frac{T_{x1}}{T_1}\right) = \left(\frac{\frac{\delta T_{x1}}{\delta T_o} T_1 - T_{x1}\frac{\delta T_1}{\delta T_o}}{{T_1}^2}\right) \quad \text{Eq3.12b}$$

$$\vdots$$

i=n $$\frac{\delta}{\delta T_o}\left(\frac{T_{x(n-1)}}{T_{n-1}}\right) = \left(\frac{\frac{\delta T_{x(n-1)}}{\delta T_o} T_{n-1} - T_{x(n-1)} \frac{\delta T_{n-1}}{\delta T_o}}{{T_{n-1}}^2}\right) \qquad \text{Eq3.12}$$

2) The derivation $\Delta Y_n$ by $T_o$, which shows in follows:

From i(=1, 2, …, n) node, the derivation of $\Delta Y_n$ by $T_o$ is

i=1 $$\frac{\delta \Delta Y_1}{\delta T_o} = \frac{\delta Y_o}{\delta T_o} + L \frac{\delta}{\delta T_o}\left(\frac{T_{yo}}{T_o}\right) \qquad \text{Eq3.13a}$$

i=2 $$\frac{\delta \Delta Y_2}{\delta T_o} = \frac{\delta Y_1}{\delta T_o} + L \frac{\delta}{\delta T_o}\left(\frac{T_{y1}}{T_1}\right) \qquad \text{Eq3.13b}$$

⋮

i=n-1 $$\frac{\delta \Delta Y_{n-1}}{\delta T_o} = \frac{\delta Y_{n-2}}{\delta T_o} + L \frac{\delta}{\delta T_o}\left(\frac{T_{y(n-2)}}{T_{n-2}}\right) \qquad \text{Eq3.13c}$$

i=n $$\frac{\delta \Delta Y_n}{\delta T_o} = \frac{\delta Y_{n-1}}{\delta T_o} + L \frac{\delta}{\delta T_o}\left(\frac{T_{y(n-1)}}{T_{n-1}}\right) \qquad \text{Eq3.13}$$

where the sub-derivation $\frac{\delta}{\delta T_o}\left(\frac{T_{y(n-1)}}{T_{n-1}}\right)$ is also a series of calculations:

i=1 $$\frac{\delta}{\delta T_o}\left(\frac{T_{yo}}{T_o}\right) = \left(\frac{\frac{\delta T_{yo}}{\delta T_o} T_o - T_{yo} \frac{\delta T_o}{\delta T_o}}{{T_o}^2}\right) \qquad \text{Eq3.14a}$$

i=2 $$\frac{\delta}{\delta T_o}\left(\frac{T_{y1}}{T_1}\right) = \left(\frac{\frac{\delta T_{y1}}{\delta T_o} T_1 - T_{y1} \frac{\delta T_1}{\delta T_o}}{{T_1}^2}\right) \qquad \text{Eq3.14b}$$

⋮

i=n $$\frac{\delta}{\delta T_o}\left(\frac{T_{y(n-1)}}{T_{n-1}}\right) = \left(\frac{\frac{\delta T_{y(n-1)}}{\delta T_o} T_{n-1} - T_{y(n-1)} \frac{\delta T_{n-1}}{\delta T_o}}{{T_{n-1}}^2}\right) \qquad \text{Eq3.14}$$

3) The derivation $\Delta X_n$ by $\theta_o$, which shows in follows:

From i(=1, 2, …, n) node, the derivation of $\Delta X_n$ by $\theta_o$ is

i=1 $$\frac{\delta \Delta X_1}{\delta \theta_o} = \frac{\delta B}{\delta \theta_o} - \left[\frac{\delta X_o}{\delta \theta_o} + L\frac{\delta}{\delta \theta_o}\left(\frac{T_{xo}}{T_o}\right)\right]$$ Eq3.15a

i=2 $$\frac{\delta \Delta X_2}{\delta \theta_o} = \frac{\delta B}{\delta \theta_o} - \left[\frac{\delta X_1}{\delta \theta_o} + L\frac{\delta}{\delta \theta_o}\left(\frac{T_{x1}}{T_1}\right)\right]$$ Eq3.15b

⋮

i=n-1 $$\frac{\delta \Delta X_{n-1}}{\delta \theta_o} = \frac{\delta B}{\delta \theta_o} - \left[\frac{\delta X_{n-2}}{\delta \theta_o} + L\frac{\delta}{\delta \theta_o}\left(\frac{T_{x(n-2)}}{T_{n-2}}\right)\right]$$ Eq3.15c

i=n $$\frac{\delta \Delta X_n}{\delta \theta_o} = \frac{\delta B}{\delta \theta_o} - \left[\frac{\delta X_{n-1}}{\delta \theta_o} + L\frac{\delta}{\delta \theta_o}\left(\frac{T_{x(n-1)}}{T_{n-1}}\right)\right]$$ Eq3.15

where the sub-derivation $\frac{\delta}{\delta \theta_o}\left(\frac{T_{x(n-1)}}{T_{n-1}}\right)$ is also a series of calculations:

i=1 $$\frac{\delta}{\delta \theta_o}\left(\frac{T_{xo}}{T_o}\right) = \left(\frac{\frac{\delta T_{xo}}{\delta \theta_o} T_o - T_{xo}\frac{\delta T_o}{\delta \theta_o}}{{T_o}^2}\right)$$ Eq3.16a

i=2 $$\frac{\delta}{\delta \theta_o}\left(\frac{T_{x1}}{T_1}\right) = \left(\frac{\frac{\delta T_{x1}}{\delta T_o} T_1 - T_{x1}\frac{\delta T_1}{\delta T_o}}{{T_1}^2}\right)$$ Eq3.16b

⋮

i=n $$\frac{\delta}{\delta \theta_o}\left(\frac{T_{x(n-1)}}{T_{n-1}}\right) = \left(\frac{\frac{\delta T_{x(n-1)}}{\delta \theta_o} T_{n-1} - T_{x(n-1)}\frac{\delta T_{n-1}}{\delta \theta_o}}{{T_{n-1}}^2}\right)$$ Eq3.16

4) The derivation $\Delta Y_n$ by $\theta_o$, which shows in follows:

From i(=1, 2, …, n) node, the derivation of $\Delta Y_n$ by $\theta_o$ is

i=1 $$\frac{\delta \Delta Y_1}{\delta \theta_o} = \frac{\delta Y_o}{\delta \theta_o} + L \frac{\delta}{\delta \theta_o}\left(\frac{T_{yo}}{T_o}\right)$$ Eq3.17a

i=2 $$\frac{\delta \Delta Y_2}{\delta \theta_o} = \frac{\delta Y_1}{\delta \theta_o} + L \frac{\delta}{\delta \theta_o}\left(\frac{T_{y1}}{T_1}\right)$$ Eq3.17b

$$\vdots$$

i=n-1 $$\frac{\delta \Delta Y_{n-1}}{\delta \theta_o} = \frac{\delta Y_{n-2}}{\delta \theta_o} + L \frac{\delta}{\delta \theta_o}\left(\frac{T_{y(n-2)}}{T_{n-2}}\right)$$ Eq3.17c

i=n $$\frac{\delta \Delta Y_n}{\delta \theta_o} = \frac{\delta Y_{n-1}}{\delta \theta_o} + L \frac{\delta}{\delta \theta_o}\left(\frac{T_{y(n-1)}}{T_{n-1}}\right)$$ Eq3.17

where the sub-derivation $\frac{\delta}{\delta \theta_o}\left(\frac{T_{y(n-1)}}{T_{n-1}}\right)$ is also a series of calculations:

i=1 $$\frac{\delta}{\delta \theta_o}\left(\frac{T_{yo}}{T_o}\right) = \left(\frac{\frac{\delta T_{yo}}{\delta \theta_o} T_o - T_{yo} \frac{\delta T_o}{\delta \theta_o}}{{T_o}^2}\right)$$ Eq3.18a

i=2 $$\frac{\delta}{\delta \theta_o}\left(\frac{T_{y1}}{T_1}\right) = \left(\frac{\frac{\delta T_{y1}}{\delta \theta_o} T_1 - T_{y1} \frac{\delta T_1}{\delta \theta_o}}{{T_1}^2}\right)$$ Eq3.18b

$$\vdots$$

i=n $$\frac{\delta}{\delta \theta_o}\left(\frac{T_{y(n-1)}}{T_{n-1}}\right) = \left(\frac{\frac{\delta T_{y(n-1)}}{\delta \theta_o} T_{n-1} - T_{y(n-1)} \frac{\delta T_{n-1}}{\delta \theta_o}}{{T_{n-1}}^2}\right)$$ Eq3.18

Table 3.1 Corresponding expression of other terms in the sub-derivations

| Derivation No. | In the sub-derivation | |
|---|---|---|
| 1 | $\frac{\delta T_{x(n-1)}}{\delta T_o}$ | $= \frac{\delta(T_{n-2})}{\delta T_o} cos\theta_{n-2} + T_{n-2} \frac{\delta(cos\theta_{n-2})}{\delta T_o} - \frac{\delta\left(F_{x(n-2)}\right)}{\delta T_o} + p_o \frac{\delta(sin\theta_{n-2})}{\delta T_o}$ |
| 2 | $\frac{\delta T_{y(n-1)}}{\delta T_o}$ | $= \frac{\delta(T_{n-2})}{\delta T_o} sin\theta_{n-2} + T_{n-2} \frac{\delta(sin\theta_{n-2})}{\delta T_o} + \frac{\delta\left(F_{y(n-2)}\right)}{\delta T_o} - p_o \frac{\delta(cos\theta_{n-2})}{\delta T_o}$ |
| 3 | $\frac{\delta T_{x(n-1)}}{\delta \theta_o}$ | $= \frac{\delta(T_{n-2})}{\delta \theta_o} cos\theta_{n-2} + T_{n-2} \frac{\delta(cos\theta_{n-2})}{\delta \theta_o} - \frac{\delta\left(F_{x(n-2)}\right)}{\delta \theta_o} + p_o \frac{\delta(sin\theta_{n-2})}{\delta \theta_o}$ |
| 4 | $\frac{\delta T_{y(n-1)}}{\delta \theta_o}$ | $= \frac{\delta(T_{n-2})}{\delta \theta_o} sin\theta_{n-2} + T_{n-2} \frac{\delta(sin\theta_{n-2})}{\delta \theta_o} + \frac{\delta\left(F_{y(n-2)}\right)}{\delta \theta_o} - p_o \frac{\delta(cos\theta_{n-2})}{\delta \theta_o}$ |
| 1, 2* | $\frac{\delta(sin\theta_{n-2})}{\delta T_o}$ | $= cos\theta_{n-2} \left[ -\frac{1}{\sqrt{1 - \frac{T_{x(n-2)}}{T_{n-2}}^2}} \right] \frac{\delta}{\delta T_o} (\frac{T_{x(n-2)}}{T_{n-2}})$ |
| | $\frac{\delta(cos\theta_{n-2})}{\delta T_o}$ | $= -sin\theta_{n-2} \left[ -\frac{1}{\sqrt{1 - \frac{T_{x(n-2)}}{T_{n-2}}^2}} \right] \frac{\delta}{\delta T_o} (\frac{T_{x(n-2)}}{T_{n-2}})$ |

Table 3.1 continued

| | | |
|---|---|---|
| 3, 4* | $\frac{\delta(sin\theta_{n-2})}{\delta\theta_o}$ | $= cos\theta_{n-2}\left[-\frac{1}{\sqrt{1-\frac{T_{x(n-2)}}{T_{n-2}}^2}}\right]\frac{\delta}{\delta\theta_o}(\frac{T_{x(n-2)}}{T_{n-2}})$ |
| | $\frac{\delta(cos\theta_{n-2})}{\delta\theta_o}$ | $= -sin\theta_{n-2}\left[-\frac{1}{\sqrt{1-\frac{T_{x(n-2)}}{T_{n-2}}^2}}\right]\frac{\delta}{\delta\theta_o}(\frac{T_{x(n-2)}}{T_{n-2}})$ |

*In the derivation of sin $\theta$ and cos $\theta$, the angle $\theta$ has two equations that could use in the derivation, which is $\mathrm{acos}(\frac{T_{x(n-2)}}{T_{n-2}})$ and $\mathrm{asin}(\frac{T_{y(n-2)}}{T_{n-2}})$. In Table 3.1, the $\mathrm{acos}(\frac{\mathrm{T_{x(n-2)}}}{\mathrm{T_{n-2}}})$ one is chose.

The initial terms showed in Eq3.11a, Eq3.12a, Eq3.13a to Eq3.18a is simply calculated by the known values and its derivation

$$X_0, Y_0 = 0$$

$$T_0, \theta_0 = input\ value$$

$$T_{x0} = T_0 cos\theta_0$$

$$T_{y0} = T_0 sin\theta_0$$

Since the series sub-derivation computes in a value instead of formulas, the final result could be calculated by the substitution of summation that express as Eq3.12, Eq3.14, Eq3.16, and Eq3.18.

Finally, the Eq3.10 would be modified into two equations:

$$T_o' = T_o - \frac{\frac{\delta \Delta Y_n}{\delta \theta_o}\Delta X_n - \frac{\delta \Delta X_n}{\delta \theta_o}\Delta Y_n}{\frac{\delta \Delta X_n}{\delta T_o}\frac{\delta \Delta Y_n}{\delta \theta_o} - \frac{\delta \Delta X_n}{\delta \theta_o}\frac{\delta \Delta Y_n}{\delta T_o}} \qquad \text{Eq3.19}$$

$$\theta_o' = \theta_o - \frac{\frac{\delta \Delta X_n}{\delta T_o}\Delta Y_n - \frac{\delta \Delta Y_n}{\delta T_o}\Delta X_n}{\frac{\delta \Delta X_n}{\delta T_o}\frac{\delta \Delta Y_n}{\delta \theta_o} - \frac{\delta \Delta X_n}{\delta \theta_o}\frac{\delta \Delta Y_n}{\delta T_o}} \qquad \text{Eq3.20}$$

The method is repeating until the misclosure is acceptable which means $\Delta X_n$ and $\Delta Y_n$ is much close to zero or accurate to a digit of 0.0001. The effect of misclosure is then could be avoided.

# CHAPTER 4 COMPUTER PROGRAMMING PROCESS

### *4.1 Non-Linear Structural Computer Program*

The computer program is based on the theoretical assumption and numerical method discussed in chapter 2 and 3. The program was wrote by FORTRAN and it could be directly divided into serval processes as shown in follows flow charts

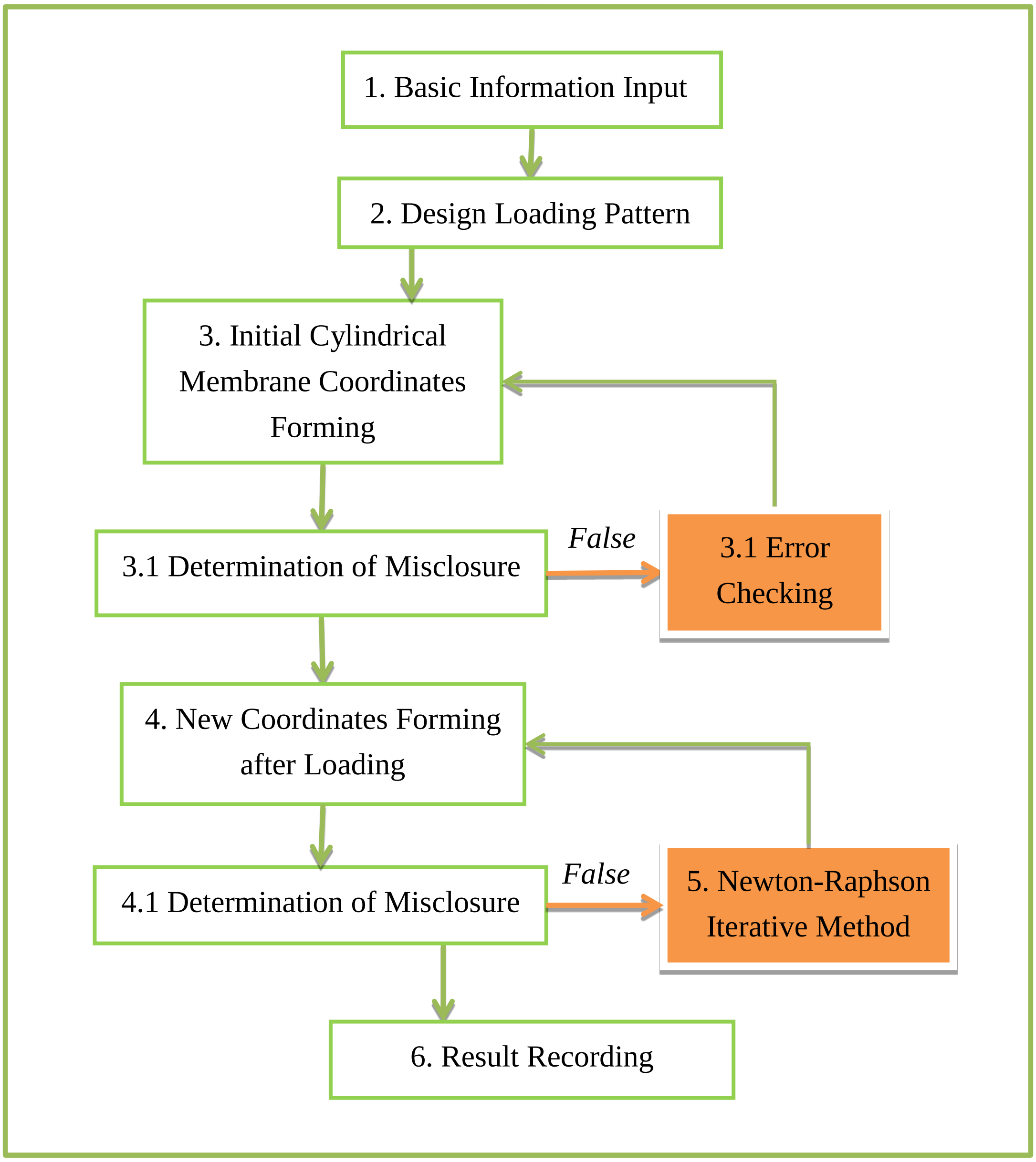


Figure 4.1 Flow chart of computer program

Figure 4.1 explained the sections during the process of computer program. The brief description of each term as shown below,

1. Basic information input

Basically the input items involve dimensions and initial stresses.

Dimensions: Two of the base width ($B$), height ($H$) and initial angle ($\theta_o$), are required to input, usually the third item could be calculated by other two knowns. The other dimensions such as radius of curvature (a), arc length ($\ell$) and Equal length ($L$) of original inflated membrane at each node, which also could be determined in this process.

Initial stress: Internal pressure ($p_o$) and weight of membrane ($Wg$) are input at the beginning. In the chapter 2, the assumption of a weightless membrane was made since it might be acceptable to ignore it. However, the weight of membrane still exists in the reality and it might be needed to consider. Thus, the weight of membrane remains its variability for a reasonable analysis.

In general, the initial angle ($\theta_o$) is selected according to the similar value in the past literatures and the initial tension ($T_o$) is the function of internal pressure and radius of curvature (Eq2.4). The recommendation of internal pressure will discuss in Section 5.1, Chapter 5. The radius of curvature could be calculated in the geometry once the initial angle is inputted.

2. Design loading pattern

Design loading pattern is another part of input. The magnitude, direction and location of design loading should be determined in this section. The location is defined as the coordinates where the node numbers exists, therefore, the behaviors of each node can be showed by acting the loading on the node system. For the wind load and internal pressure, which applied on the circumferential direction as the distributed load, the angles with the horizontal axis will be calculated in the section 4 below. The loading patterns would have detail discussion in Chapter 5.

3. Initial Cylindrical Membrane Coordinates Forming

Original cylindrical membrane model is simply created by the inputs in section 1 and then an initial node system could be formed. The misclosure would be acceptable to three significant digits that compared with the initial dimensions.

4. New Coordinates Forming after Loading

In this section, the design loading is taken into consideration on forming the new node coordinate system. An appropriate value of $X_n$ and $Y_n$ usually do not come up at the first time of new coordinate forming since the initial tension is an approximate value for prediction. Thus, the Newton-Raphson method always performs after the first run.

5. Newton-Raphson Iterative Method

The principle of Newton-Raphson iterative method is to find out the approximation of internal tension and initial angle in which the cylindrical membrane behaves reasonably to have a negligible misclosure.

6. Result Recording

By comparing the results of original and new coordinate, the displacement can be determined at each node.

In the computer program, the computing formulas are same as the Eq3.1 to 3.20. But a problem of domain occurred in the determination of the degree $\theta_i$ by the inverse of cosine, sine in the section 4. The issue mainly focuses on the definition of domain for obtaining reasonable degree in terms of inflated cylindrical membrane behaviours. Thus, the problem could be solved from the predetermination of value $T_{xi}$, and $T_{yi}$, and then defining the domain whether it is compatible to the inverse of cosine or sine and finally return a reasonable degree. This numerical method of computer program will finish when the misclosure and results are obtained properly. To define how a result is correct, the comparison will make in chapter 5.

For determining the number of node, the typical load pattern such as concentrated load acting centrally on the cylindrical membrane is selected to compare with the theoretical result by using some of the critical data points in Figure 2.2.2. Moreover, the accuracy of computer program would be discussed by the comparison of present study and the result of Turkkan and Srivastava (1992).

# CHAPTER 5 CYLINDRICAL MEMBRANE MODEL

In the cylindrical membrane model, the membrane is made of the inextensible material, and assumed to be circle shape which is inflated by internal air and anchor on the ground with two end supports. For the long cylindrical membrane, only 2D frame will be considered in the model (Figure 5.1).

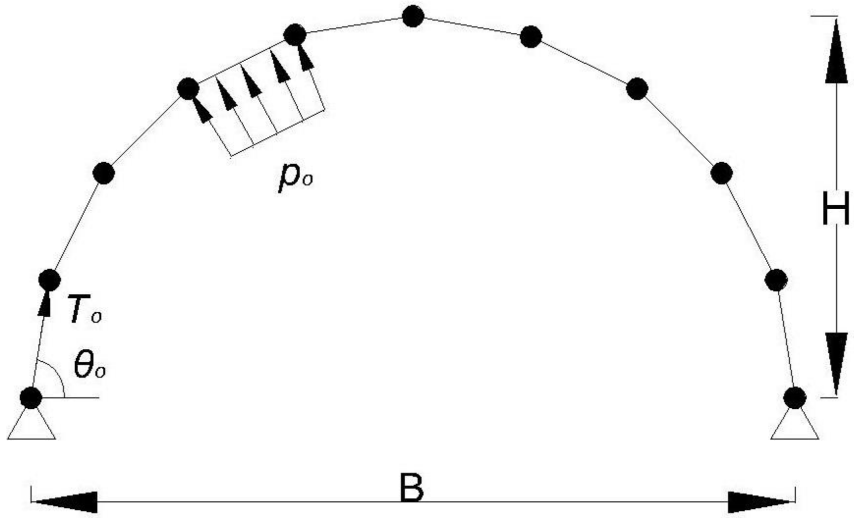


Figure 5.1 Notations of membrane model

The number of bar elements affects the accuracy of model. To determine the number, preliminary analysis is necessary to check the most precise result with a particular number of bar elements (Table 5.1).

Table 5.1 Comparison of number of bar elements on the typical case in chapter 2 with initial angle of 90 degree

| Number of elements | 100 | 200 | 400 | 1000 |
|---|---|---|---|---|
| $\bar{k}$ | Percentage difference of $\bar{\Delta}_v$ ($\frac{\bar{\Delta}_v - \bar{\Delta}_v{}'}{\bar{\Delta}_v} * 100\%$) | | | |
| 0.25 | 75.28% | 87.363% | 93.579% | 97.583% |
| 0.5 | 89.96% | 95.001% | 97.385% | 98.986% |
| 0.75 | 94.90% | 97.621% | 98.534% | 99.463% |
| 1.25 | 99.56% | 99.872% | 99.826% | 99.918% |
| 1.5 | 99.97% | 99.836% | 99.976% | 99.926% |
| 1.75 | 99.49% | 99.637% | 99.792% | 99.928% |
| 2 | 99.50% | 99.613% | 99.832% | 99.907% |
| Average | **94.093%** | **96.992%** | **98.418%** | **99.387%** |
| Standard Deviation | 21.890% | 11.117% | 5.645% | 2.101% |

In the Table 5.1, the comparison of theoretical and experimental result is made by the difference of percentage in two results on the same situation of dimensionless loading parameters ($\bar{k}$ = 0.25, 0.5, 0.75, 1.25, 1.5, 1.75 and 2). The reason of omitting $\bar{k}$ = 1 is because a series of $\bar{\Delta}_v$ exists within $\bar{k}$ = 1 which was showed on the curve of 90 degree (Figure 2.2.2). It involves the uncertainty in the comparison which may make an error in deciding the number of elements since the computer program only provides a result of $\bar{\Delta}_v$ corresponding to a $\bar{k}$.

The average percentage on four numbers of elements was indicated that there were 99.387±2.101(%) for 1000 nodes of membrane. Even though a higher number of nodes would give more accuracy, but in terms of rapid convergence of misclosure, the 1000 nodes was fast enough to perform at least an average accuracy of 97.286% that was acceptable to avoid the error from the computation of numerical equations under the assumption of model. By using 1000 nodes, the result can be calculated within a second; otherwise higher number of nodes might need additional time. Furthermore, 1000 nodes of cylindrical membrane have almost 99.99% of arc length similar to the arc length of half circle.

### *5.1 Design Loads*

1. Internal Pressure

An internal pressure is necessary to maintain the stability and stiffness of inflated cylindrical membrane which subjected to the loadings. The particular magnitude of internal pressure is decided by the consideration of initial geometry, anchor force and different loading patterns.

As the research in Turkkan and Srivastava (1992) that mentioned the CSA standard (1981), the minimum internal pressure $p_o$ equals or greater of

$$p_o = 0.38kPa\ (38mm\ water) \qquad \text{Eq5.1}$$

It also suggested that a pressure of 20 to 100 mm of water gauge was commonly used in the practice of air-supported structure. Therefore, the internal design pressure will base on the suggestions and actual behaviour of membrane to set up the value.

2. Wind Load

The common type of loading pattern is wind load which around an exposed membrane structure. As the flexibility of membrane, it will be a degree of instability under the effect of wind load pattern. Basically, the wind load acting on the side of membrane structure has a nonlinear behavior which causing displacement under the tensile and compressive stress (Figure 5.1.1).

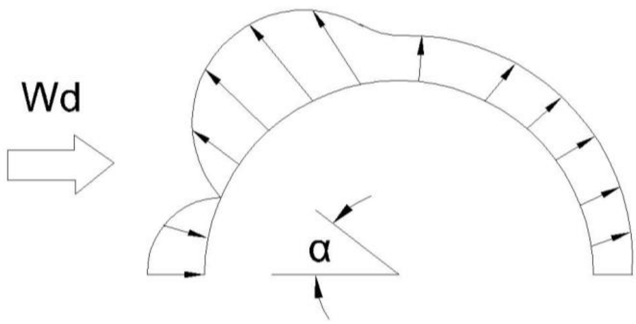


Figure 5.1.1 wind load pattern

According to IASS (1985) and CSA (1981), the equivalent static wind pressure as shown in follows

$$W_d = C_p q' \qquad \text{Eq5.2}$$

where $q'$ is dynamic wind pressure( $q' = \frac{1}{2}\rho v^2$ ), $\rho$ is density of air, $v$ is approximate wind speed and the coefficient of wind pressure $C_p$ is a function of internal pressure, dynamic wind pressure and the angle $\alpha$ which defined in Figure 5.1.1

$$C_p = 0.8^{p_o/q'}(-0.7 + 0.3cos\alpha + cos2\alpha + 0.4cos3\alpha - 0.1cos4\alpha) \qquad \text{Eq5.3}$$

The determination of $C_p$ was found by the researchers (Srivastava *et al.* 1985a, 1985b) who performed the wind tunnel tests on cylindrical membranes. The equation 5.3 behaves similar to the wind load perpendicular to the structure and it was proved by the laboratory experiments as a close approximation.

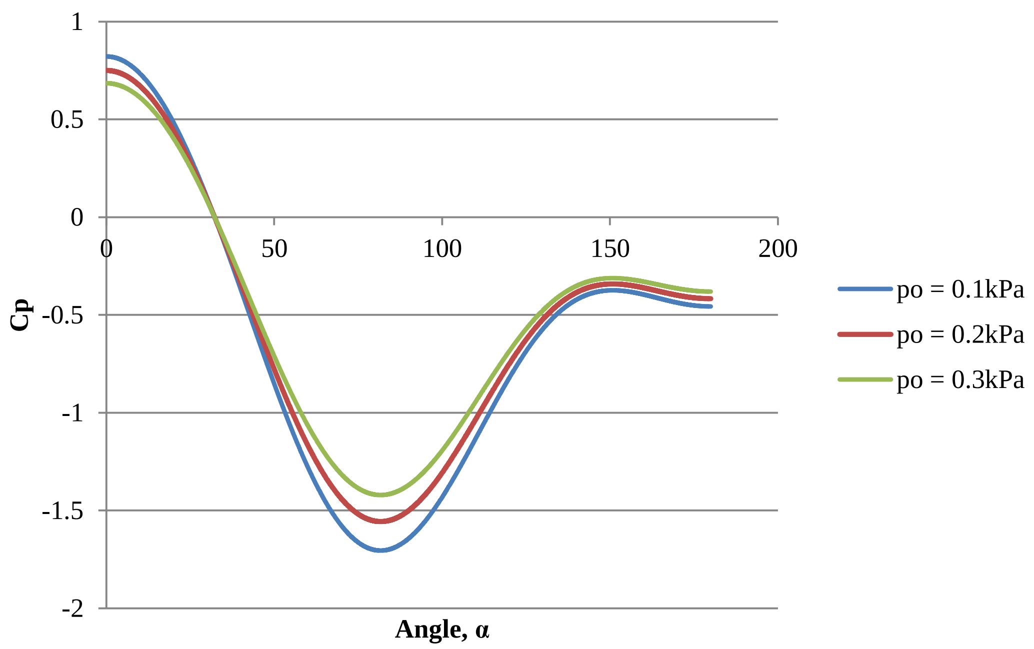


Figure 5.1.2 Distribution of coefficient of wind load with $v$ = 20 m/s

Since the angle should be the range from 0 to 180 degrees, the curve of $C_p$ distribution (Figure 5.3) is mainly determined by the ratio of $p_o/q'$ which suggested and referred from the research in Turkkan and Srivastava (1992).

In the wind speed of 20 m/s, the $q'$ is a constant value which approximately equals to 0.245 kPa when the air density of 1.225 kg/m$^3$ is used (at the sea level and at 15℃). The behaviour is showed on Figure 5.3 which the portion of positive $C_p$ means one side of the cylindrical membrane which the wind pressure is directly applied, is principally subjected to compressive stress from the wind pressure. On the contrary, the negative $C_p$ represents the behaviour of tensile stress on another side of membrane which does not directly resist the wind pressure.

The instability of membrane would happen when the decrease of $p_o$ and the increase of $C_p$ caused the increase of difference in external compressive and tensile stress, in the front and back side respectively. In this situation, the superposition of two stresses causes the deformed membrane structure in three main portions which is an unstable behaviour should be considered in the analysis. Thus, for the analysis, a reasonable ratio will be selected referring to the curve of $C_p$ in Figure 5.3.

3. Snow Load

According to the research in Turkkan and Srivastava (1992) that recommended in Canadian standard (CSA(1981)), the German standard and international recommendation (IASS(1985)), full snow load or half snow load distribution (Figure 5.1.3) will be included in the loading pattern for the numerical analysis.

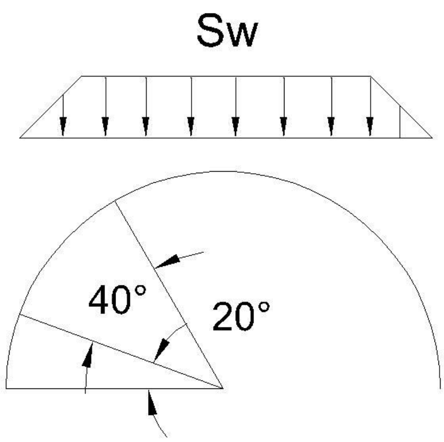


Figure 5.1.3 snow load pattern

Figure 5.1.3 indicates the snow load pattern that formed on the membrane. The snow load have a triangular distribution in the two side is because the snow load will collapse on the position. Thus, the research suggested that the triangular distribution starts from the angle of 20 degree to 60 degree and same as the other side.

4. Concentrated Load

For the concentrated load, it is a kind of accidental loading case which the snow or water may accumulate on the top of cylindrical membrane due to displacement. The ponding is usually around the center of top where the static condition exists and it may further concentrate on the center after the ponding force was increased. Thus, the concentrated load is assumed to be applied centrally.

### *5.2 Comparison of Present Study and the Past Research*

To explain cylindrical membrane model, some of the typical loading cases would be performed on the program. Moreover, the comparison of present study and the results done by Turkkan and Srivastava (1992) will carry out later in order to check the accuracy or reasonable error. The relevant loading combination, geometry and initial pressure of each typical case are listed on the following tables,

| **Typical case 1–Wind Load, wind speed = 20 m/s** |
|---|
| Geometry: Height = 10m, Span = 20m, Initial angle = 90°;<br>Initial pressure: Internal pressure = 0.1 kPa, Weight = 0, |

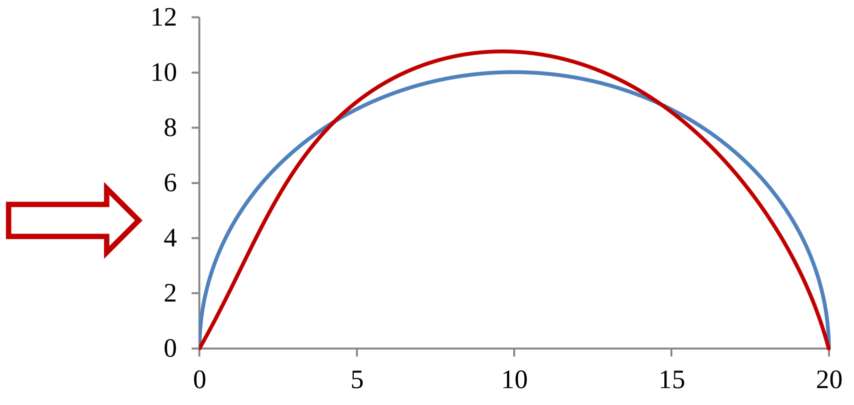


Figure 5.2.1 Graphical result of membrane subjected to wind load

**Typical case 2– Full Snow Load = 0.35kPa**

Geometry: Height = 10m, Span = 25m, Initial angle = 77°;

Initial pressure: Internal pressure = 0.3 kPa, Weight = 0,

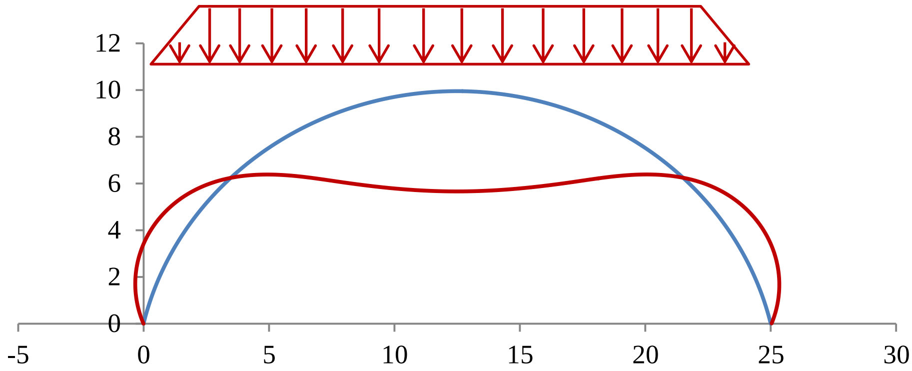


Figure 5.2.2 Graphical result of membrane subjected to full snow load

**Typical case 3– Half Snow Load = 0.3kPa**

Geometry: Height = 10m, Span = 18m, Initial angle = 96°;

Initial pressure: Internal pressure = 0.3 kPa, Weight = 0,

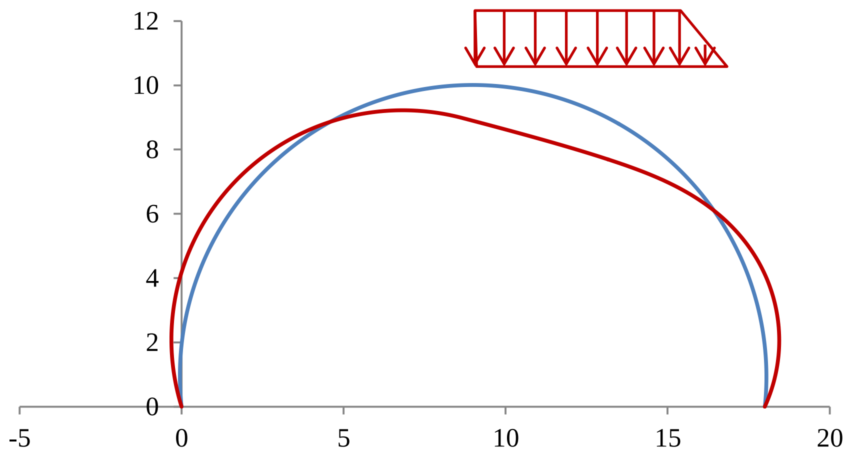


Figure 5.2.3 Graphical result of membrane subjected to half snow load

| **Typical case 4– Concentrated Load = 1 kN** |
| --- |
| Geometry: Height = 5m, Span = 10m, Initial angle = 90°;<br><br>Initial pressure: Internal pressure = 0.3 kPa, Weight = 0, |
| 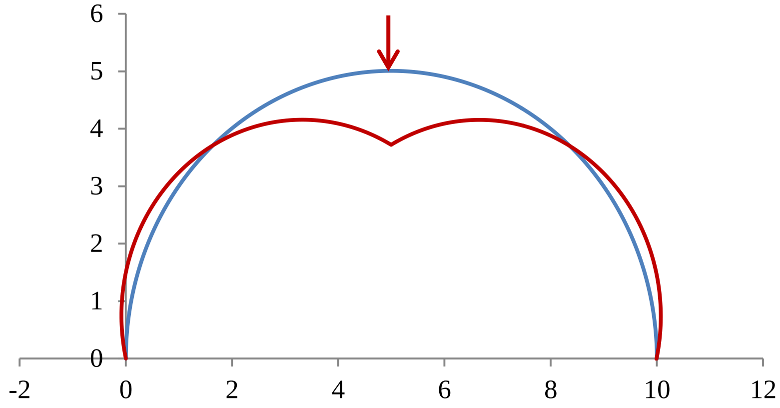<br>Figure 5.2.4 Graphical result of membrane subjected to concentrated load |

| **Typical case 5 –Wind Load (wind speed=15 m/s) + Half Snow Load=0.3kPa** |
| --- |
| Geometry: Height = 12m, Span = 25m, Initial angle = 88°;<br><br>Initial pressure: Internal pressure = 0.2 kPa, Weight = 0, |
| 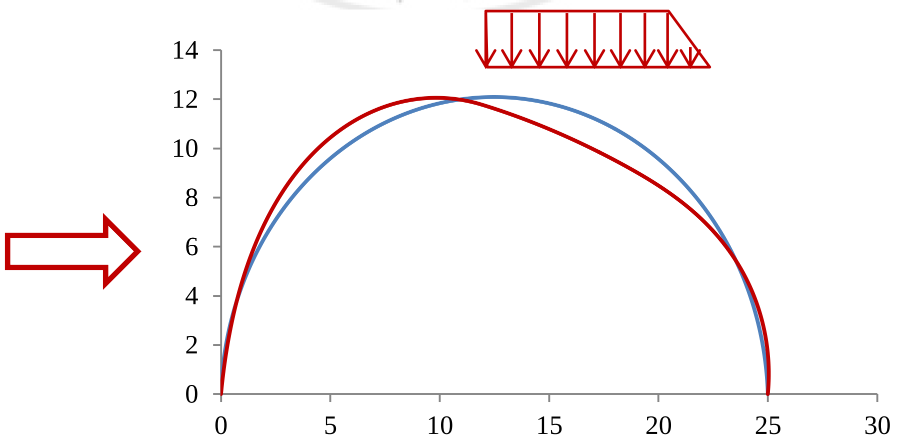<br>Figure 5.2.5 Graphical result of membrane subjected to wind load and half snow load |

**Typical case 6 –Wind Load (wind speed = 20 m/s) + Concentrated Load = 5kN**

Geometry: Height = 6m, Span = 20m, Initial angle = 62°;

Initial pressure: Internal pressure = 0.2 kPa, Weight = 0,

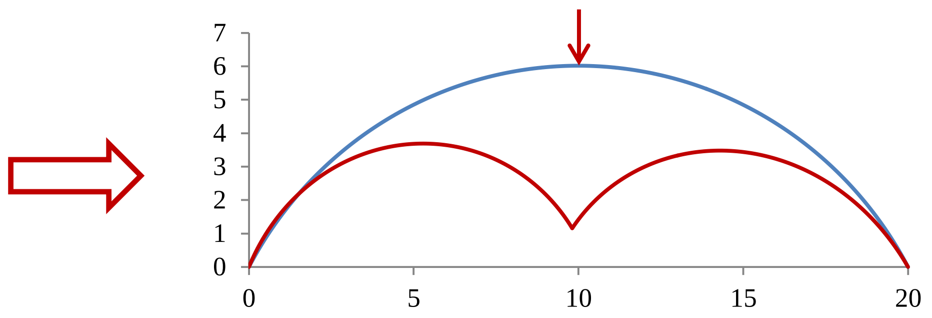


Figure 5.2.6 Graphical result of membrane subjected to wind load and concentrated load

Table 5.2.1 Result of present study and the Turkkan and Srivastava (1992) (T&S) in different typical loading cases

| | Present Study | T&S | Present Study | T&S |
|---|---|---|---|---|
| Loading Cases: | Wind Load | | Full Snow Load | |
| $T_{max}$ (kN/m) | 3.74 | 3.79 | 2.38 | 1.54 |
| $d_{max}$ (m) | 1.07 | 1.06 | 4.66 | 3.97 |
| AncF (kN/m) | 3.74 | 3.79 | 1.47 | 1.42 |
| $Anc\theta$ ° | 61.18 | 61.38 | 114.86 | 109.13 |

| Loading Cases: | Half Snow Load | | Concentrated Load | |
|---|---|---|---|---|
| $T_{max}$ (kN/m) | 2.40 | 2.22 | 1.34 | 1.31 |
| $d_{max}$ (m) | 1.51 | 1.71 | 1.23 | 1.23 |
| AncF (kN/m) | 2.21 | 2.22 | 1.03 | 1.02 |
| Anc$\theta$ ° | 107.64 | 110.15 | 104.56 | 101.45 |
| Loading Cases: | Wind Load + Half Snow Load | | Wind Load +Concentrated Load | |
| $T_{max}$ (kN/m) | 3.08 | 3.00 | 4.01 | 3.94 |
| $d_{max}$ (m) | 1.44 | 1.68 | 3.60 | 3.48 |
| AncF (kN/m) | 2.96 | 2.90 | 2.06 | 2.12 |
| Anc$\theta$ ° | 83.55 | 84.75 | 68.90 | 67.34 |

In the Table 5.2.1, $T_{max}$ = maximum tension, $d_{max}$ = maximum displacement, AncF = Anchor Force (first tension) and Anc$\theta$ = deflected Anchor angle (deflected angle)

The behavior of maximum tension is predicted by the anchor force. Thus, the comparison would only discuss with AncF, $d_{max}$ and Anc$\theta$ which is made by the difference of two results (Present study – T&S) in the following Table 5.2.2 and 5.2.3.

Table 5.2.2 Comparison summary of present study and Turkkan and Srivastava (1992)

| Loading Cases: | Wind Load | Concentrated Load | Wind Load + Concentrated Load |
|---|---|---|---|
| $\Delta d_{max}$ (m) | **0.01** | **0** | **0.12** |
| ΔAncF (kN/m) | **-0.05** | **0.01** | **-0.06** |
| $\Delta Anc\theta^{\circ}$ | **-0.2** | **3.11** | **1.56** |

As the results compared in the Table 5.2.2, the cases of wind load, concentrated load and its combination showed the behaviour of the anchor force is proportional to the displacement. For a simple loading such as concentrated load, it is apparent to explain the tendency that if a membrane has less displacement, the radius of each circle in Figure 2.1.1 would be less also under a constant of internal pressure. Thus, the internal tension should be less in consistency of Eq2.4 or 2.5. For a wind load, the behaviour could be referred to the curve of $C_p$ in Figure 5.1.2. Since the internal pressure is proportional to initial tension (Eq2.4, 2.5), similarly to the anchor force or first tension, the relation of internal pressure and $C_p$ was practically available for that of anchor force and $C_p$. As a result, the less anchor force on the supports, the more displacement is made by the increase of external compressive and tensile stress from the wind pressure. The combination of these two cases is explicitly a development of the behavior which the wind load is leading loads and the concentrated load is accompanying. Then, the behavior of the combination will follow the wind load cases.

Table 5.2.3 Comparison summary of present study and Turkkan and Srivastava (1992)

| Loading Cases: | Full Snow Load | Half Snow Load | Wind Load + Half Snow Load |
|---|---|---|---|
| $\Delta d_{max}$ (m) | **0.69** | **-0.2** | **-0.24** |
| ΔAncF (kN/m) | **0.05** | **-0.01** | **0.06** |
| $\Delta Anc\theta^{\circ}$ | **5.73** | **-2.51** | **-1.2** |

For the cases of full snow load, half snow load and combination of wind load and half snow load in Table 5.2.3 which are either a snow load pattern or incorporated with it, the behaviour is similar to the concentrated loading case. The snow load pattern (Figure 5.1.3) is a pressure distribution which made the membrane structure subjected to the external compressive stress on the upper part and that is similar to apply a distribution of concentrated load. The behavior should be consistent with the concentrated loading cases which the displacement and anchor force will increase when a higher snow load is applied. In the combination of wind load and half snow load, the observation tells the similarity compared with the combination of wind load and concentrated. In general, based on the discussion above, the results of these three cases have showed the consistency.

In the summary of accuracy check, firstly, the Anc$\theta$ is a little acceptable since $\Delta$Anc$\theta$ is within 6 degree of difference and the anticipation of deformed cylindrical membrane behaves normally as the graphical result in Figure 5.2.1-5.2.6.

Secondly, the AncF is reasonable within a small of deviation of $\pm 0.06$. On the other hand, $d_{max}$ might have some error in the loading cases in the loading cases that involve the snow load, but the overall tendency of typical cases is well acceptable for the analysis of behaviours.

The comparisons are just a preliminary analysis of the accuracy of modeling, the further discussion would continue in the chapter 6.

### *5.3 Limitation*

As mentioned in chapter 2, the accuracy of program has a limit that it is difficult to provide further precision in the misclosure. Some of the reason may be because of the assumptions. To use the node equilibrium, the distributed load needed to be divided into two components on the principle axis. The continuous behaviours occurred in the cylindrical membrane might not be ideally matched to the reality, and thus the misclosure will exist and increase during the iteration. The accumulation of misclosure is why the accuracy is hard to develop further up to four or higher significant digits.

# CHAPTER6 ANALYSIS

### *6.1 Cylindrical Membrane under Single Loading Cases*

The single loading cases such as concentrated load, wind load, full and half snow load will be presented in this chapter.

#### *6.1.1 Concentrated Loads*

For a cylindrical membrane structure subjected to concentrated load, the theory mentioned in chapter 2 had explained that the shape would form two circular arc in symmetrical. The behaviour of deformed shape has shown below with the increase of dimensionless loading parameter $(\bar{k} = 0.5, 1, 1.5, 2)$. The basic information is initial angle = 90°, height = 5 m and internal pressure = 0.1kPa.



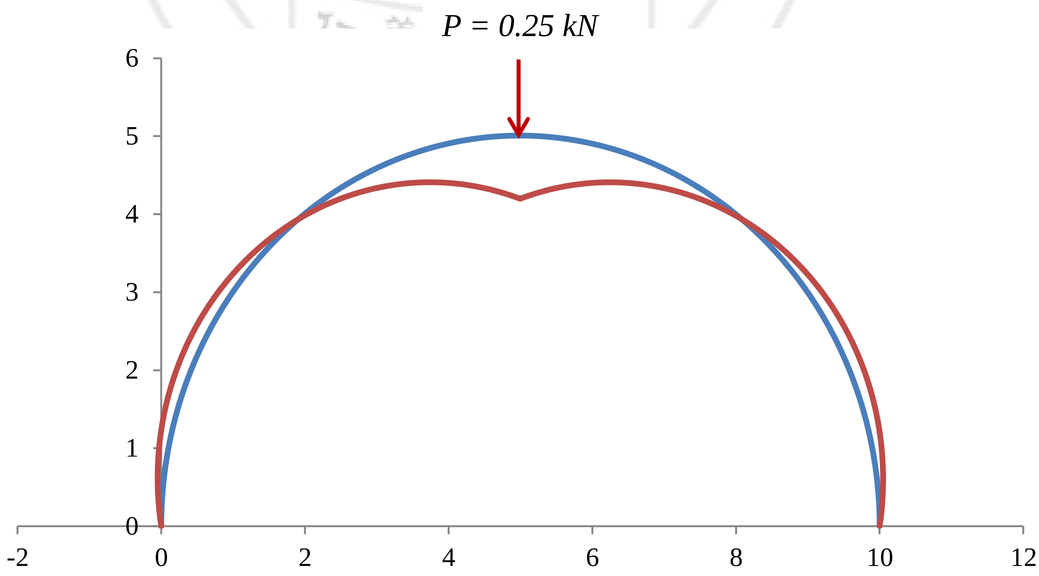


Figure 6.1.1 Symmetrical displacement of cylindrical membrane, $\bar{k} = 0.5$

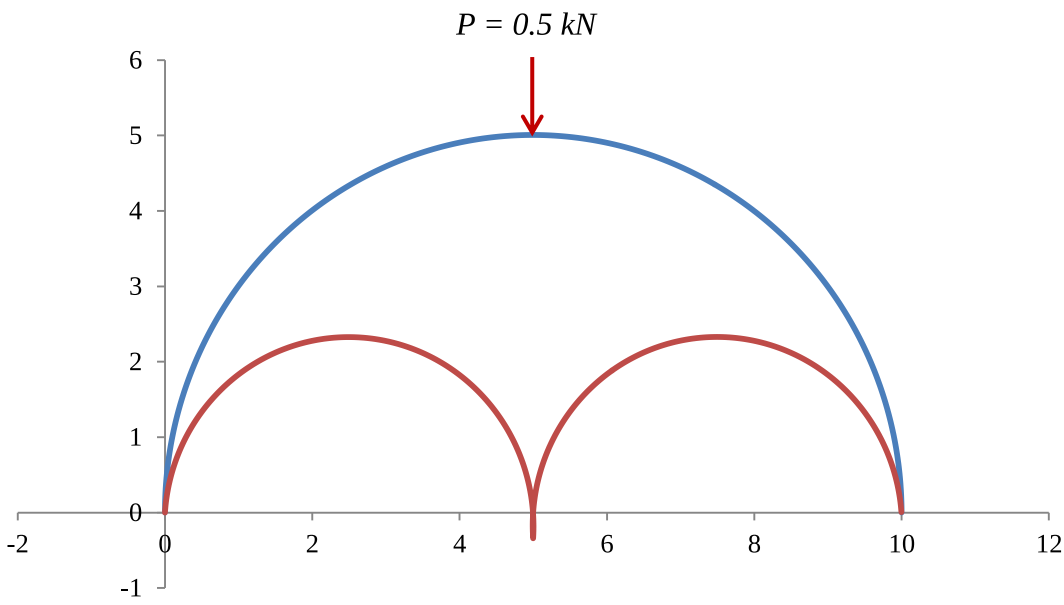


Figure 6.1.2 Symmetrical displacement of cylindrical membrane, $\bar{k} = 1$

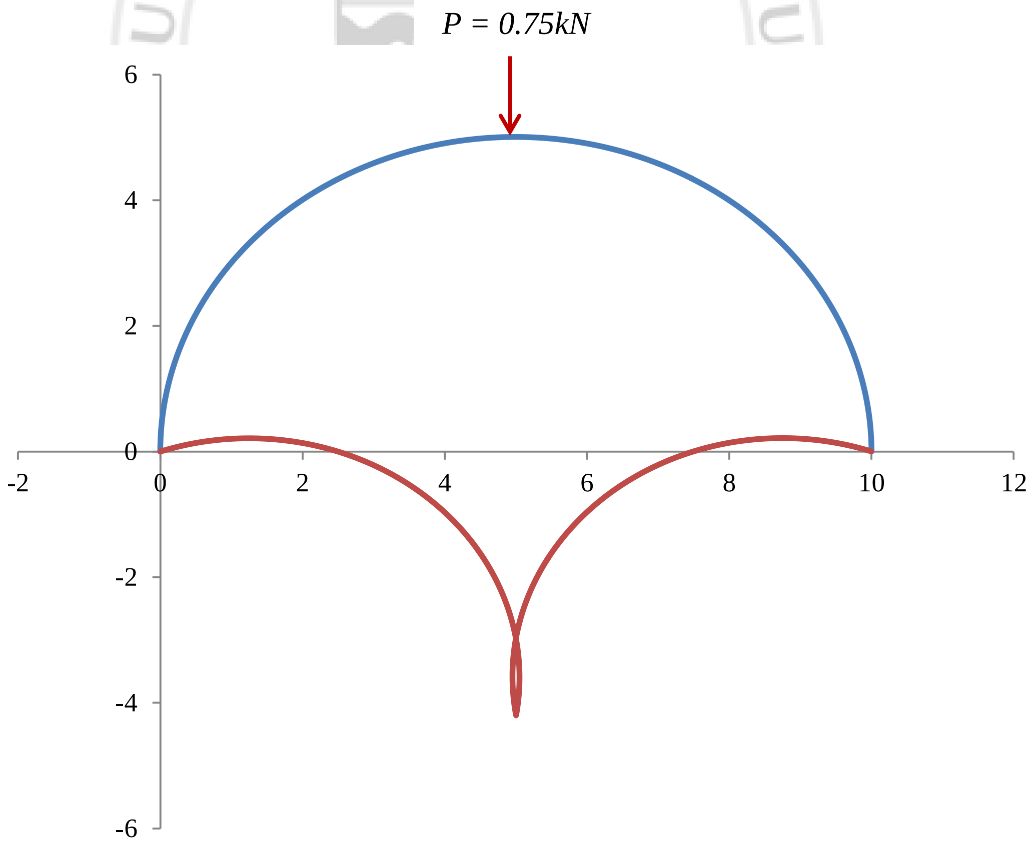


Figure 6.1.3 Symmetrical displacement of cylindrical membrane, $\bar{k} = 1.5$

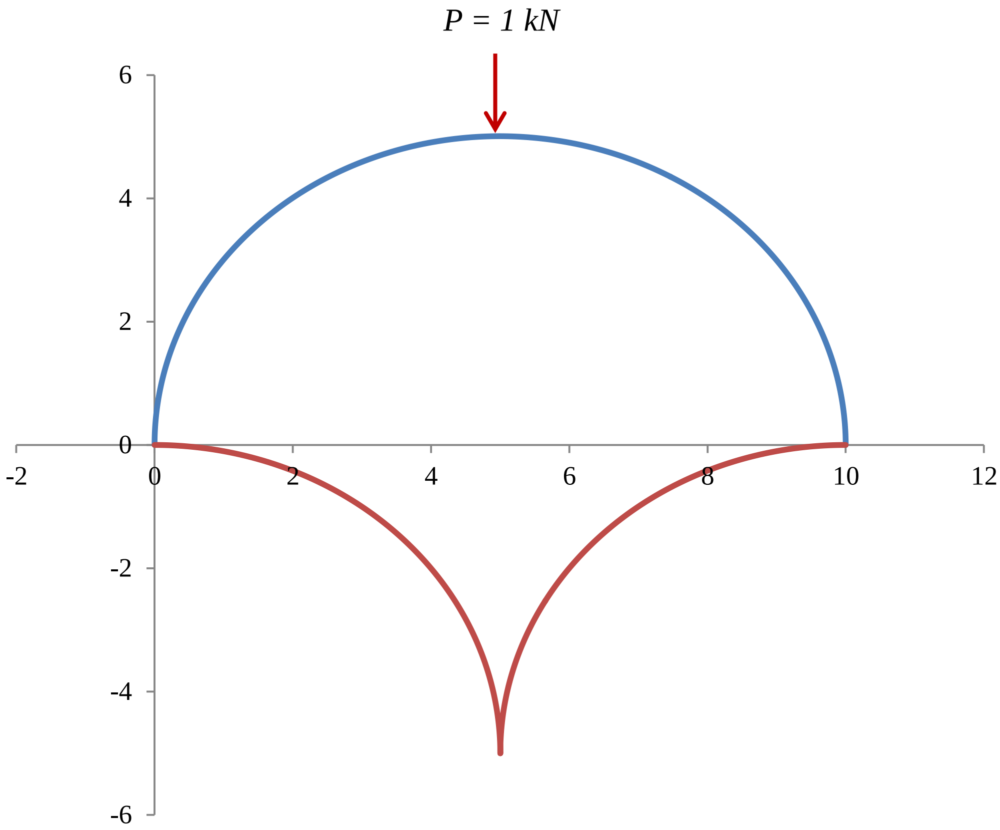


Figure 6.1.4 Symmetrical displacement of cylindrical membrane, $\bar{k} = 2$

In the first figure $\bar{k} = 0.5$ above, the displacement is still acceptable to maintain the stability. By the increase of loading up to $\bar{k} = 1$, the magnitude of displacement is over its original height that means most of the space is occupied and the structural stability probably reaches the limit state. While the $\bar{k} = 1.5$, the entire structure is failed. In the Figure 6.1.3, the behaviour is physically impossible in the real structure since the membrane has overlapped to each portion. The similar behaviour is expressed in Figure 6.1.4 without overlapping. This situation exists only if an underground space had built under the supports of membrane and at least same height as membrane. But it is a rare case.

In the reality, the deformation will stop in $\bar{k} = 0.5$ since the membrane is commonly built on the ground without underground space. Thus, the behaviour of cylindrical membrane structure may likely to have a limit state in Figure 6.1.2.

Under the concentrated load, the characteristics can be summarized as the membrane can have a certain level of stability with large displacement but the occupied space should be taken into account whether it is available for the activities inside the structure. Hence, the different geometry ratio will be decided for the further analysis of subjecting to concentrated load.

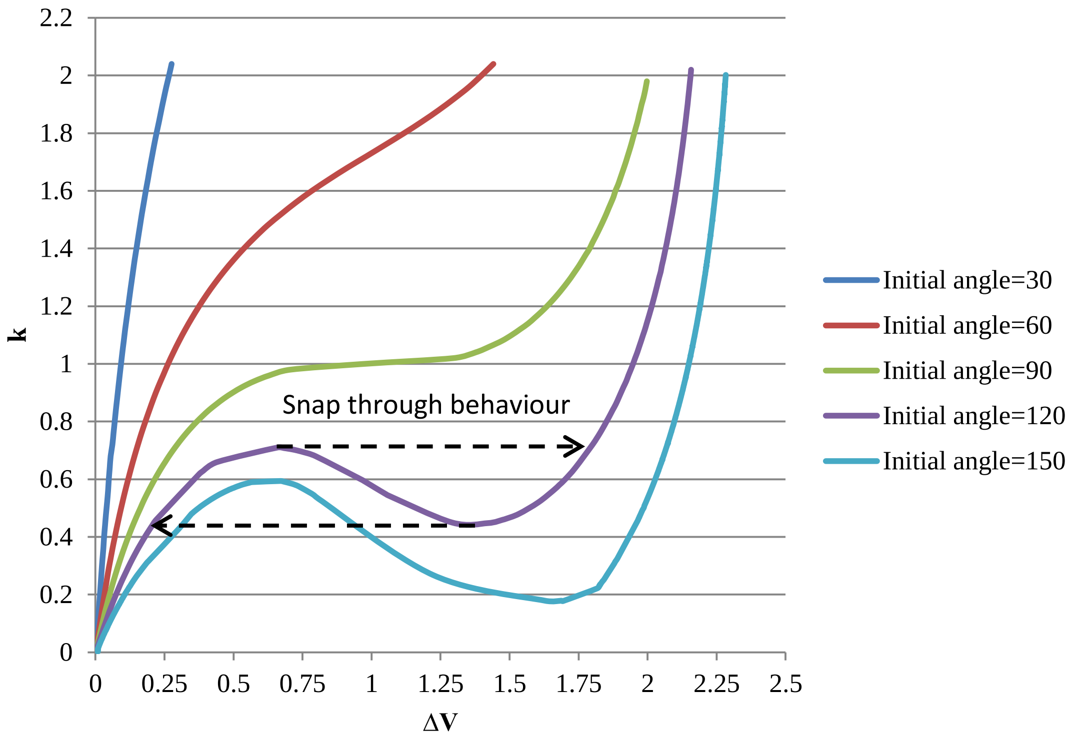


Figure 6.1.5 Relation of loading parameter and vertical displacement factor

Figure 6.1.5 describes the behaviour of cylindrical membrane subjected to concentrated load in different initial angle.

Firstly, the positive slopes represent a proportional relation between the loading and displacement that correspond to stable equilibrium. In the curve of initial angle of 30 degree, it is an approximate linear relation, which has only a displacement less than 0.5 of its original height with the loading parameter $\bar{k}$ of 2. That means a 30-degree cylindrical membrane is able to resist most of the stress from the loading. In this case, it makes the structure with a considerable stability.

When the initial angle increases to 60 degree, the linear range will narrow down and the turning point is about $\bar{k} = 0.8$ which the structure can provide less displacement within about 0.25 of its original height. But the displacement will enhance gradually with the increase of loading after $\bar{k} = 0.8$. In the initial angle of 90 degree, or like a semi-circle, there is a range of zero slopes that the displacement keeps raising without the change of force. Then, the stability will no longer exist.

For the initial angle within 90 degree, in terms of displacement, the smaller initial angle will provide a better behaviour of subjecting to concentrated load. In addition, the force should be controlled within $\bar{k} = 0.6$ or 0.8 for 60 and 90 degree respectively in order to prevent a further development of displacement.

Secondly, at the limit point or zero slopes, the structures will snapthrough to an unstable position when further loaded or to opposite direction when unloaded which is noted in Figure 6.1.5 Basically the behaviour is related to the properties of membrane material such as structural fabric if a statically unstable condition is created by a large concentrated load, the structure is possible to have large displacement in positive or reverse direction.

Thirdly, the negative slopes represent the unstable configuration that the membrane is overlapped, or pass through the two ends that showed similarly in Figure 6.1.3. Although the situation does not exist physically, the mathematical calculation is able to find it out. Thus, for the initial angle greater than 90 degree, the cylindrical membrane has the limit state before the large displacement happened.

In conclusion of concentrated load, the cylindrical membrane structure will has a better condition to perform the structural stability when it is a smaller initial angle. But it usually needs a large place to maintain the structure of a small initial angle, thus, an initial angle of 90 degree may be able to accomplish the requirement in a limited area. Nevertheless, different initial angle can have an acceptable displacement if the loading is predictable. The concentrated loading case is just an accidental loading case and usually the combination of different loading cases will be more reliable.

*6.1.2 Full Snow Loads*

In the full snow loads, a distributed load on the top of membrane, when the load increases (Snow load=0.2, 0.3, 0.4 and 0.5 kPa), the series behaviour will express as below. The basic information is initial angle = 90˚, height = 10 m and internal pressure = 0.3kPa.

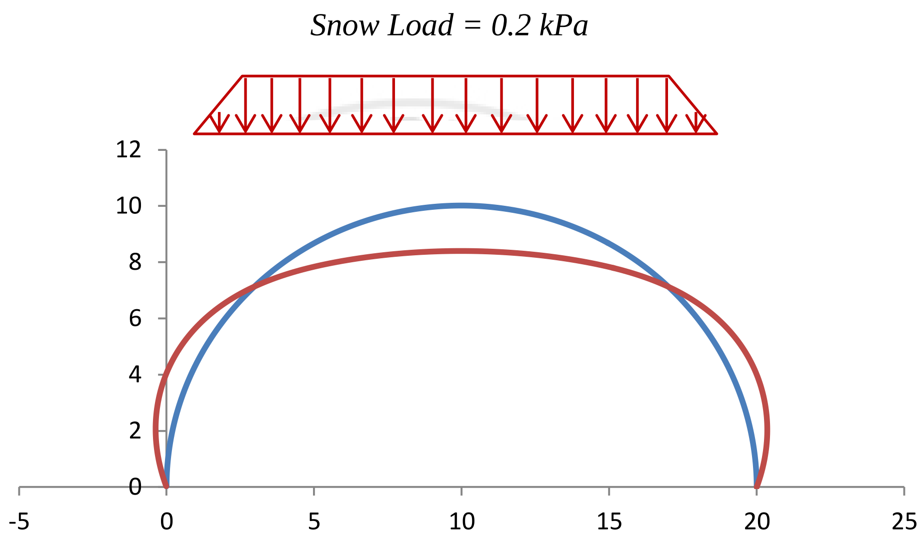


Figure 6.1.6 Deformed cylindrical membrane under a full snow loads = 0.2kPa

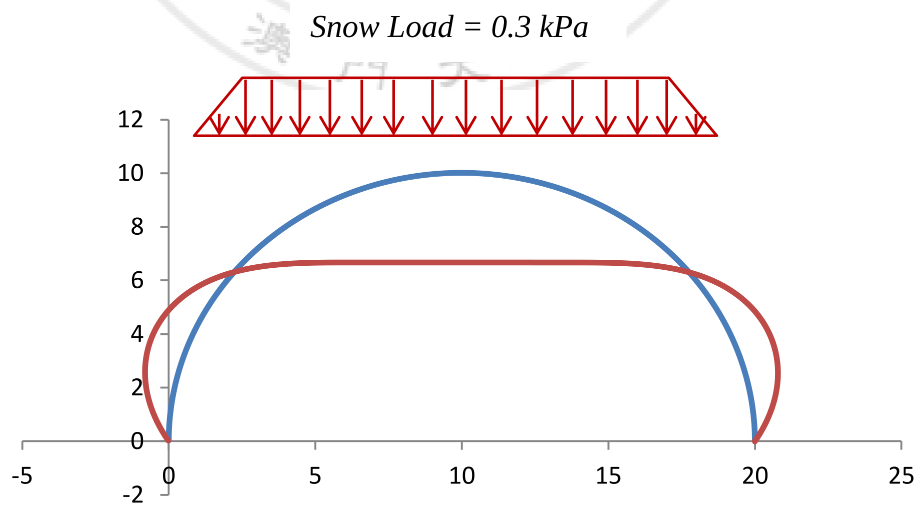


Figure 6.1.7 Deformed cylindrical membrane under a full snow loads = 0.3kPa

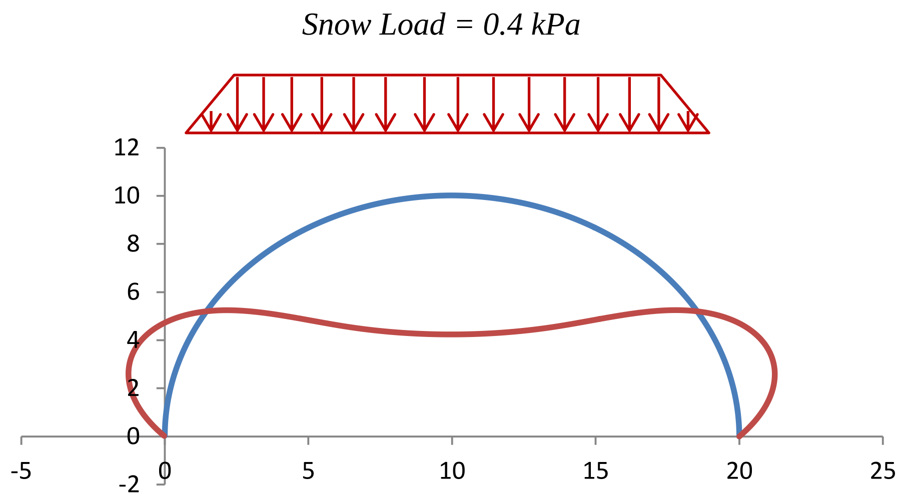


Figure 6.1.8 Deformed cylindrical membrane under a full snow loads = 0.4kPa

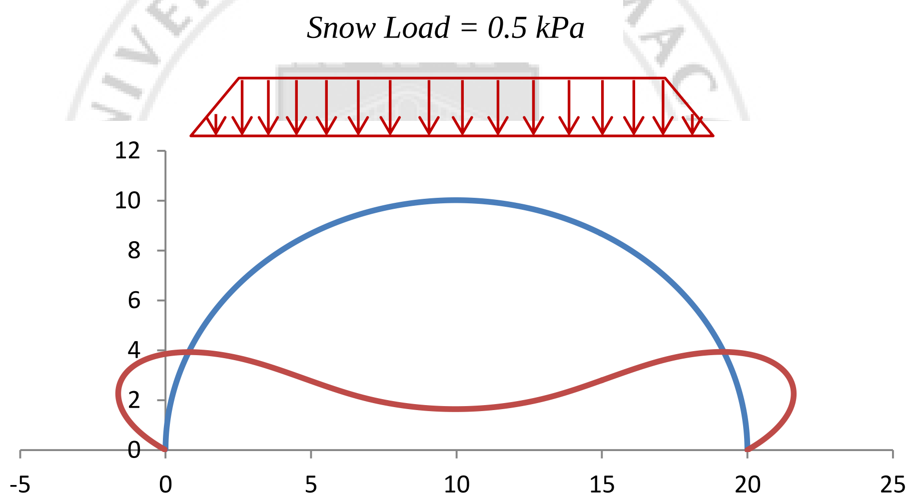


Figure 6.1.9 Deformed cylindrical membrane under a full snow loads = 0.5kPa

In the Figure 6.1.6 to 6.1.9, the full snow load concentrates on the upper and middle part of membrane and creates the entire movement in the direction of snow load.

In the snow load equals to 0.3kPa, the upper part of membrane is likely to form a horizontal roof where is mainly subjected to compressive stress and the left and right portions will be subjected to the tensile stress. The leading compression and accompanying tension are not an appropriate loading distribution for the cylindrical membrane structure. Thus, while the snow load increases to 0.4kPa, the tensile portions will reduce that means the membrane cannot resist the compression to keep stability.

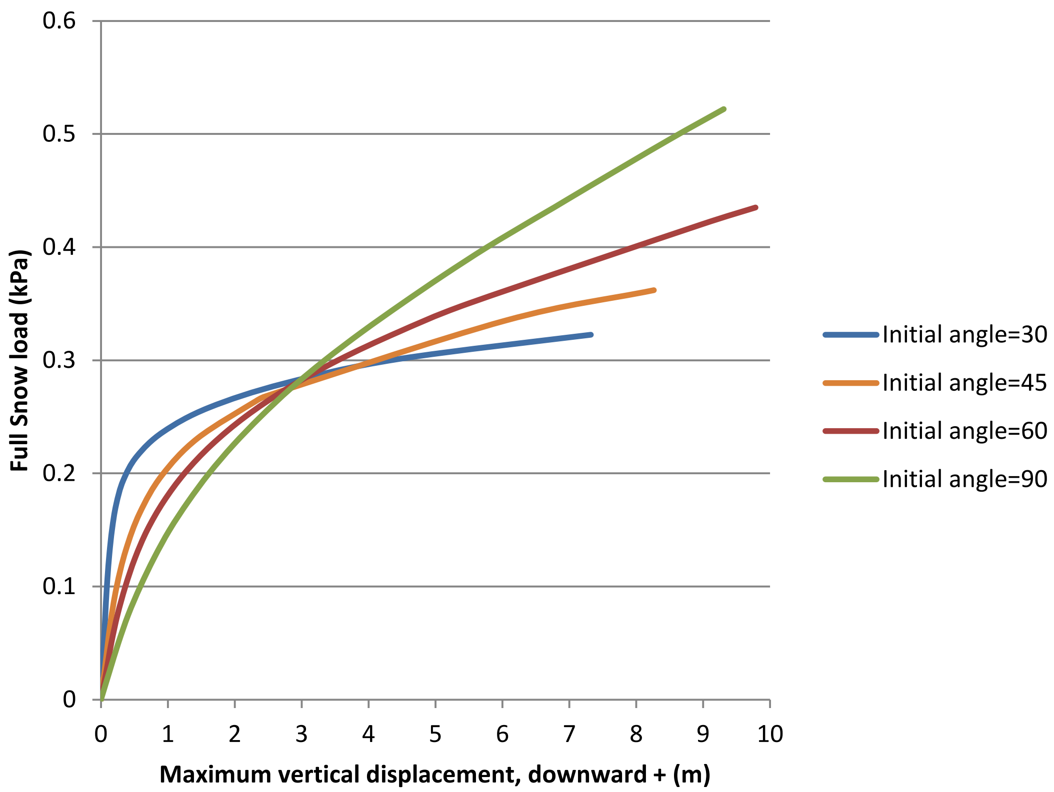


Figure 6.1.10 Relation of snow load and maximum vertical displacement for initial angle within 90 degree

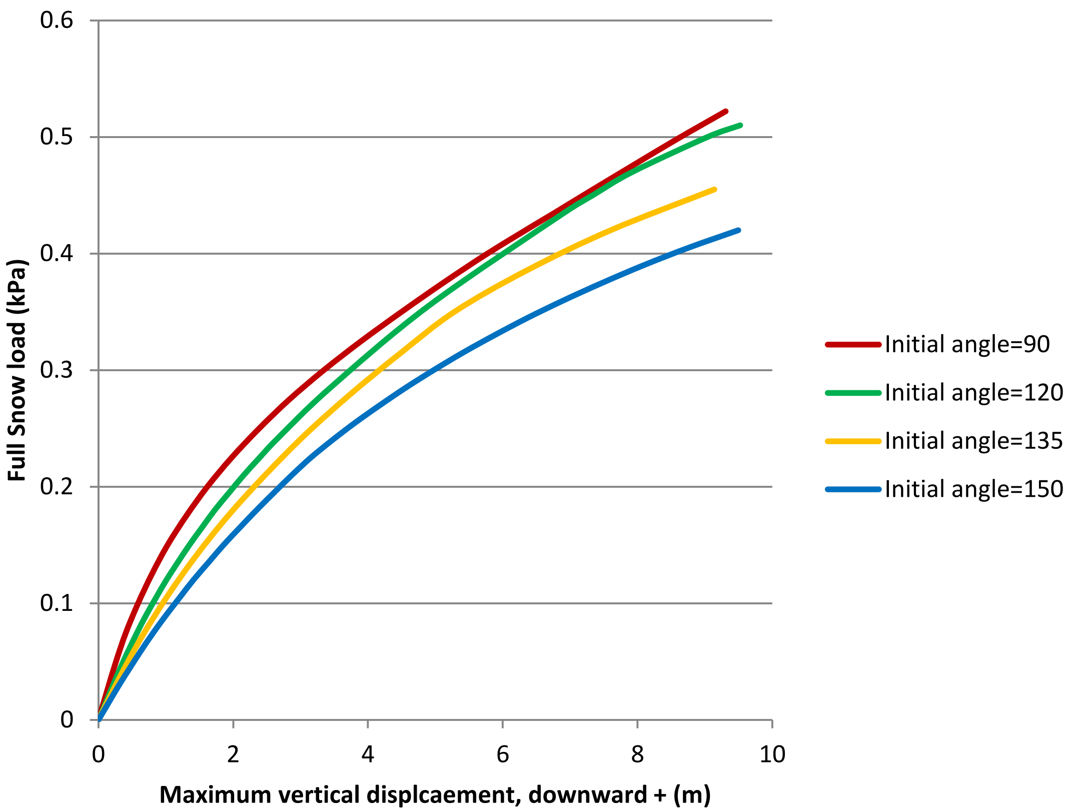


Figure 6.1.11 Relation of snow load and maximum vertical displacement for initial angle equals to and over 90 degree

In the Figure 6.1.10 and 6.1.11, the location of maximum vertical displacement has been found in the model or approximately observed from the Figure 6.1.9 that is at the center of cylindrical membrane.

By observing on the Figure 6.1.10, some of the behaviour can be pointed out. First, there is a point of intersection where exists the same loading and displacement within initial angle of 90 degree. Second, the curve below the point of intersection shows the smaller initial angle will have the superiority to against the compression from the snow loads. Third, the behaviour is reversed when loaded above the point of intersection and it seems the bigger initial angle can stand for a large loading. Other than that, the large displacement may probably affect the practicability of structure if there are internal activities. On the other hand, the bigger initial angle may appropriate for some long-term structure since it can provide a stable change in the displacement and the structural failure can be observed easily. In general, the balance between these angles depends on the function of membrane structure and it will be another valuable study.

In the initial angle equals to or greater than 90 degree, the behaviour is clearly showed that a bigger initial angle is weak in the resisting the concentrated load (Figure 6.1.11). But in terms of continuous and stable behaviour during the time of increasing load, the initial angle will be suitable in this range.

### *6.1.3 Half Snow Loads*

Another snow load pattern is half snow load, which is a special case when a half of full snow load is heavier than the other half, the heavier half snow will collapse. In this case, the loading can be larger than full snow load (Snow load=0.3, 0.5, 0.7 and 0.9 kPa). Then, the graphical development of behaviour is described below. The basic information is initial angle = 90°, height = 10 m and internal pressure = 0.3kPa.

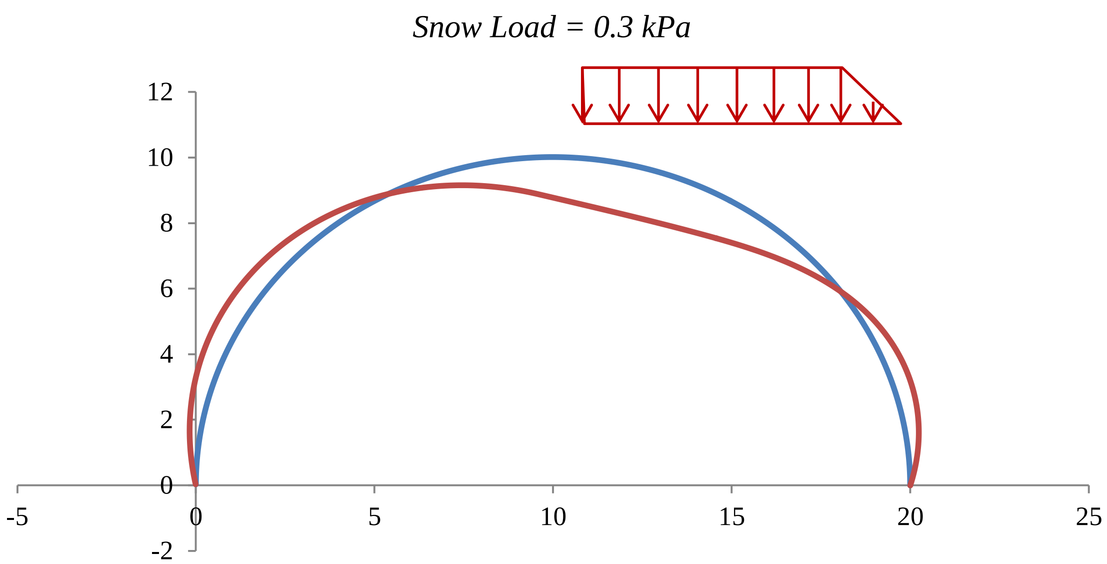


Figure 6.1.12 Deformed cylindrical membrane under a half snow loads = 0.3kPa

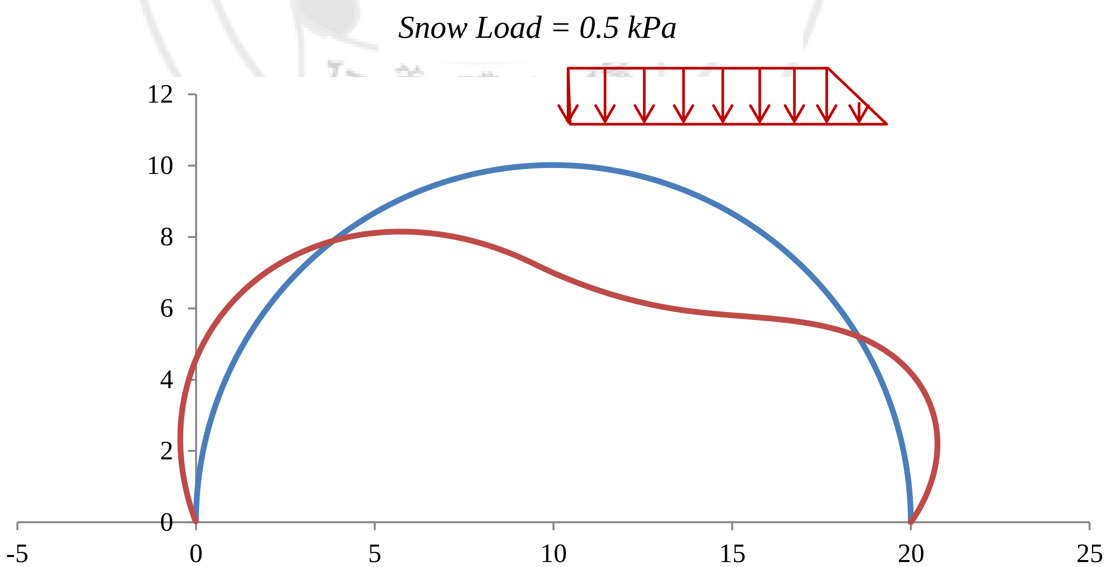


Figure 6.1.13 Deformed cylindrical membrane under a half snow loads = 0.5kPa

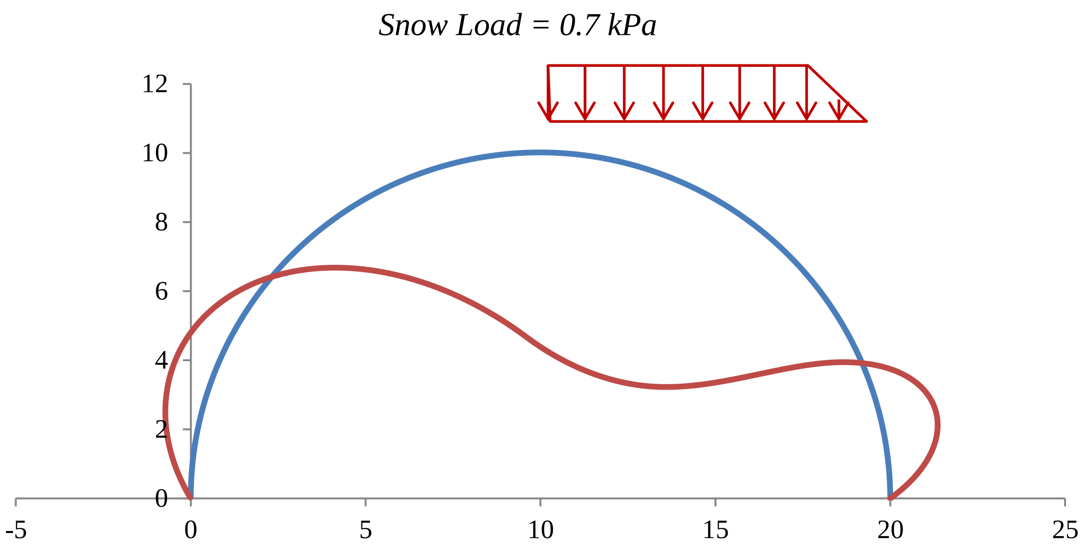


Figure 6.1.14 Deformed cylindrical membrane under a half snow loads = 0.7kPa

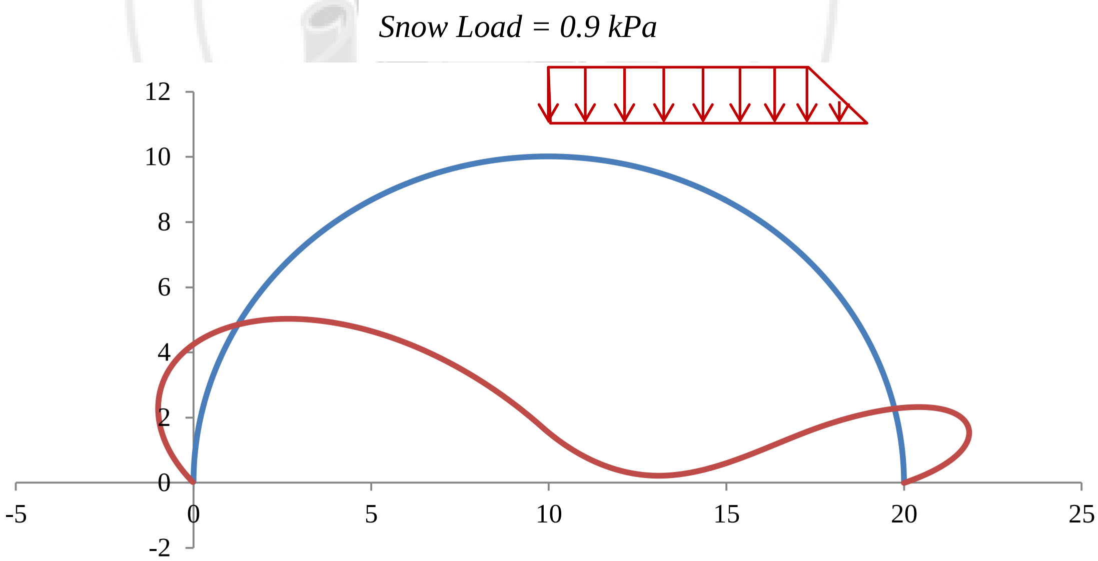


Figure 6.1.15 Deformed cylindrical membrane under a half snow loads = 0.9kPa

For the half snow load, the side effect on the membrane makes an unsymmetrical displacement. Other than the full snow load, the members are majorly in tensile stress that is able to prevent the large displacement. Since the half snow load is continuous applied to the membrane, the statically unstable equilibrium will not occur while the load keeps increasing. When the snow load is 0.9kPa (Figure 6.1.15), the magnitude of displacement increases to about its original height, which compared to the full snow load case the membrane is more capable of subjecting to half snow loads. The behaviour can be observed from the following figures.

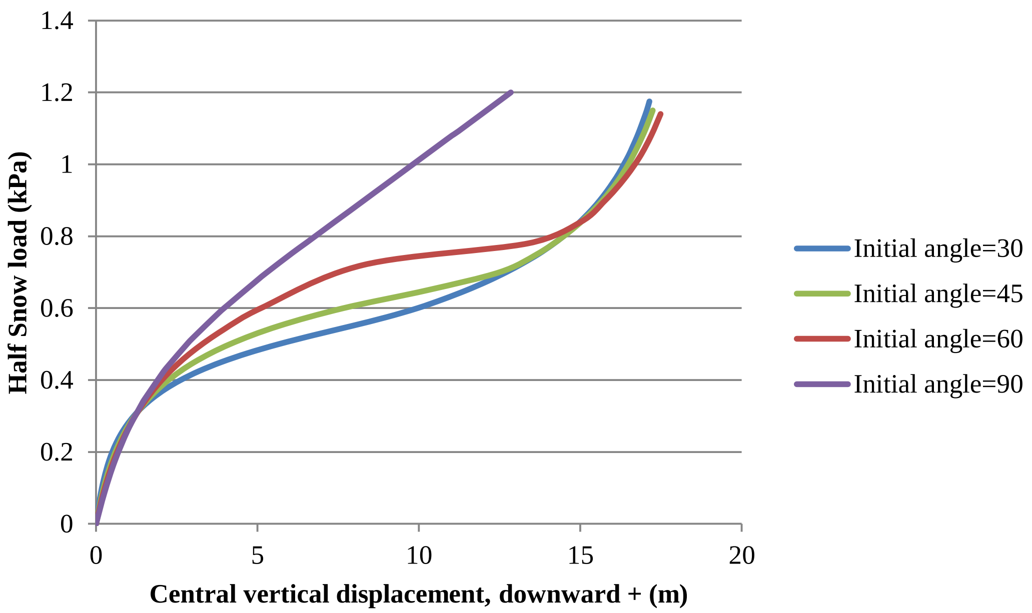


Figure 6.1.16 Relation of snow load and central vertical displacement for initial angle within 90 degree

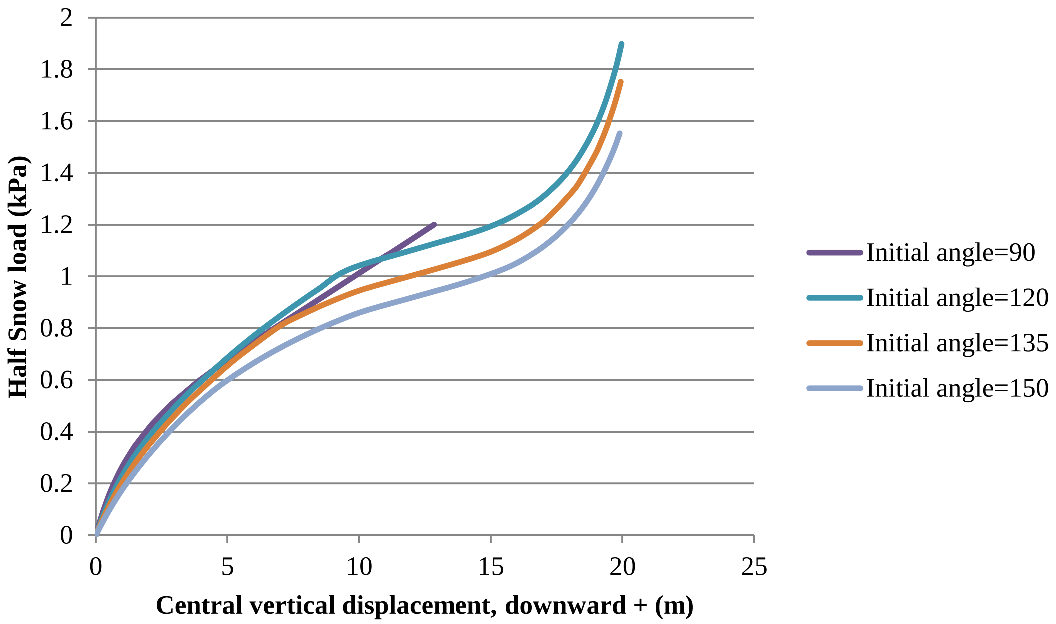


Figure 6.1.17 Relation of snow load and central vertical displacement for initial angle equals to and over 90 degree

The data point for the analysis is selected at the center and its corresponding snow load and central vertical displacement relation shown in the Figure 6.1.16 and 6.1.17. For the initial angle within 90 degree (Figure 6.1.16), it tends to be stable in the higher initial angle. If the loading is under about 0.3 kPa, the curves will have a similar and approximate linear relation to each other. Once the curves are over the point of 0.3kPa, which will be a turning point, the characteristics of each initial angle are diverged gradually and converged again at about 0.8kPa excluding 90 degree, which explicitly shows in Figure 6.1.16. The final convergence path indicates the limited behaviour of half snow load on the membrane, which the central displacement is difficult to develop further more.

Besides, the initial angle equals to and greater 90 degree (Figure 6.1.17) gives a relatively divergence curve compared to previous one. The behaviour is more stable in the lower initial angle. As the previous Figure 6.1.16 shows that the 90 degree is the steady behaviour compared to the others, the 120 degree can have a similar standard of that behaviour. In the observation, there may have a particular initial angle between the initial angle of 90 and 120 degree will result in the most stable behaviour.

In the half snow load, the entire behaviour is appropriate for the membrane structure. The half snow load pattern may be evolved from the full snow load that means if the membrane is designed for resisting the full snow load and it will be also capable of half snow load. On the other hand, the side effect of half snow is the potential issue, which the membrane may have the possibility to shift suddenly to another side of half snow load, since the snow load pattern may be more realistically complicated than the recommendation from the codes.

### *6.1.4 Wind Loads*

As a common loading pattern for such a membrane structure, wind load is usually a long-term effect to the membrane. To describe the behaviour with the increasing wind speed, the graphical result will show in the figures below. The basic information is initial angle = 90°, height = 10 m and internal pressure = 0.2kPa.

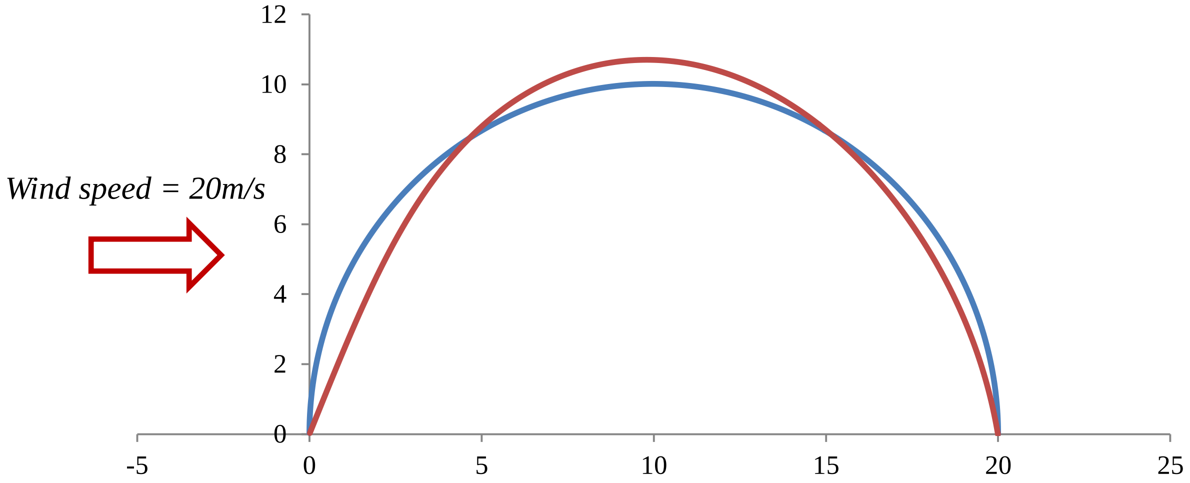


Figure 6.1.18 Deformed cylindrical membrane under a wind load of speed = 20 m/s

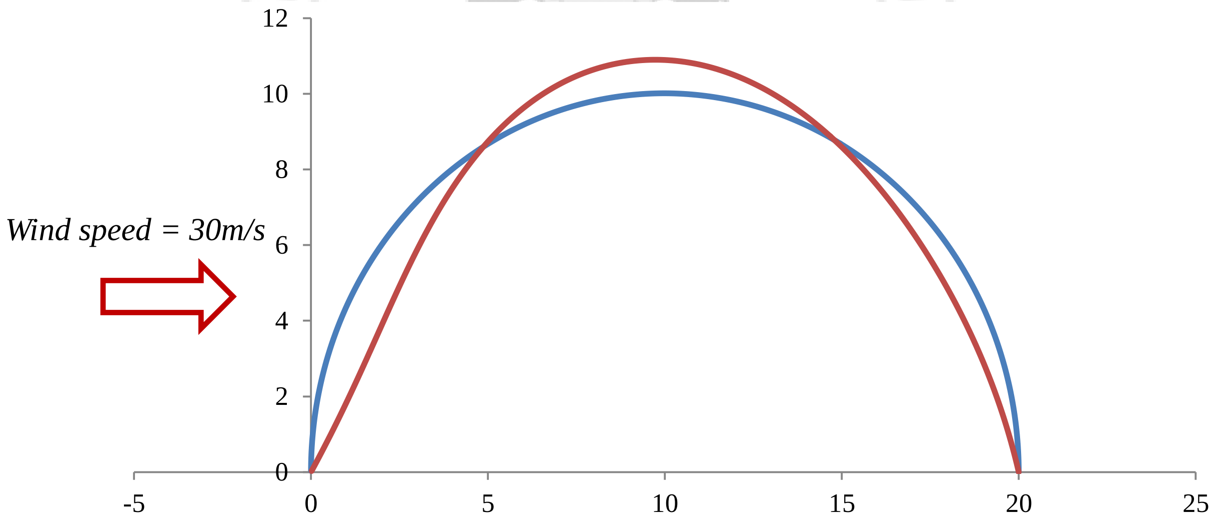


Figure 6.1.19 Deformed cylindrical membrane under a wind load of speed = 30 m/s

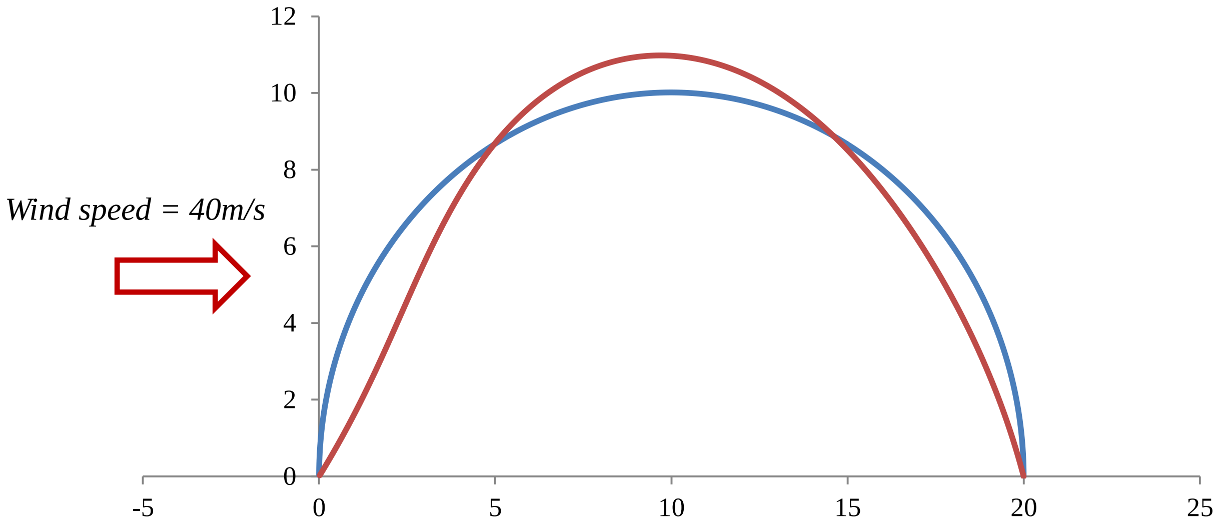


Figure 6.1.20 Deformed cylindrical membrane under a wind load of speed = 40 m/s

Due to the property of wind load coefficient *Cp*, the effect of tension and compression in the left side and right side respectively in Figure 6.1.18 to 6.1.20, will be reduced if it is subjected to less speed in wind load. The deformed portions are mainly divided into the left, right and top, and thus, the maximum displacement can be found in these three portions. While the wind speed increases from 30m/s to 40m/s, the change in behaviour will be not obviously between two Figures 6.1.19 and 6.1.20. The reason of the behaviour is probably because of the assumption of inextensible membrane that limits the lateral movement.

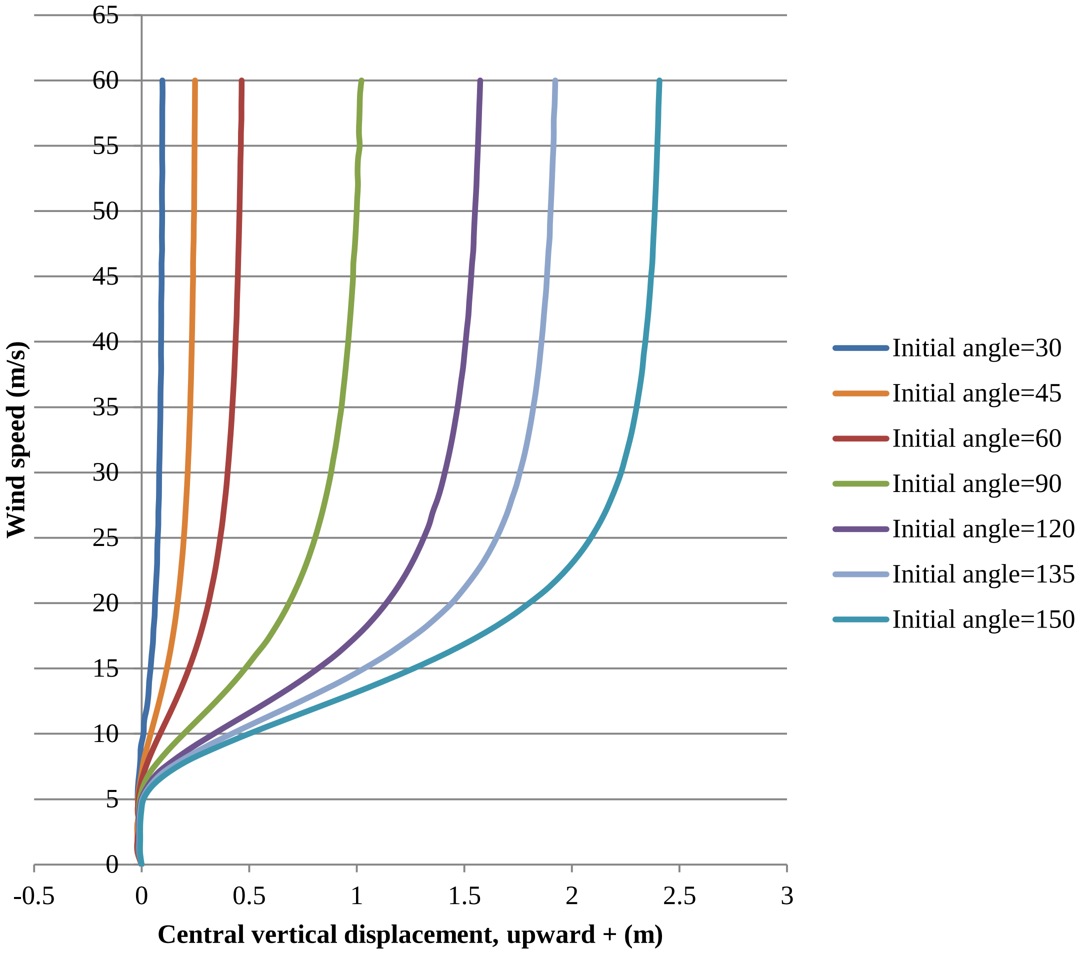


Figure 6.1.21 Relation of wind speed and central vertical displacement

In the Figure 6.1.21, the data point is at the center of membrane for plotting the relation of wind speed and central vertical displacement.

The behaviour converges under about wind speed of 5m/s at the first part of curves and then diverges until it reaches the limited displacement. The behaviour can be developed further to over the wind speed of 100m/s, but the supports may not able to carry out such large tension. Thus, the wind speed of 60m/s that is approximate to some of the speed in typhoon is enough to show the entire behaviour.

### *6.2 Cylindrical Membrane under Load Combinations*

According to the single cases discussed in pervious section, the load combinations will be the concentrated loads & wind loads and the half snow loads & wind loads.

### *6.2.1 Concentrated Loads and Wind Loads*

The behaviour of concentrated load and wind load is a special combination since the displacement in concentrated load is downward and in wind load is upward, both at the center. The effect of this combination will have a balance range which the membrane can resist both loadings and still maintain the stability. For this case, two sets of results will make for the comprehensive analysis. One is the increasing wind loads at constant concentrated loads = 3 and 6kN, another is the increasing concentrated loads at constant wind loads = 20 and 40m/s. The graphical behaviour will show at the beginning of the two results. The basic information is initial angle = 90°, height = 10 m and internal pressure = 0.3kPa.

### *6.2.1.1 Increasing Wind Loads with Constant Concentrated Loads*

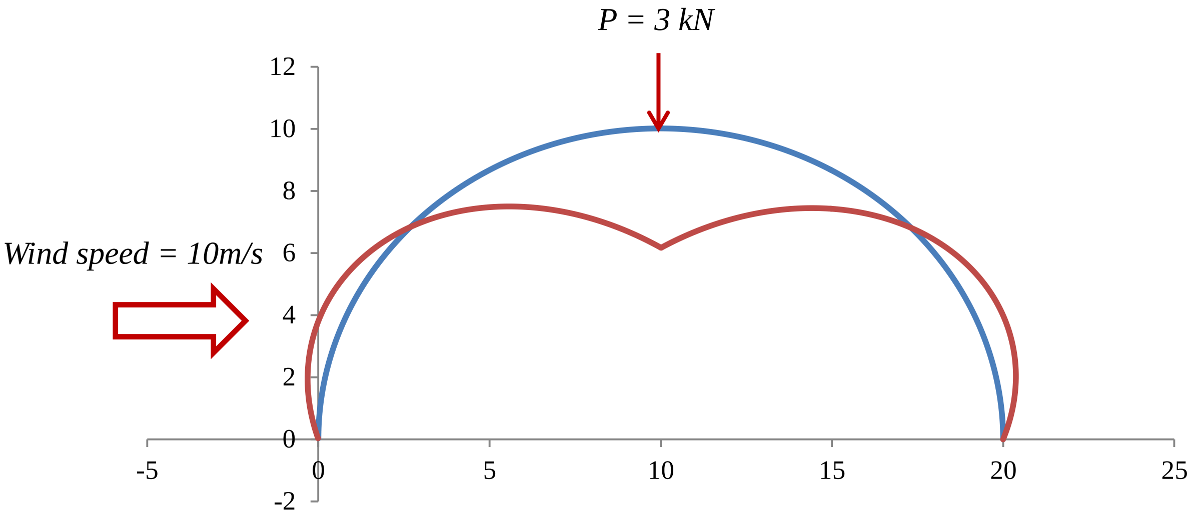


Figure 6.2.1 Deformed cylindrical membrane under a wind load of speed = 10 m/s and concentrated load = 3kN

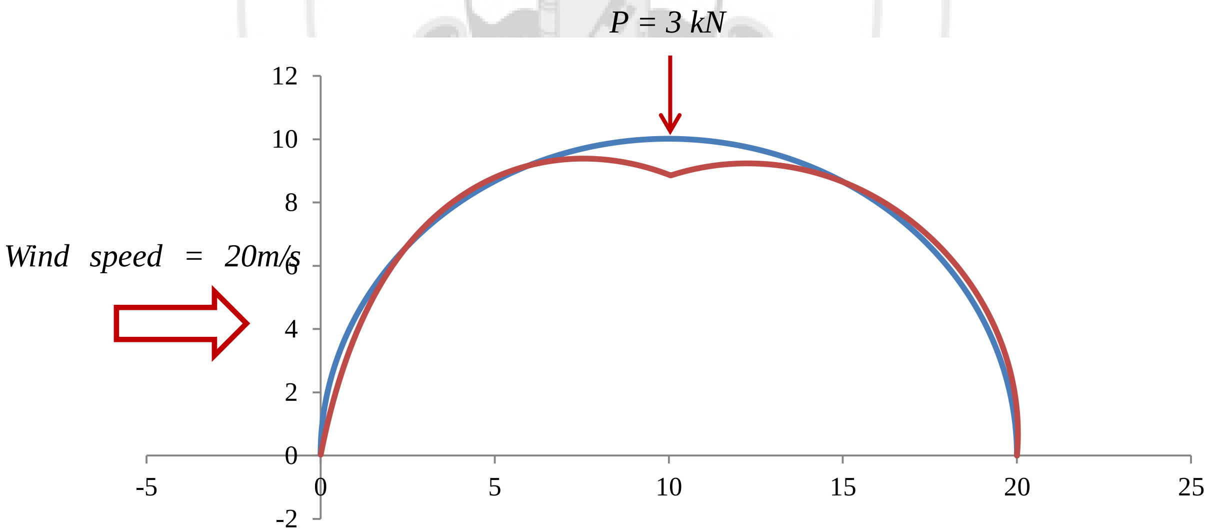


Figure 6.2.2 Deformed cylindrical membrane under a wind load of speed = 20 m/s and concentrated load = 3kN

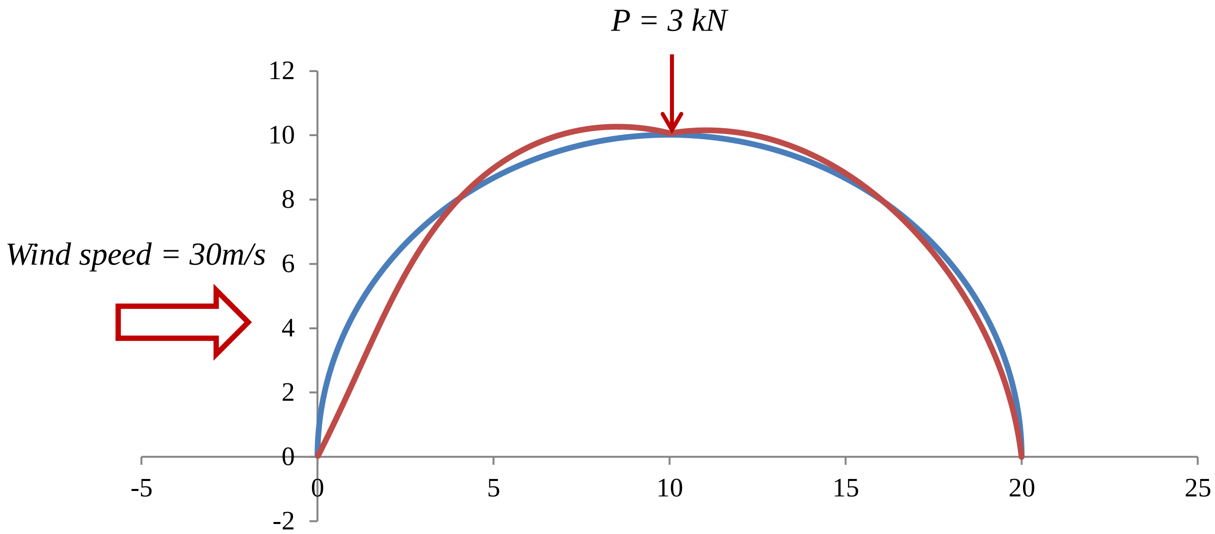


Figure 6.2.3 Deformed cylindrical membrane under a wind load of speed = 30 m/s and concentrated load = 3kN



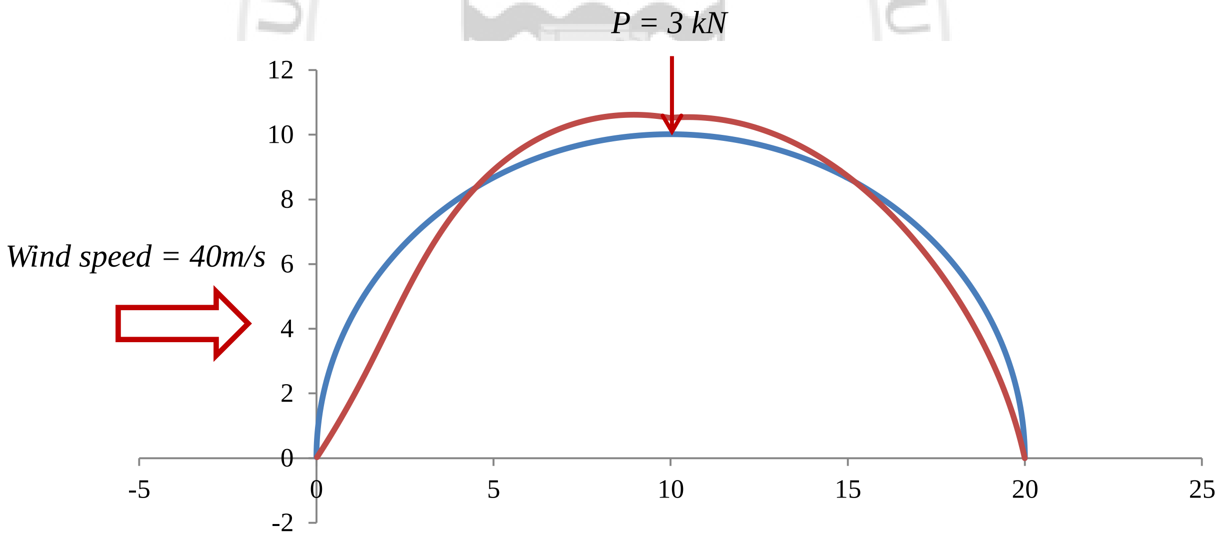


Figure 6.2.4 Deformed cylindrical membrane under a wind load of speed = 40 m/s and concentrated load = 3kN

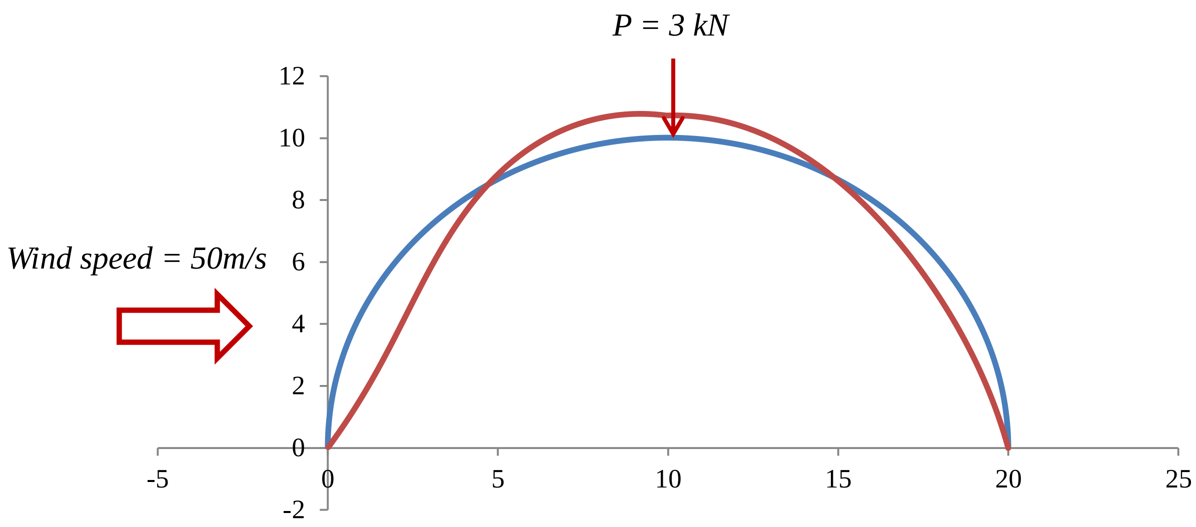


Figure 6.2.5 Deformed cylindrical membrane under a wind load of speed = 50 m/s and concentrated load = 3kN

The behaviour changes from the leading concentrated load to the leading wind load (Figure 6.2.1 to 6.2.5). In the extreme behaviour of two figures 6.2.1 and 6.2.5, the deformed shape is most likely same as the corresponding single loading cases of concentrated loads and wind loads. For the figures between two extremes, the wind load offsets a part of displacement that is made by the concentrated load. If the wind load is at a high wind speed, the displacement will be increased again (Figure 6.2.6 and 6.2.7).

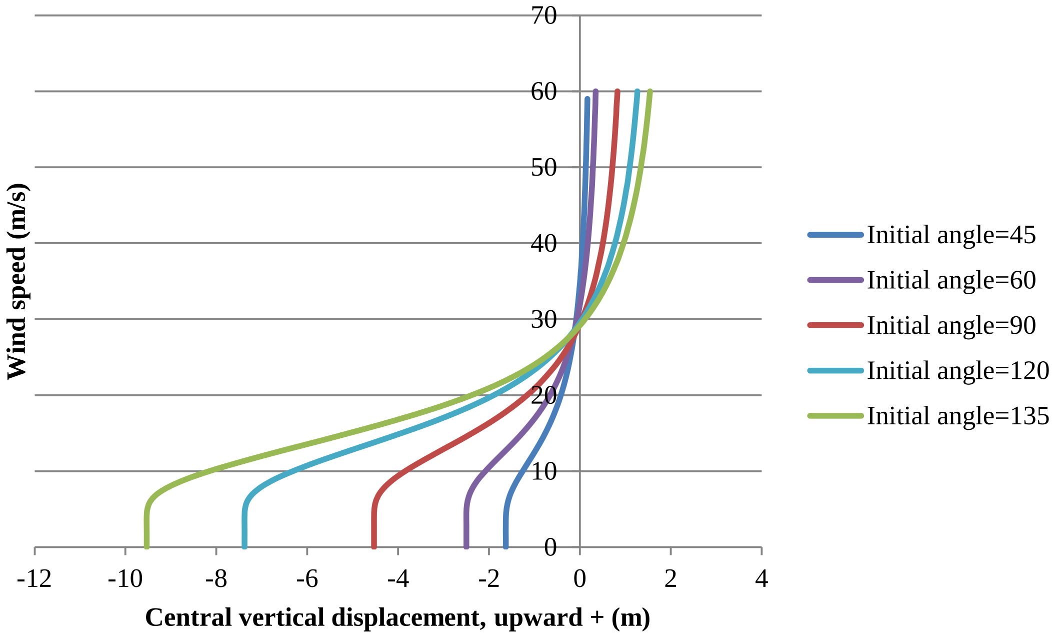


Figure 6.2.6 Relation of wind speed, a concentrated load of 3kN and central vertical displacement

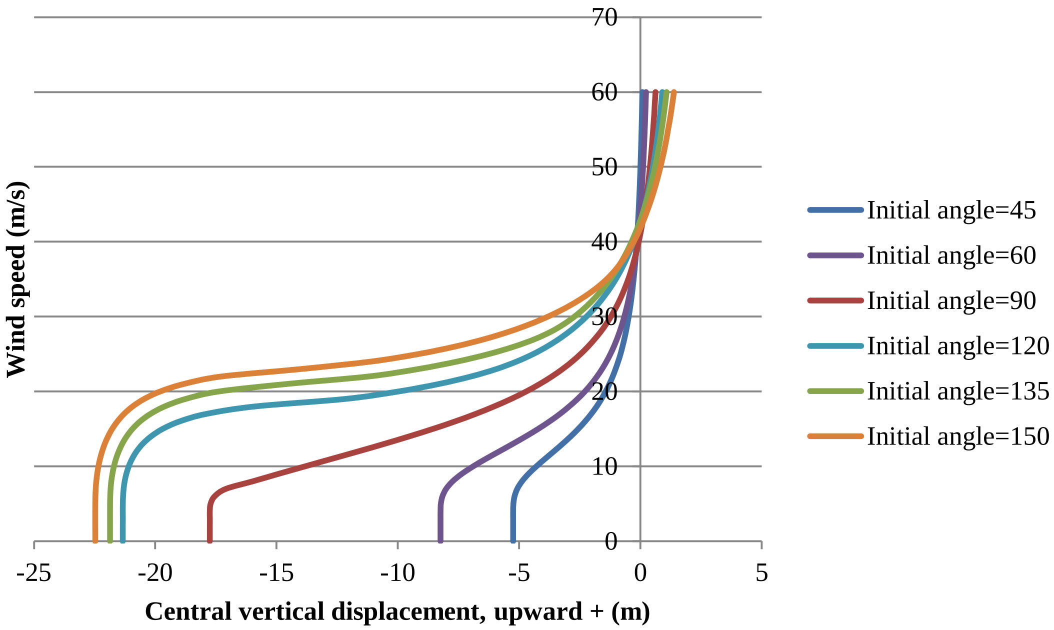


Figure 6.2.7 Relation of wind speed, a concentrated load of 6kN and central vertical displacement

At the beginning of the curves in Figure 6.2.6 and 6.2.7, the concentrated load is leading until the wind load is large enough to against to it and thus the membrane moves to opposite direction. Although a smaller initial angle has a less displacement, all the curves will pass through the same zero displacement point and keeps increasing to the limited range of displacement.

The differences of Figure 6.2.6 and 6.2.7 have two points. For the concentrated load of 6kN, first, the initial displacement will exist for a longer time during the increasing of wind speed in the initial angle greater than 90 degree. Second, the zero displacement point moves upward and the behaviour of two loads against to each other will appear in a later stage.

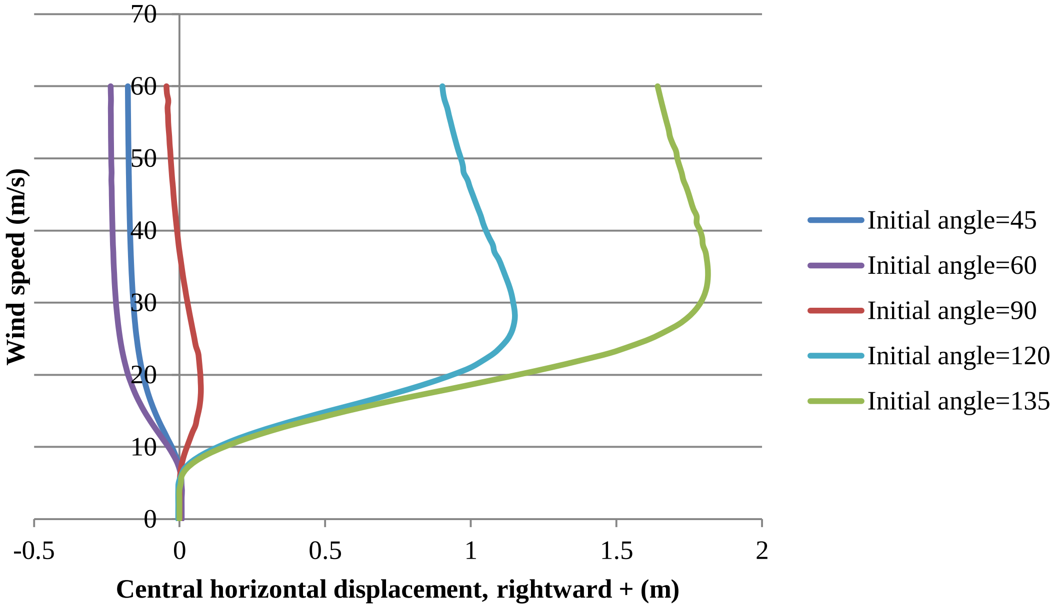


Figure 6.2.8 Relation of wind speed, a concentrated load of 3kN and central horizontal displacement

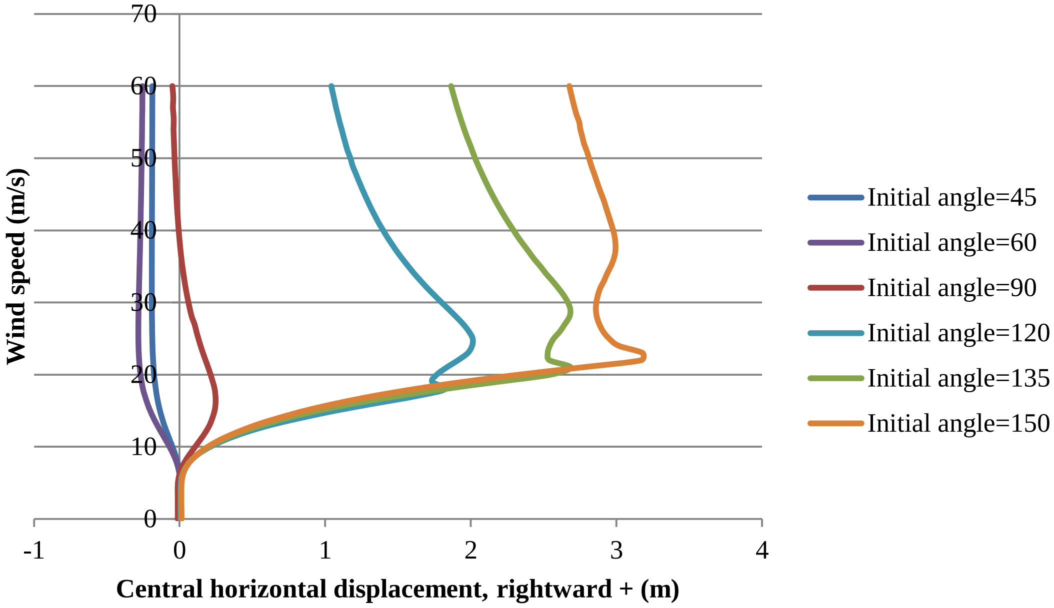


Figure 6.2.9 Relation of wind speed, a concentrated load of 6kN and central horizontal displacement

For the central horizontal displacement in Figure 6.2.8 and 6.2.9, the curves have a converging portion at first because of the leading concentrated load. When the curve diverges, the initial angles smaller than 90 degree will have negative (leftward) displacement, the initial angles greater than 90 degree will have a positive (rightward) displacement and the 90-degree initial angle is relatively stable compared to the others.

The difference of behaviour in Figure 6.2.8 and 6.2.9 is in the portion between wind speed of 20 and 40 m/s. The uncertainty of the curve in higher concentrated load case may be because of the effect between a particular range of wind loads and a high concentrated load which causing the unstable behaviour on the membrane.

In this load combination, the wind loads is able to resist some of the compressive stress from the concentrated load and have an acceptable displacement. The large displacement may be the major problem, which needs to deal with it if a higher concentrated load has applied. Therefore, the design of membrane should be mainly concern on the effect of concentrated load in the consideration of this combination.

#### *6.2.1.2 Increasing Concentrated Loads with Constant Wind Loads*

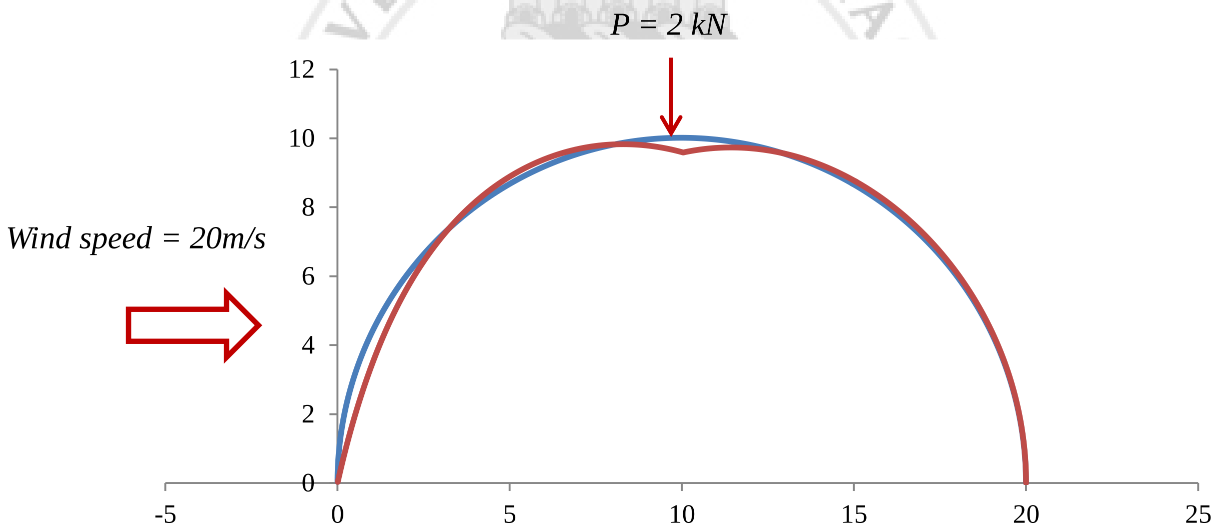


Figure 6.2.10 Deformed cylindrical membrane under a concentrated load = 2kN and wind load of speed = 20 m/s

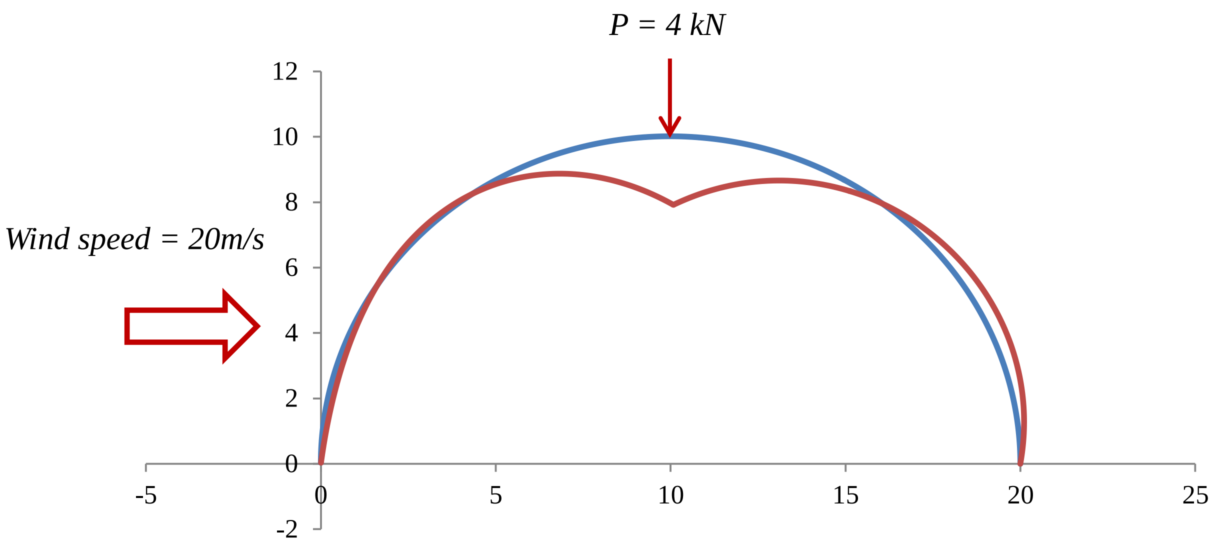


Figure 6.2.11 Deformed cylindrical membrane under a concentrated load = 4kN and wind load of speed = 20 m/s

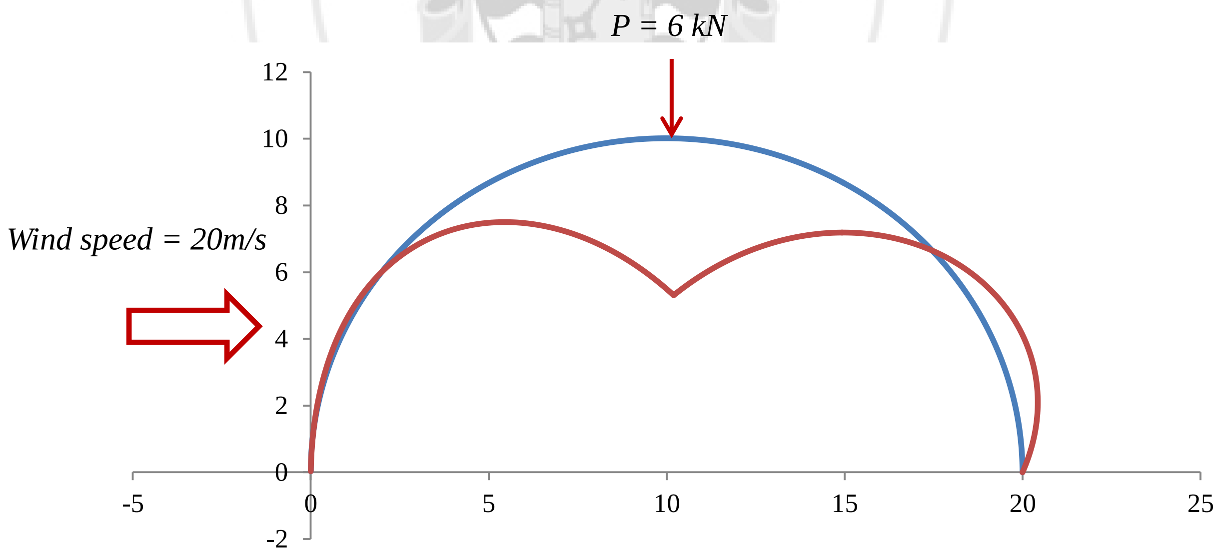


Figure 6.2.12 Deformed cylindrical membrane under a concentrated load = 6kN and wind load of speed = 20 m/s

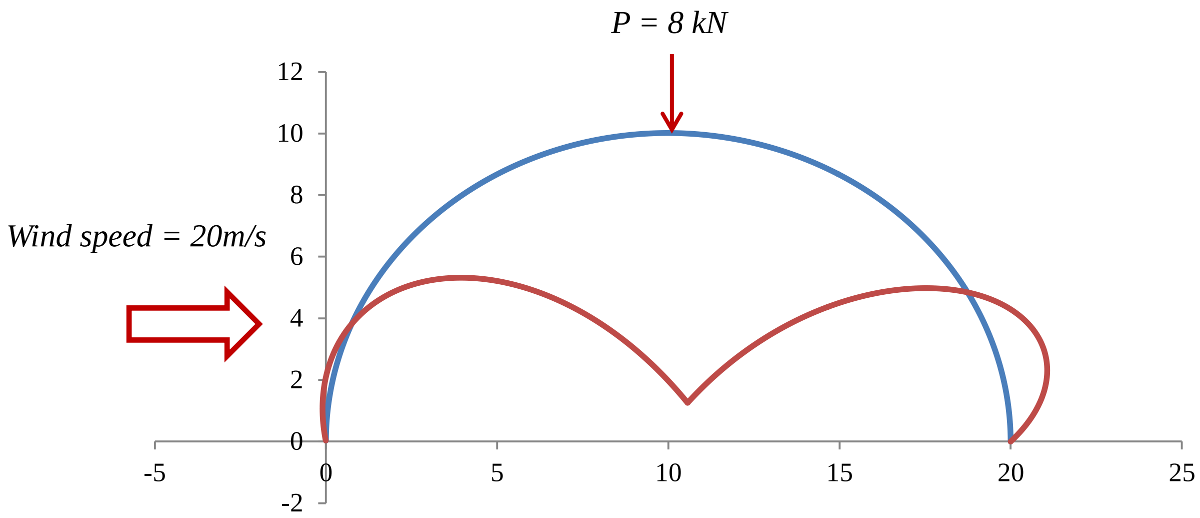


Figure 6.2.13 Deformed cylindrical membrane under a concentrated load = 8kN and wind load of speed = 20 m/s

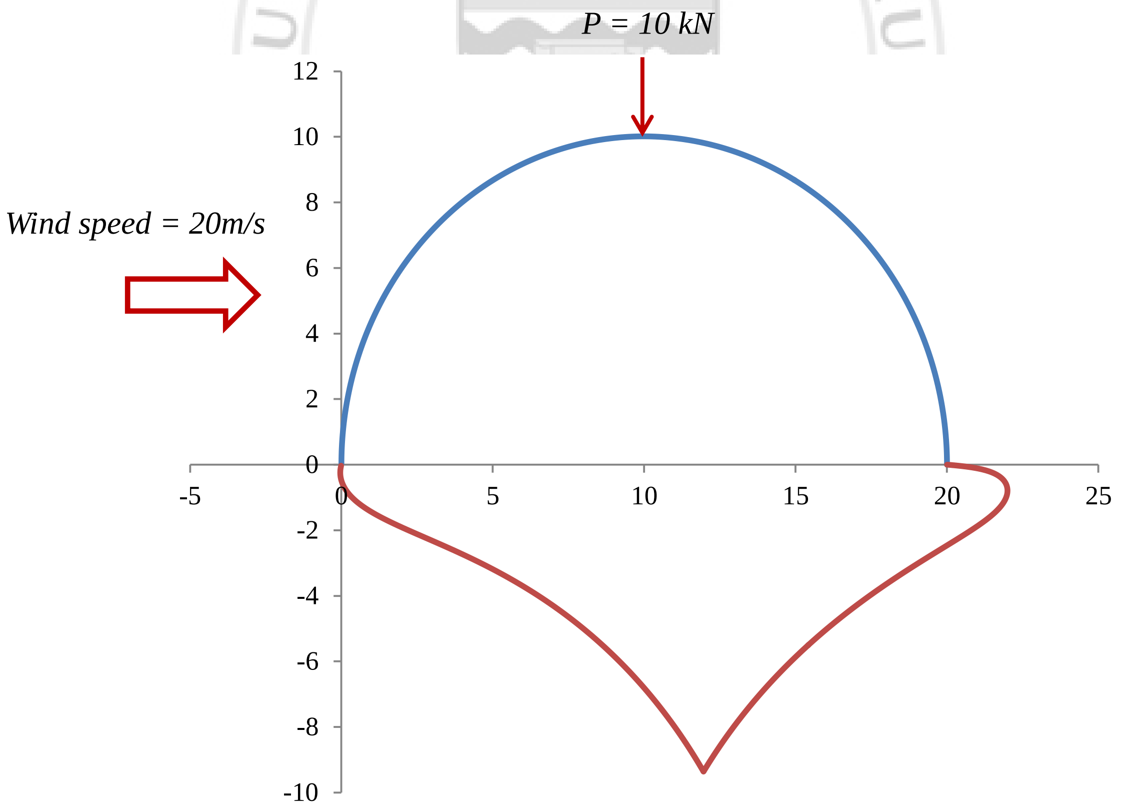


Figure 6.2.14 Deformed cylindrical membrane under a concentrated load = 10kN and wind load of speed = 20 m/s

For the behaviour in Figure 6.2.10 to 6.2.14, the effect of wind load makes the membrane has an unsymmetrical displacement, which can be explicitly observed in the higher concentrated. Once the concentrated load is up to 8kN, the membrane is in an unstable state, which will suddenly have a large displacement in downward direction. Then, the displacement behaviour is similar to the singe loading case of concentrated loads and the similarity can be found out in the following figures.



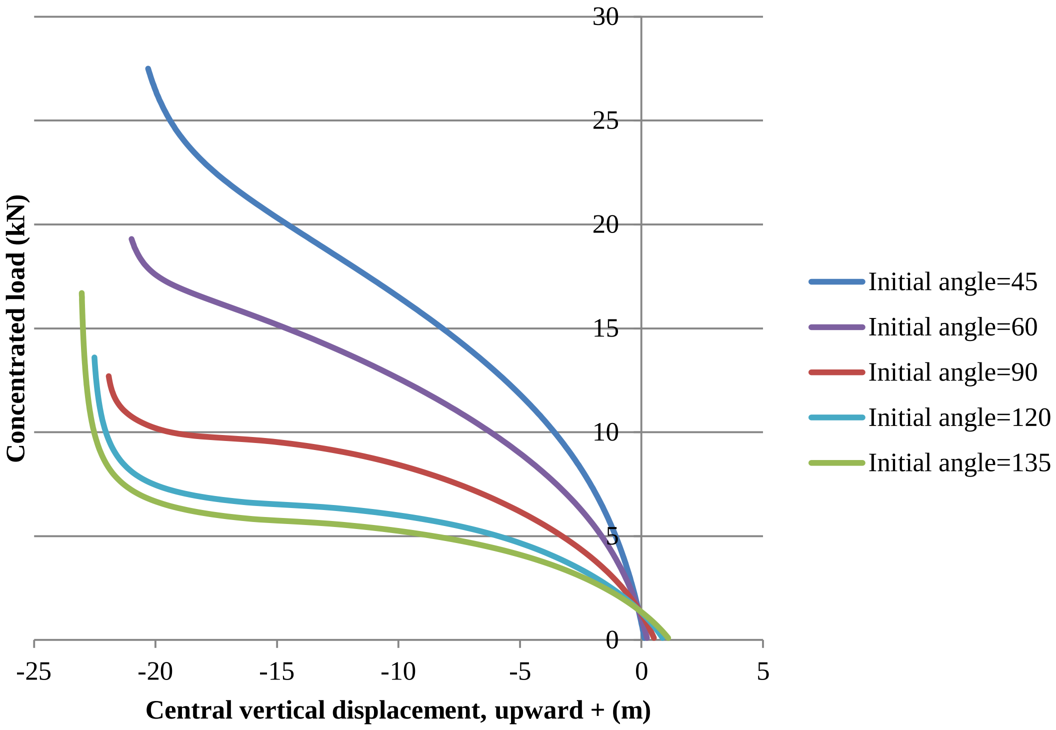


Figure 6.2.15 Relation of concentrated load, wind load at 20 m/s and central vertical displacement

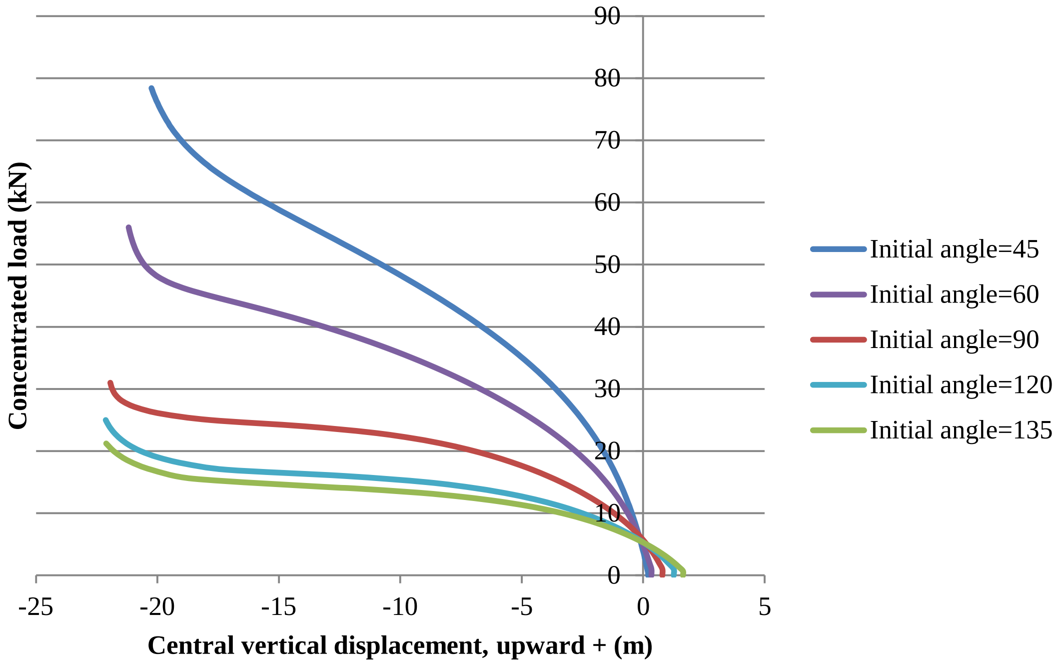


Figure 6.2.16 Relation of concentrated load, wind load at 40 m/s and central vertical displacement

In the Figure 6.2.15 and 6.2.16, the data point is selected at the center of membrane. As the figure shows that there is a zero displacement point which is the effect of interaction of wind load and concentrated load. After this point, the curves diverge until the displacement reaches its limit, in this path, the slope is near to the zero which means the wind load has less effect on the concentrated load and the behaviour will change mainly following the leading concentrated load.

The difference of two wind speeds is that the zero displacement point may develop in a higher wind speed case and the curves is likely to have a scale of increase.

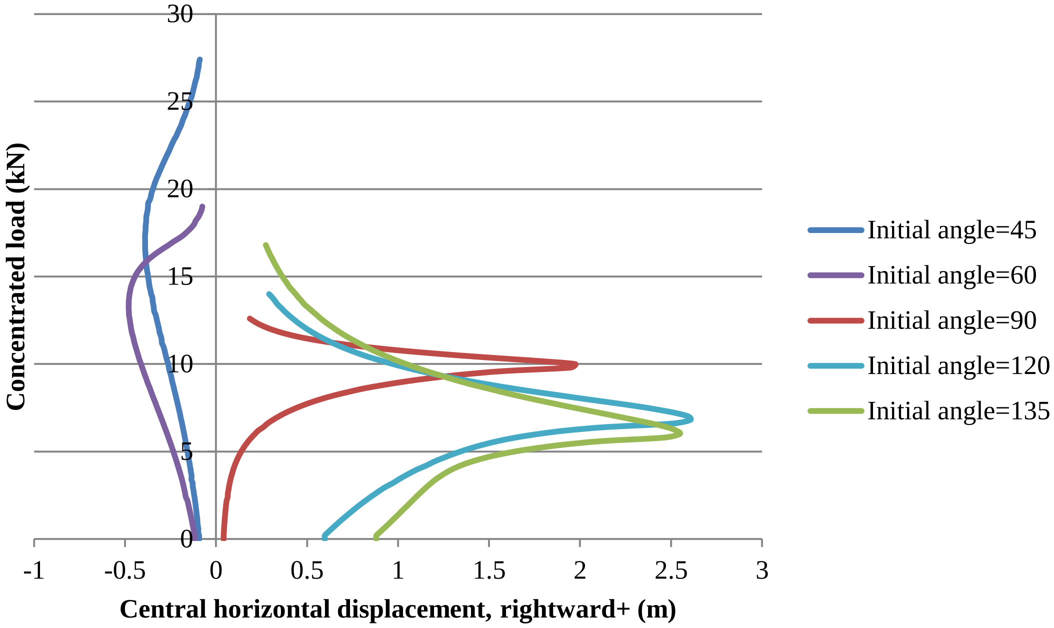


Figure 6.2.17 Relation of concentrated load, wind load at 20 m/s and central horizontal displacement

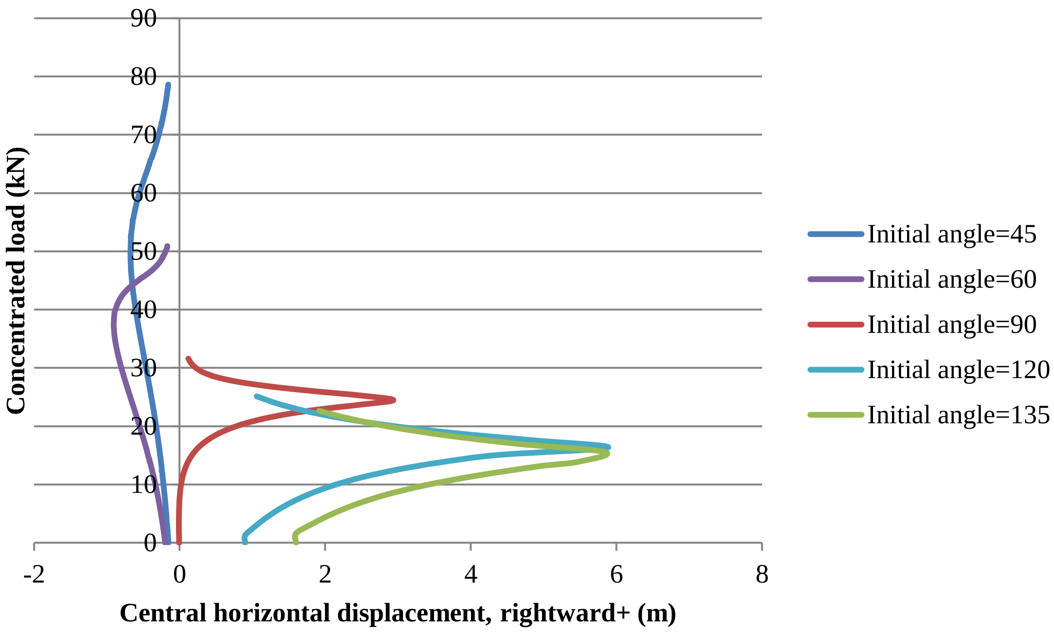


Figure 6.2.18 Relation of concentrated load, wind load at 40 m/s and central horizontal displacement

For the central horizontal displacement in Figure 6.2.17 and 6.2.18, the smaller initial angles have a stable horizontal movement. The extreme horizontal movement in the initial angles of 90 degree and over 90 degree explains the behaviour of membrane is in a significant unstable state in this combination. Finally the horizontal displacement decreases but the magnitude of vertical displacement has been development to the twice of original height.

In general, the wind loads is able to resist some of the compressive stress from the concentrated load but only in the early stage. In this combination, the large horizontal displacement usually follows the small vertical displacement. In addition, if the concentrated load takes the main effect in the combination, the worst behaviour may occur in the membrane.

### *6.2.2 Half Snow Loads and Wind Loads*

In this case, the two sets of results will be performed. One is the increasing wind loads with constant half snow loads = 0.3 and 0.5kPa. Another is the increasing half snow loads with constant wind loads = 20 and 40m/s. The graphical behaviour will show at the beginning of the two results. The basic information is initial angle = 90$^{\circ}$, height = 10 m and internal pressure = 0.3kPa.

#### *6.2.2.1 Increasing Wind Loads with Constant Half Snow Loads*

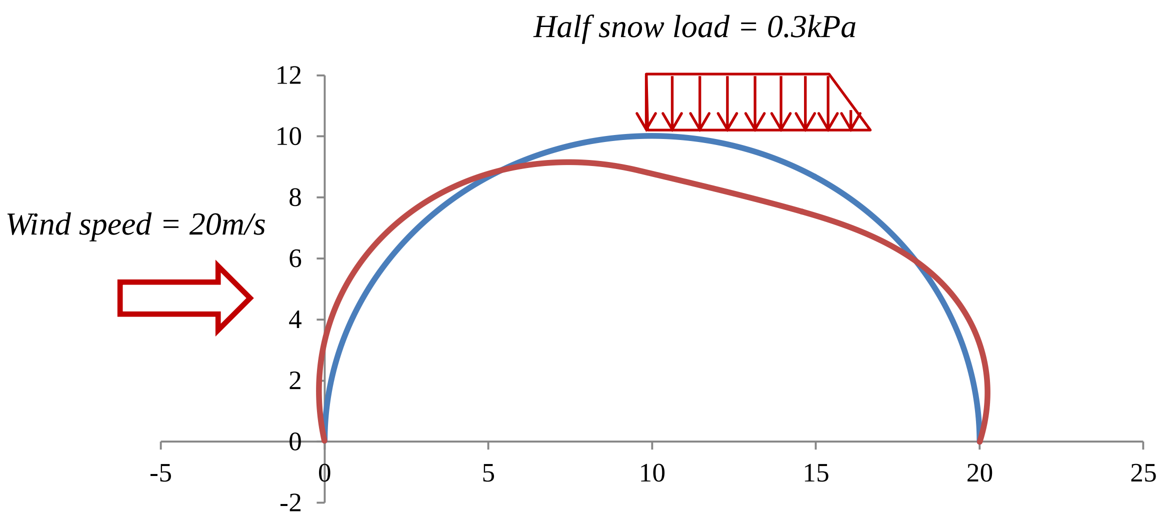


Figure 6.2.19 Deformed cylindrical membrane under a wind load of speed = 20 m/s and half snow load = 0.3kPa

In the Figure 6.2.19, the displacement, which made by the half snow load may offset by the wind load. But the effect of half snow load is continuous on the top of membrane; the membrane will have large displacement in this combination compared to the previous combination. The reason of only a graphical behaviour will show in the following figures.

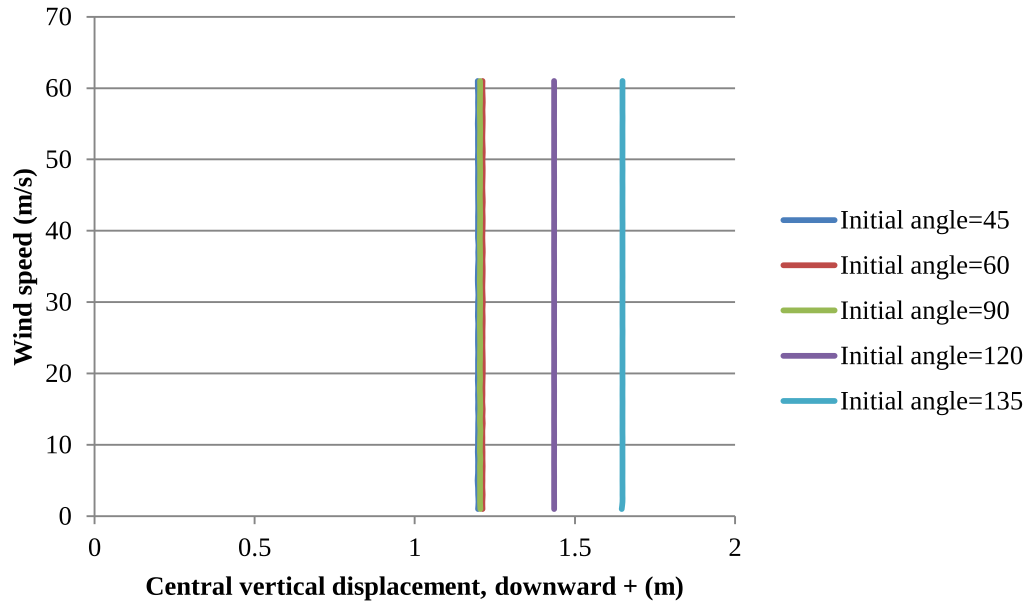


Figure 6.2.20 Relation of wind speed, half snow load at 0.3 kPa and central vertical displacement

The behaviour in Figure 6.2.20 shows that the half snow load is the leading load. Even though the wind speed increases to about 60 m/s, the membrane still maintain the deformed shape under the effect of half snow load. In general, the smaller initial angle provides an appropriate geometry for the membrane in this combination.

### *6.2.2.2 Increasing Half Snow Loads with Constant Wind Loads*

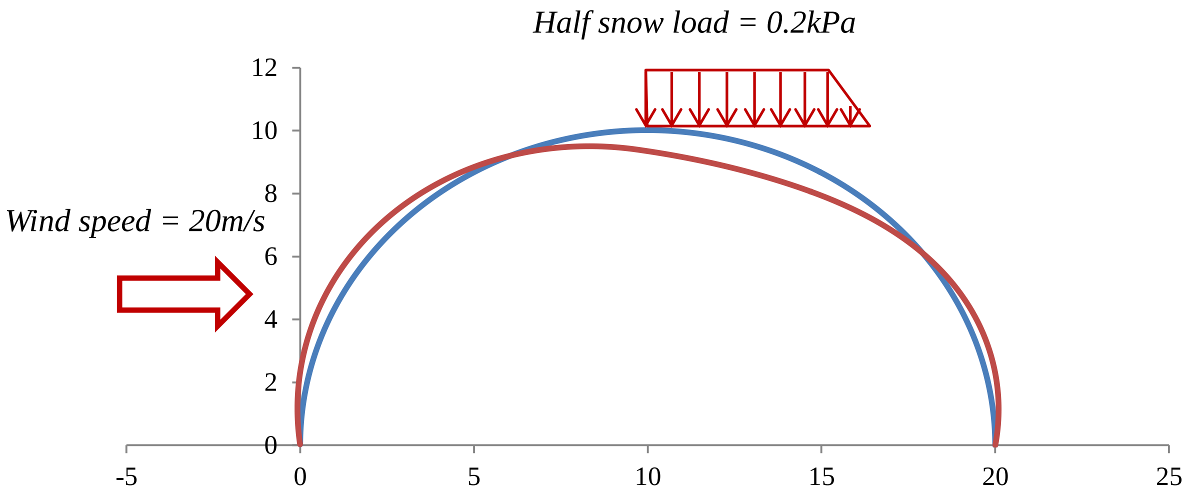


Figure 6.2.21 Deformed cylindrical membrane under a half snow load = 0.2kPa and wind load of speed = 20 m/s

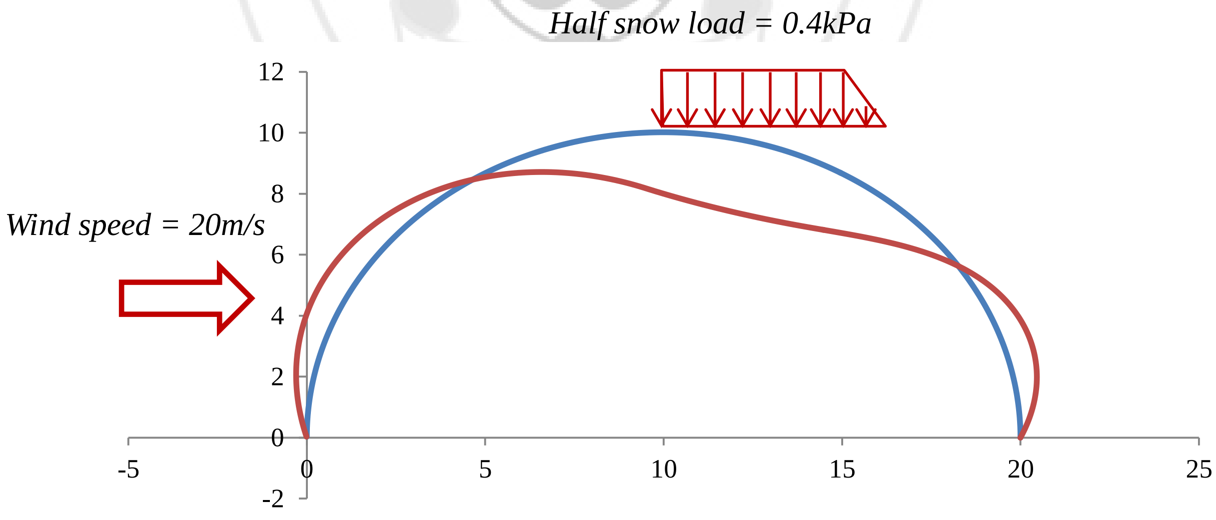


Figure 6.2.22 Deformed cylindrical membrane under a half snow load = 0.4kPa and wind load of speed = 20 m/s

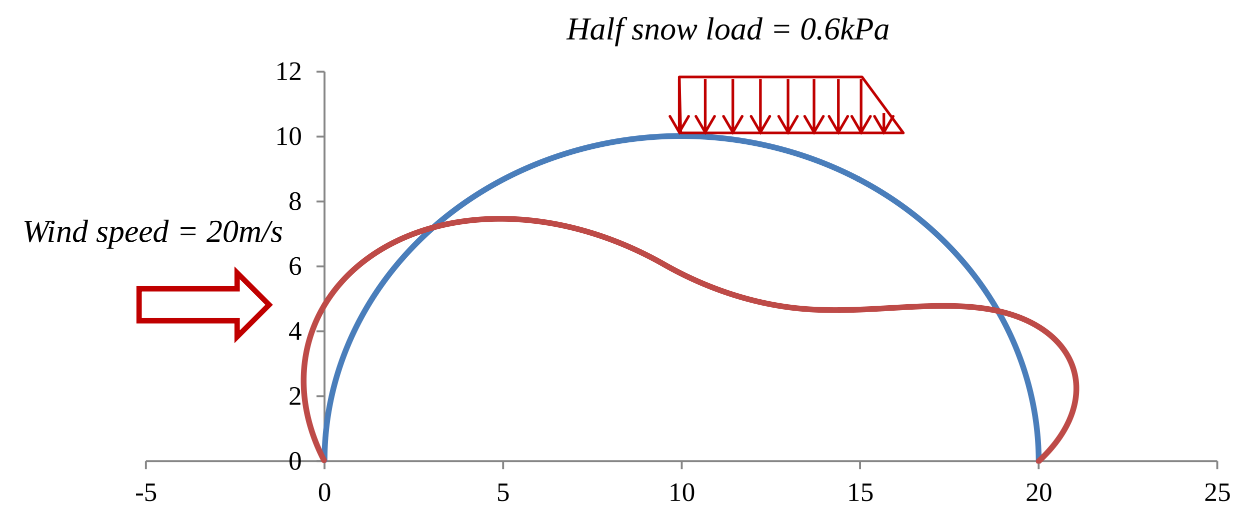


Figure 6.2.23 Deformed cylindrical membrane under a half snow load = 0.6kPa and wind load of speed = 20 m/s

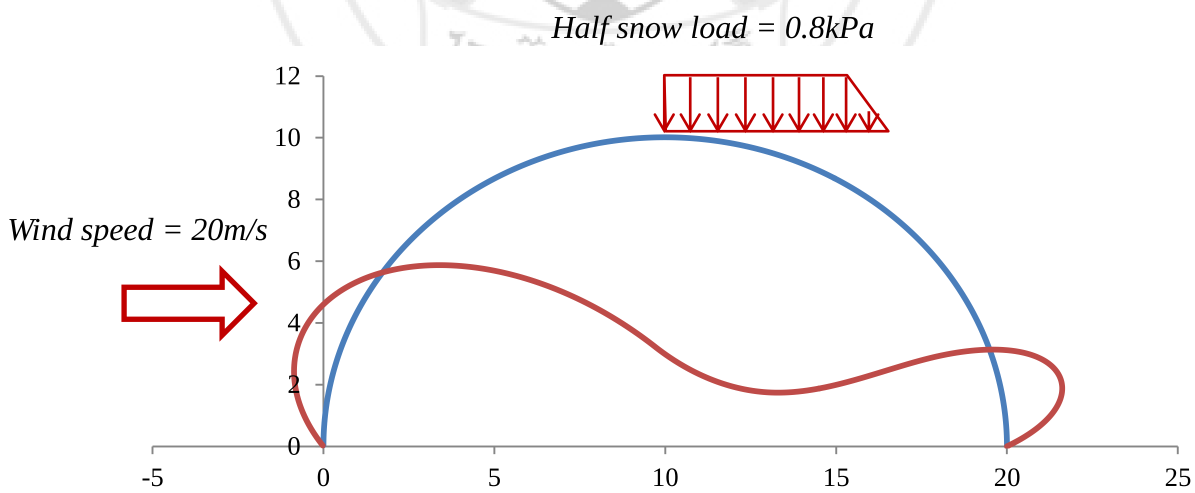


Figure 6.2.24 Deformed cylindrical membrane under a half snow load = 0.8kPa and wind load of speed = 20 m/s

In the Figure 6.2.21 to 6.2.24, the series behaviour is similar to the single loading case of half snow load and it is consistent with the result in Figure 6.2.20. In the early comparison in Table 5.2.1, the result also indicates the slight difference of two loading cases (half snow load to wind load and half snow load). Thus, the similarity can be observed in following figures.

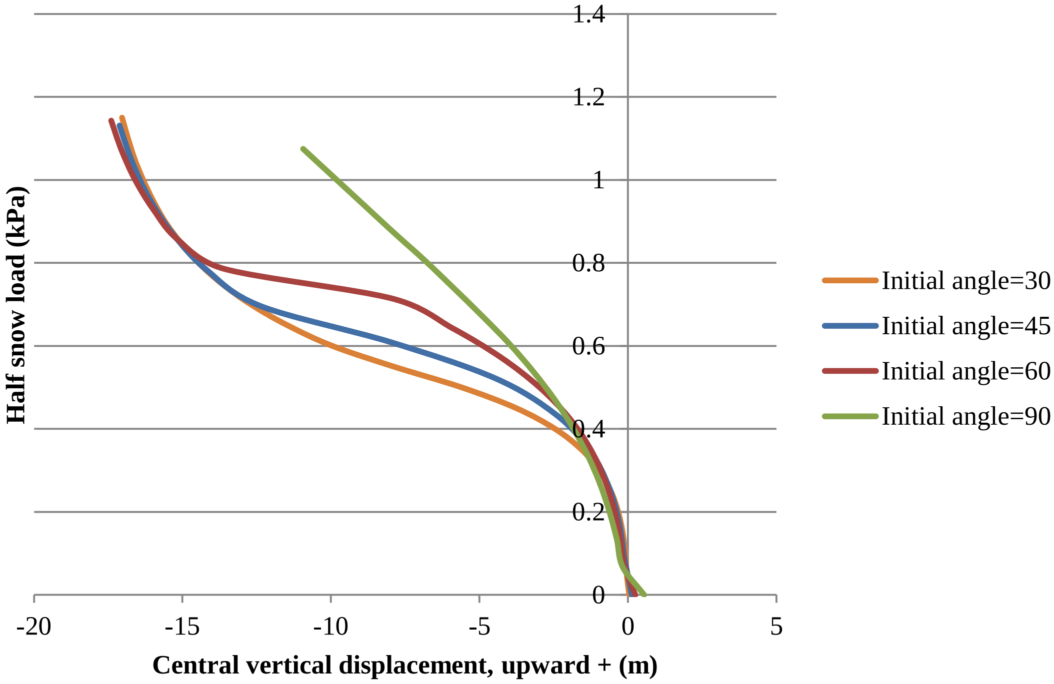


Figure 6.2.25 Relation of half snow load, wind speed at 20 m/s and central vertical displacement for initial angle within 90 degree

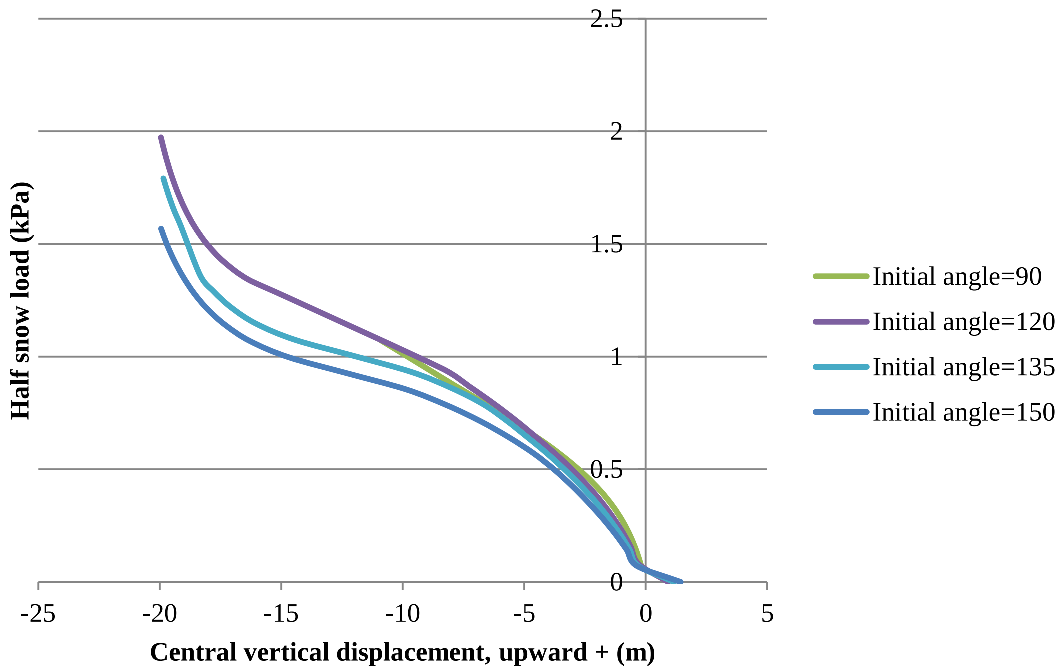


Figure 6.2.26 Relation of half snow load, wind speed at 20 m/s and central vertical displacement for initial angle equals to and over 90 degree

Although the curves have the same behaviour as the single loading case of half snow load, the entire internal force system is different with it. For the membrane model, it can easily form the equilibrium without the consideration of how much internal energy can be spent, the internal system may have been resisted most of the external loading. Consequently, the membrane subjected to half snow load and wind load has little change in displacement; the internal tension has been increased to a certain amount.

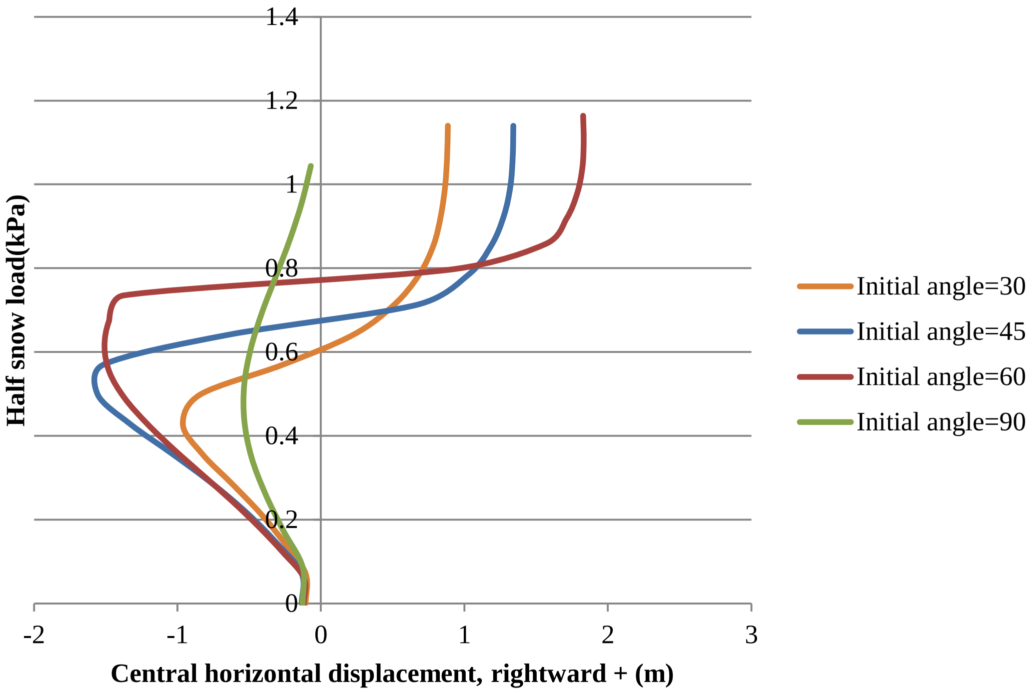


Figure 6.2.27 Relation of half snow load, wind speed at 20 m/s and central horizontal displacement for initial angle equals to and over 90 degree

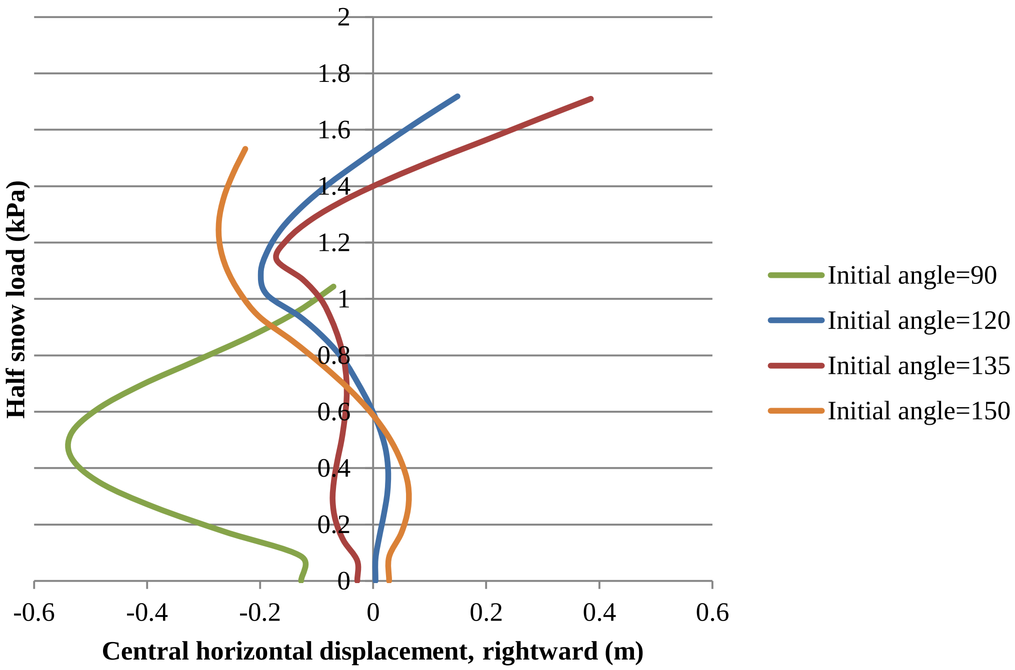


Figure 6.2.28 Relation of half snow load, wind speed at 20 m/s and central horizontal displacement for initial angle equals to and over 90 degree

In the Figure 6.2.27, the negative horizontal displacement is where the vertical displacement is not over the level of ground, and the initial angle of 90 degree is the better case. Once the initial angle greater than 90 degree (Figure 6.2.28), the possible horizontal movement may hard to predict but the horizontal displacement is relatively less compared to the initial angle under the 90-degree.

### *6.3 Comparison of Loading Cases with Different Internal Pressure*

Based on the results of single loading case which have discussed in previous sections, the stable initial angle as the geometry of membrane will be selected for the further analysis with different internal pressure so as to find out a specific cylindrical membrane that is completely appropriate for the loading case in reality. The basic information for each case is the height of 10m.

### *6.3.1 Concentrated Loads*

For the concentrated load, the initial angle of 30 degree is used.

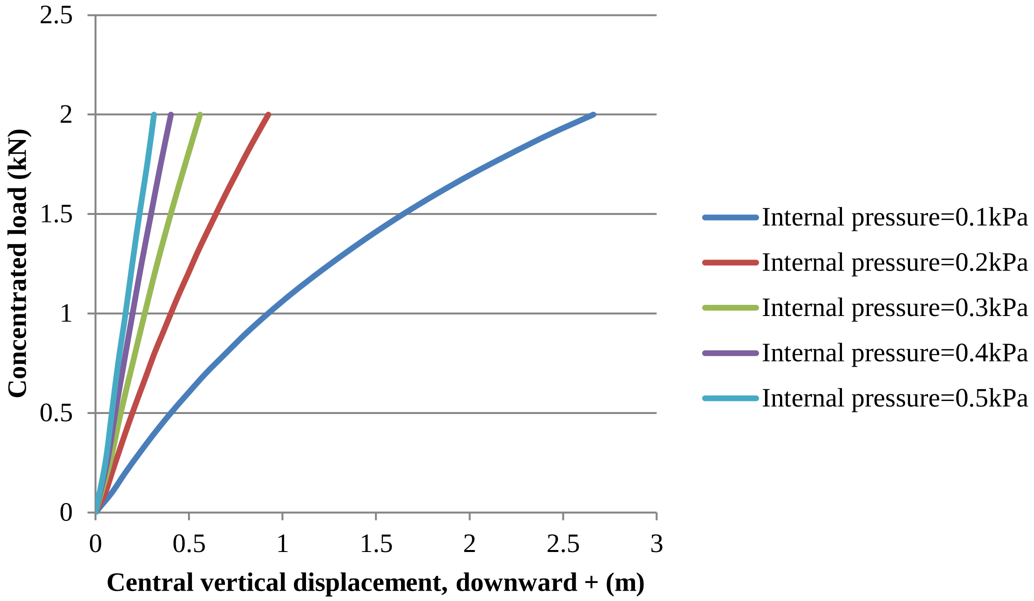


Figure 6.3.1 Relation of concentrated load and central vertical displacement in different internal pressure

In the Figure 6.3.1, the membrane is likely to have an internal pressure of 0.2 kPa at least since the effect of 0.1 kPa is serious. The difference will decrease when the internal pressure increases gradually. In the model, the 0.3kPa is selected and it seems to be the most balance internal pressure in both the stability and cost concern.

### *6.3.2 Full Snow Loads*

For the full snow load, the initial angle of 90 degree is used.

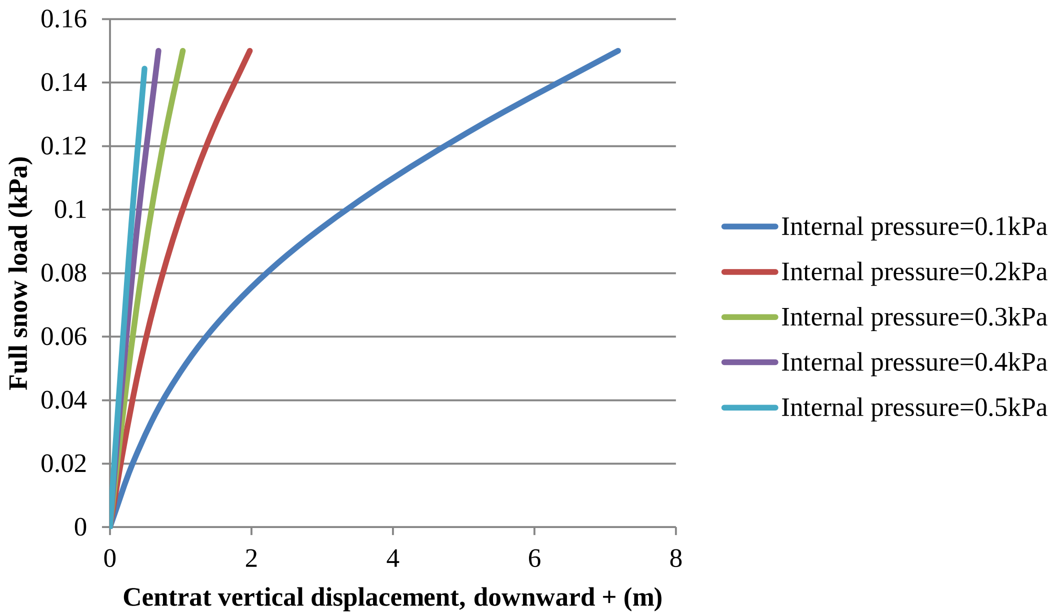


Figure 6.3.2 Relation of full snow load and central vertical displacement in different internal pressure

The curve of internal pressure of 0.1 kPa gives a large potential displacement compared to the others. For the 0.2kPa, the displacement is about 2m, which may be a little bit acceptable for the membrane of 10m high. Hence, in the safety concern, the recommended internal pressure should be equaled or over 0.3kPa.

### *6.3.3 Half Snow Loads*

For the half snow load, the initial angle of 90 degree is used.

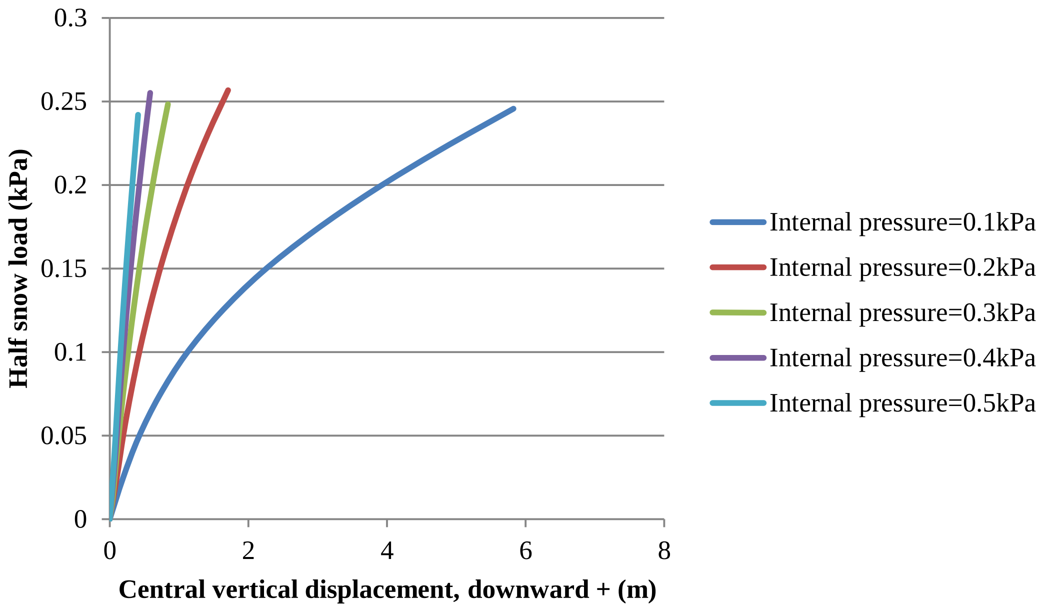


Figure 6.3.3 Relation of half snow load and central vertical displacement in different internal pressure

The curve of internal pressure of 0.1kPa is not reasonable in the membrane structure. For the 0.2 kPa, if the half snow load is under a small value, this internal pressure may be acceptable. In general, it is recommended to have an internal pressure of 0.3kPa or even higher.

### *6.3.4 Wind Loads*

For the wind load, the initial angle of 90 degree is used.

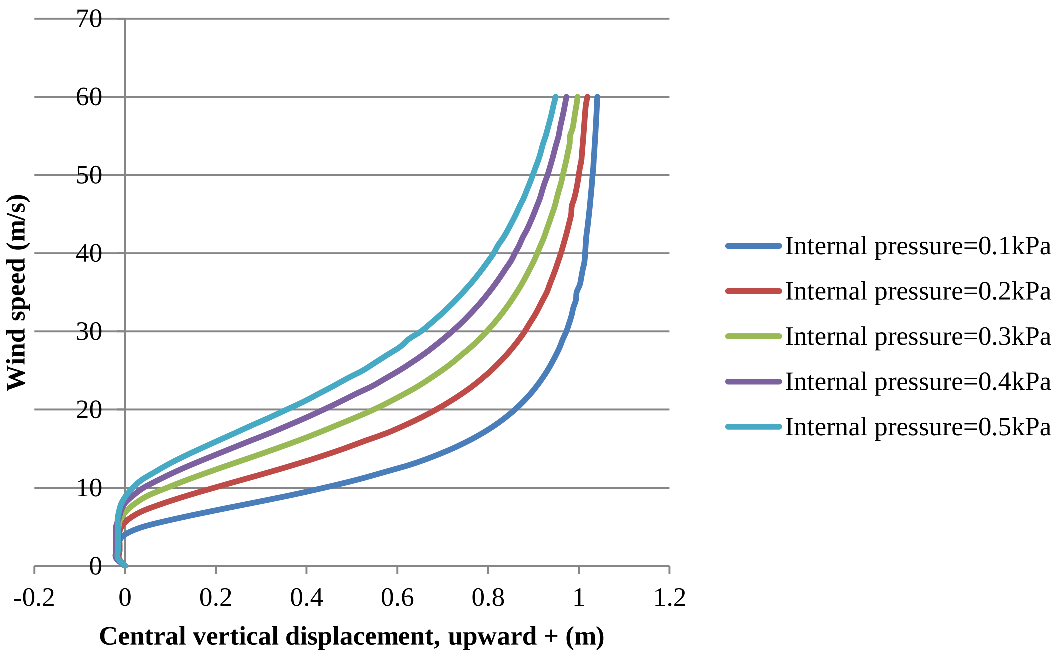


Figure 6.3.4 Relation of wind speed and central vertical displacement in different internal pressure

In the smallest internal pressure of 0.1 kPa have a vertical displacement of 1m which may be a little acceptable in the membrane which is 10 m high, but the membrane will have more displacement even in the low wind speed compared to the others. In some place where the typhoons always exist, the lower internal pressure may be available. On the contrary, the inland where in less contact with winds, may need a higher internal pressure. However, the higher internal pressure should be applied if the anchor tension is limited.

### *6.3.5 Concentrated Loads and Wind Loads*

For the concentrated load and wind load, the initial angle of 45 degree is used.

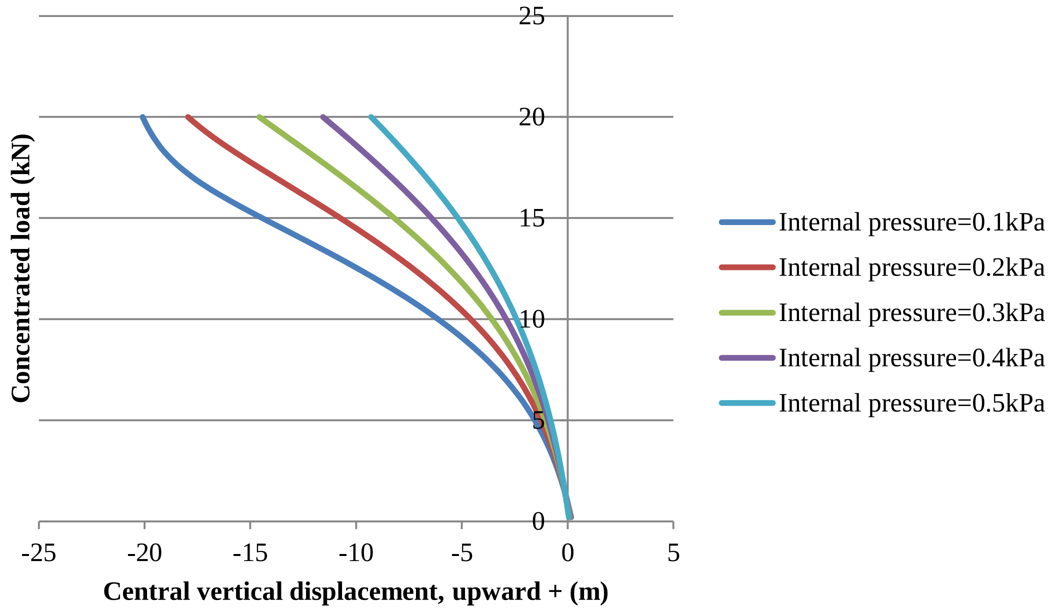


Figure 6.3.5 Relation of concentrated load, wind load of speed 20 m/s and central vertical displacement in different internal pressure

The effect of higher internal pressure is increasing regularly. Since the membrane is under a loading combination and have the potential movement vertically and horizontally, the higher internal may need to make sure the stability of membrane.

*6.3.6 Half Snow Loads and Wind Loads*

For the half snow load and wind load, the initial angle of 90 degree is used.

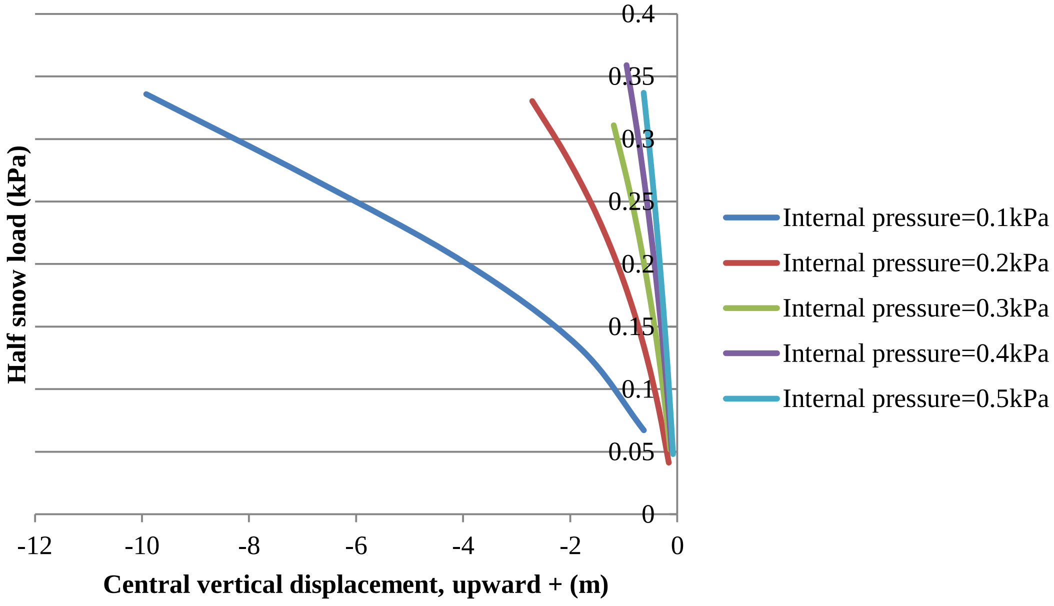


Figure 6.3.6 Relation of half snow load, wind load of speed 20 m/s and central vertical displacement in different internal pressure

As the Figure 6.3.6 shows the instability of membrane in the internal pressure of 0.1kPa. The internal pressure of 0.2 kPa may more reasonable than 0.1 kPa but only if the snow load is within a small value. Thus, the internal pressure of 0.3 kPa was used in the model can be acceptable for maintaining the stability of membrane or a higher internal pressure can be used for other purposes.

# CHAPTER 7 CONCLUSION

## *7.1 Behaviour of Cylindrical Membrane Structure*

Cylindrical membrane structure is a special structure that can resist the loadings with the large displacement. In the behaviour of membrane subjected to vertical loads, the smaller initial angle provides a better internal tension system for resisting the compression. In the behaviour of membrane subjected to horizontal loads, the smaller initial angle also performs a well behaviour in terms of less displacement. In the combination of vertical and horizontal loads, the analysis shows the effect of vertical loads is significant in the behaviour of large displacement compared to horizontal loads. For the flexibility of membrane structure, the applied loadings have the probability to indirectly influence the other loadings. As a result, the membrane will have a more complicated behaviour in the load combinations. Besides, the initial angle of 90 degree is basically applicable for all loading cases, which is stable for the membrane structure. In addition, the inextensible assumption limits the effect of loadings in resulting large displacement.

In general, the structure can be subjected to different load combinations but the continuous air-supported system is required to maintain the stability. The stiffness of cylindrical membrane structure can be proportionally related to the internal pressure.

Finally, the results indicate the potential of cylindrical membrane structure is appropriate as a part of buildings. However, this paper only introduces the inextensible cylindrical membrane structure in 2D-frame. The other feasibility of membrane can be found if using the 3D-frame in the model.

# REFERENCES

Chan, C. O. (2012), "Analysis of Air-Supported Structure", *Final Year Report,* University of Macau, Macau.

Maaskant, R. and Roorda, J. (1985), "Stability of Cylindrical Air-Supported Structures", *Journal of Engineering Mechanics*, Vol. 111 No. 12 ,pp.1487-1501.

Merritt, S. F. and Ricketts, T. J. (1958), *Building Design and Construction Handbook, Air-Stabilized Structures*, *Chapter 5,* Sixth Edition. (McGraw-Hill Professional, 2001 1994 1982 1975 1965 1958), AccessEngineering.

Turkkan, N. and Srivastava, N. K. (1992), "A Microcomputer-Based Analysis and Design of Air-Supported Cylindrical Membranes", *Canadian Journal of Civil Engineering*, School of Engineering, Universite de Moncton, Moncton, *N.B.*, Canada E1A 3E9, pp.1032-1040.